STUDIES ON THE EFFECTIVENESS OF FILM COOLING FOR ROCKET THRUST CHAMBER SAFETY

A DISSERTATION

Submitted in partial fulfilment of the requirements for the award of the degree
of
MASTER OF TECHNOLOGY
in
CHEMICAL ENGINEERING
(With Specialization in Industrial Safety and Hazards Management)

By

V. SUMESH

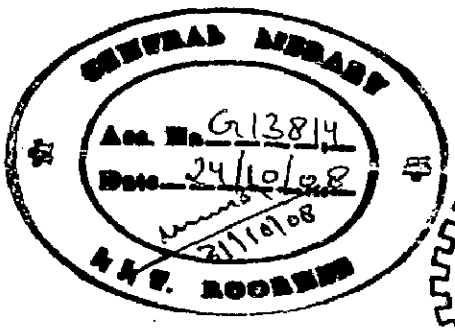

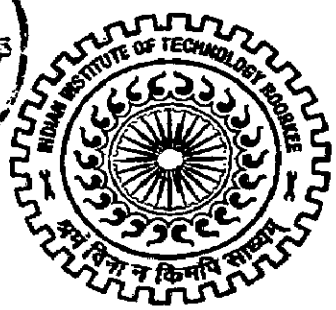

DEPARTMENT OF CHEMICAL ENGINEERING
INDIAN INSTITUTE OF TECHNOLOGY ROORKEE
ROORKEE -247 667 (INDIA)

JUNE, 2008

CANDIDATE'S DECLARATION

I hereby declare that the work which is being presented in this dissertation report titled **"STUDIES ON THE EFFECTIVENESS OF FILM COOLING FOR ROCKET THRUST CHAMBER SAFETY"**, in partial fulfillment of the requirements for the award of the degree of **Master of Technology** in Chemical Engineering with specialization in "**Industrial Safety and Hazards Management**", submitted to the Department of Chemical Engineering, Indian Institute of Technology, Roorkee, is an authentic record of the work carried out by me during the period from May 2007 to June 2008, under the guidance of **Dr. I.M Mishra,** Professor, Department of Chemical Engineering, Indian Institute of Technology Roorkee, Roorkee (India) and **Dr. S. Sunil Kumar,** Deputy Division Head, Thermal, Propulsion Research and Studies (PRS), Liquid Propulsion System Centre, ISRO, Thiruvananthapuram. The matter embodied in this work has not been submitted for the award of any other degree.

Date: 27-06-2008
Place: IIT, Roorkee

(V. SUMESH)

CERTIFICATE

This is to certify that the above statement made by the candidate is correct to the best of my knowledge.

Dr. S. Sunil Kumar
Deputy Division Head,
Thermal, PRS, LPSC, ISRO,
Thiruvananthapuram,
Kerala – 695 547 (India).

Dr. I. M. Mishra,
Professor,
Department of Chemical Engineering,
Indian Institute of Technology Roorkee,
Roorkee, Uttarakhand (India).

ACKNOWLEDGEMENT

I am greatly indebted to my guide Prof. I. M. Mishra, Department of Chemical Engineering, Indian Institute of Technology Roorkee, Roorkee for his support and guidance for the work without which this dissertation work would not have been possible.

I am very thankful to Dr. B. Prasad, Associate professor, Department of Chemical engineering, Indian Institute of Technology Roorkee, Roorkee for his timely help.

I would like to thank Dr. Shri Chand, Head of the Department, Department of Chemical Engineering and Chairman, DRC, for the support that he extended.

I would like to thank Dr S. Sunil Kumar, Deputy Division Head, Thermal, Propulsion Research studies (P.R.S), L.P.S.C., I.S.R.O., Thiruvananthapuram for all the support and guidance extended to me and appreciate his profound insight that contributed to prepare this dissertation report.

I would like to extent my sincere gratitude to Shri. Jophy Peter, P. R. S. lab, L. P. S. C., I. S. R. O. for his enormous helps in making the experimental work successful.

I am thankful to the Professor and Coordinator and other staffs of the QIP Centre, Indian Institute of Technology Roorkee, Roorkee for their encouragement and cooperation.

I sincerely acknowledge my wife and son for their encouragement and moral support.

I also thank my friends for their help and support to make this work success

(V. SUMESH)

ABSTRACT

An experimental investigation was carried out to determine the extent of reduction in wall temperature in a model thrust chamber of liquid rocket engines for various configurations of film cooling. The experimental test rig comprised a 100 kW hot air supply system, test section and required instrumentation. Hot air simulates the hot combustion products and nitrogen gas is used as the film coolant. Coolant gas injectors of three different configurations, viz., straight and compound angles of 30°–10° and 45°–10°, were used for the experiments. Experiments were carried out for different core gas flow temperature over a range of blowing ratios. The study brought out the relative merit of each of the injector configurations with respect to film cooling effectiveness, film cooled length and its uniformity. The main-stream hot gas used at two different temperatures of 343 K and 397 K with flow rates of 0.13 and 0.094 Nm^3/s for both temperature and the coolant gas applied at 308 K with flow rates of 0.0028 and 0.0021 Nm^3/s. Initially, the observations of surface temperature of test section were made with the help of thermocouples without applying the coolant and then with coolant for different coolant injections. The data that are available from the experiments is used to evaluate the film cooled length, film cooling effectiveness, film stability and the effects of blowing ratio. It is also used to compare the above evaluations for all configurations and hence to conclude the effect of the configurations on film cooling. It was noticed that the film cooling effectiveness was higher in the case of injector configuration with compound angle injection of 30°–10° as compared to that of straight and the compound angle of 45°-10° injection configurations. The film cooled length was also found to increase with blowing ratios. Higher core gas temperature lead to a reduction in the effective film cooled length.

CONTENTS

		DESCRIPTION	PAGE NO.
		CANDIDATE'S DECLARATION	I
		ACKNOWLEDGEMENT	II
		ABSTRACT	III
		CONTENTS	IV
		NOMENCLATURE	VI
		LIST OF FIGURES	VII
		LIST OF TABLES	IX
Chapter 1		INTRODUCTION	1
	1.1	Objective of the work	3
Chapter 2		LITERATURE REVIEW	4
	2.1	Thrust Chamber Failures	4
	2.2	Status of Film Cooling Research	4
Chapter 3		THRUST CHAMBER HEATING MECHANISM	13
	3.1	Heat transfer from the hot gases to the walls	13
	3.2	Thrust chamber cooling techniques	14
	3.3	Rocket Thrust Chamber Heat Transfer	17
	3.4	General Steady-state Heat-transfer relations	18
	3.5	Film Cooling Effectiveness	20
	3.6	Blowing Ratio	20
Chapter 4		EXPERIMENTAL SETUP AND MEASUREMENT PLAN	21
	4.1	Flow system	21
	4.2	Coolant injection system	33
	4.3	Test section chamber	33

	4.4	Film Coolants	37
	4.5	Instrumentation	37
	4.6	Test matrix	40
	4.7	Test procedure	40
	4.8	Uncertainty in measurements	40
Chapter 5		**RESULTS AND DISCUSSIONS**	45
Chapter 6		**CONCLUSIONS AND RECOMMENDATIONS**	75
	6.1	Conclusions	75
	6.2	Recommendations	76
		REFERENCES	77

NOMENCLATURE

Q	Heat transferred per unit time (W-s)
A	Surface area (m^2)
T	Temperature (K)
V	Velocity (m/s)
M	Blowing ratio = $(\rho V)_c/(\rho V)_\infty$
D	Diameter (m)
R	Radius (m)
(dT/dL)	Temperature gradient (K/m)
k	Thermal conductivity (W/m K)
h	Heat transfer coefficient (W/m^2 K)
q	Flow rate (m^3/s)
x	Distance (m)

Greek

η	Film cooling effectiveness = $\frac{(T_w - T_\infty)}{(T_c - T_\infty)}$
ρ	Density (kg/m^3)
σ	Standard deviation on temperature

Subscripts

c	Coolant
g	Gas
l	Liquid
w	Wall
aw	Adiabatic wall
wg	Gas side wall
wl	Liquid side wall
c	Coolant
∞	Main stream

LIST OF FIGURES

Figure No.	Caption / Title	Page No.
3.1	Eroded test chamber and the injector	14
3.2	Regenerative cooling	15
3.3	Uncooled liquid propellant thrust chamber with ceramic liners	16
3.4	Three ways of cooling the combustion chamber	17
3.5	Heat transfer rate distribution along thrust chamber wall	18
3.6	Temperature gradients in rocket thrust chamber	19
4.1	Schematic of Experimental set-up	22
4.1A	Test section-Copper	23
4.1B	Test section assembly	24
4.1C	Pressure adaptor of test section	25
4.1D	Injector-straight orifice	26
4.1E	Injector-Part I of 45°-10°	27
4.1F	Injector-Part II (Typical)	28
4.1G	Details of injector orifices	29
4.1H	Pressure adaptor of injector	30
4.1I	Coolant adaptor of injector (2 no.)	31
4.2	Photographic view of experimental set-up	32
4.3	Flow straightner	34
4.4	Injection head assembly	35
4.5	Coolant Injectors	36
4.6	Injector and Test section with thermocouples	38
4.7	Thermocouple positions on the test section	39
4.8	Data acquisition system	41
5.1	Temperature distribution on the test section circumference (T_∞=343 K)	46
5.2	Temperature distribution on the test section circumference (T_∞=397 K)	46

5.3	*Temperature profile for M = 2.4*	48
5.4	Temperature profile for M = 1.8	49
5.5	Temperature profile for M = 3.4	50
5.6	Temperature profile for M = 2.5	51
5.7	Temperature profile for M = 2.8	52
5.8	Temperature profile for M = 2.1	53
5.9	Temperature profile for M = 3.9	54
5.10	Temperature profile for M = 2.9	55
5.11	Variation of film cooled length with temperature for M=2.5 and 2.9	57
5.12	Variation of film cooled length with temperature for M=1.8 and 2.1	58
5.13	Variation of film cooled length with temperature for M=2.4 and 2.8	59
5.14	Variation of film cooled length on blowing ratio	60
5.15	Variation of Effectiveness for M=2.4	62
5.16	Variation of Effectiveness for M=1.8	63
5.17	Variation of Effectiveness for M=3.4	64
5.18	Variation of Effectiveness for M=2.5	65
5.19	Variation of Effectiveness for M=2.8	66
5.20	Variation of Effectiveness for M=2.1	67
5.21	Variation of Effectiveness for M=3.9	68
5.22	Variation of Effectiveness for M=2.9	69
5.23	Film uniformity along the circumference for M=2.4	70
5.24	Film uniformity along the circumference for M=2.8	71
5.25	Film stability for all injectors (M=1.8)	72
5.26	Film stability for all injectors (M=3.4)	73
5.27	Film stability for all injectors (M=3.9)	74

LIST OF TABLES

Table No.	Caption / Title	Page No
4.1	Matrix for straight injector orifice	42
4.2	Matrix for compound angle injector orifice of 30°-10°	43
4.3	Matrix for compound angle injector orifice of 45°-10°	44
5.1	Comparison of film cooled length	56

Chapter 1

INTRODUCTION

High thrust-high specific impulse rocket engines, which are being developed as the propulsion devices for heavier pay load capacity, use liquid propellants instead of solid fuel. The temperature and pressure that are developed in such a thrust chamber (rocket nozzle) because of combustion of the propellants is of high magnitudes (3800 to 4000 K and 450 to 550 psi) and have direct impact on the safety of the launch facilities and the personnel. The hot combustion gases cause the wall temperature to go beyond the melting point of the material itself leading to burn-through and explosions. Inadequate measures to manage these adverse pressure and temperature conditions had led to a significant number of failures of engine thrust chamber during the developmental phase of several high thrust engines. The primary concern is therefore the development of techniques to manage such high temperatures (~3800 K). No margin of error is to be allowed and the rocket engines are to be made 100% foolproof to withstand engine temperatures and pressures.

One way of alleviating high temperature problem is to cool the walls of the thrust chamber. However, one has to deal with high heat flux levels (~50 MW/m^2) at the nozzle throat. This calls for employing a host of technique for efficient wall cooling. The following cooling methods are available for such a purpose.

(1). **Regenerative cooling**

This is the method in which the rocket chamber is cooled by circulating a part or all of the liquid propellant (fuel or oxidizer) through a jacket (or coils wrapped) around the hot gas chamber. The heat absorbed by the coolant in the jacket (or coils) is, therefore, not wasted but helps in augmenting the heat content of the propellant.

(2). **Film cooling**

Large reductions in over–all heat transfer to rocket engine walls have been obtained by injecting the propellant around the inner walls of the chamber, which forms a film. These two methods have been used in conjunction with each other in most of the advanced high thrust engines.

(3). ***Transpiration or sweat cooling***

Here the coolant and the hot combustion gas is separated by a porous wall and cooling is effected by sweating of the coolant through the porous wall using its latent heat of evaporation. The use of sweat cooling applications in a rocket engine has been limited because of difficulty in realizing porous plates to meet the requirement of well controlled coolant flow and its variation in flow throughout the walls to be cooled.

(4). **Ablative cooling**

This is another approach of using high-temperature-resisting materials to reduce the heat flow into rocket-engine walls. This method is widely used in earth storable rocket engines of shorter burning duration.

Out of the four methods described as above, internal film cooling is effective in conjunction with regenerative cooling and is one of the most potential methods to keep the wall temperature within safe limits. Film cooling is a method in which a solid surface is protected from the influence of high temperature combustion gases using a film of coolant medium in between the hot gases and the wall. In the case of liquid propellant rockets, fuel itself could be used as the coolant. For earth storable and semi-cryogenic propellant rockets, the coolant is initially in liquid phase whereas for cryogenic rockets the coolant is injected as a gas.

The coolant is to be injected into the combustion chamber with a tangential component of velocity in addition to the axial velocity so that it can smear over the inside wall of the combustion chamber. The coolant moves as a swirled film over the inner wall surface of the chamber and the nozzle. The axial velocity component and the viscous drag of the high velocity hot core gas on the coolant film helps in spread and coverage of progress the coolant film along the length of the chamber and the nozzle. In this manner the coolant travels along the length of the combustion chamber, forms a barrier between the hot gas and the wall and thus protects the wall from the hot combustion products. However, during its travel along the wall, it mixes with the main-stream hot gases and gets heated. Space conscious nations have been investing a lot of resources in optimizing and taming this cooling technique to be suitably adapted to the new age rocket systems due to its significance in safety promotion and assurance. It may, however, be noted that the effectiveness of the film cooling with respect to the coolant flow rate, temperature, injection angle, medium and state has neither been

investigated thoroughly nor understood fully and a lot of work needs to be done in this direction. Research centers across the world are actively pursuing ways and means of optimizing the design of such cooling mechanism, which has a direct bearing on the payload carrying capacity of the launch vehicle itself.

1.1 Objective of the work

The effectiveness of film cooling depends on the blowing ratio, compound injection angles, film adherence to wall, film stability and the thermo-physical properties of the coolant. A clear understanding of their extent of influence is still not investigated thoroughly. The present study has the following aims and objectives.

To set up an experimental test rig with adequate instrumentation for measurements for some specific experiments as in Tables I, II and III to bring out the role of blowing ratios, injection configuration angles on film cooling effectiveness, film cooled length, film uniformity and its wall adherence. The present work is limited to gas film cooling and the results obtained would be applicable for a cryogenic liquid propellant rockets.

Chapter 2

LITERATURE REVIEW

2.1 Thrust chamber failures

There are generally two basic types of heat transfer failures in combustion chambers. In one type, the wall temperature on the gas side exceeds the value at which the material is readily melted or oxidized. The resulting local loss of material and the local heating weakens the wall so that the remaining material is inadequate to take the thermo-mechanical load. This failure is characterized by melting, erosion or severe oxidation on the gas side surface of the wall. This type of failure occurs primarily in uncooled chambers and uncooled nozzles, but also in cooled chambers or nozzles with relatively thick walls.

The other type of failure is essentially caused by the local inability of the liquid film of the cooling jacket coil to transfer the heat from the wall to the liquid coolant. When the regenerative coolant medium is very near to the first critical heat flux regime, a marginal increase in heat flux would push it from nucleate boiling to transition boiling regime which reduces the heat transfer capacity of the fluid. This occurs only in liquid propellant-cooled chambers and is characterized by a sudden decrease in the local heat flux, a breakdown of the liquid film, and a sudden increase of the wall temperature, usually resulting in melting of the metal. This breakdown of the liquid film occurs if the wall temperature on the coolant side exceeds the boiling point of the coolant liquid by a considerable margin.(Sutton, 1963)

2.2 *Status of film cooling research*

Film cooling investigations had been performed over many years. Most of the work has dealt with the determination of the film cooling effectiveness. There have been numerous experimental studies and several models for the prediction of film cooling effectiveness in the literature.

Eriksen, (1971) had carried out an experimental investigation of the local film cooling effectiveness. He determined the heat transfer coefficients down stream of the region of coolant injection into a hot air stream over a flat plate. Three configurations of

coolant injection were studied. In the first, the injection was through a single hole normal to the main hot flow. In the second configuration, a row of holes spaced at three diameter intervals with an injection angle of 35° to the main flow was used. A single hole injection at an injection angle of 35° was also done. He compared the film cooling effectiveness with the results of other investigations and found that the film cooling effectiveness was the least for normal injection. Subsequent flow visualization experiments showed very large eddies and vortices caused by the interaction between the normally injected jets and the main stream.

Kuo et al. (1996) investigated the effects of mass addition in both subsonic and supersonic flow on film cooling experimentally and analytically. Experimental observation indicated film cooling to be effective in subsonic flow, but not in supersonic flow. A one dimensional steady-state analysis showed that for subsonic flow, mass addition causes a decrease in the pressure, total pressure, density and temperature. In contrast, the mass additions in supersonic flow lead to an increase in entropy, density, pressure and temperature. Film cooling effect prevails in subsonic flow because of the temperature decrease in the main stream. However, it is absent in supersonic flow because of the temperature increase, leading to the conclusion that the film cooling effect cannot penetrate into a supersonic flow region.

Papell, (1960) studied the effect of variation of coolant injection angles on gaseous film cooling effectiveness. Data were obtained for coolant injection through slots at angles up to and including 90°. He found that when the angle between the mainstream and coolant stream increases, fluid mixing increases which results in decreased film cooling effectiveness. In the correlation of his experimental data, an effective injection angle was defined by the vector summation of the coolant and mainstream gas flows. The cosine of this angle was used as a parameter to empirically develop a correction term to propose a correlating on the experimental data.

An experimental study of film cooling effects produced by injection of helium as a secondary flow into a low speed air mainstream was carried out by Goldstein et al., (1966). They injected helium through a porous section into a turbulent boundary layer flowing over a flat plate. For comparison purposes, they used air as the secondary fluid for their experiments. It is found that helium injection produces higher film cooling effectiveness than anticipated.

The applicability of film cooling to rocket engines in the 4.5 - 454 kg-thrust range using earth-storable, space-storable and cryogenic propellant combinations were investigated by Stechman et al., (1969). The accuracy of the analytical model was verified with test data using some propellant combinations. They illustrated the inter-relational effects of mixture ratio, specific impulse, wall temperature and the percent of film cooling. The study showed that the propellant combinations using one of the hydrazine-type fuels are well suited to film cooling. These fuels have large heats of vaporization, so that they remain in the more efficient liquid state for a longer time.

Goldstein et al., (1974) studied the influence of the variation of the size and geometry of the coolant gas injection holes on film cooling effectiveness. They conducted experiments in a low speed wind tunnel. The results indicated an increase in film cooling effectiveness when the geometry of the hole was modified as a stepped hole (counter sunk hole) with an increase in diameter of the hole before the injection. The reason for the increased effectiveness was attributed to the decrease in the mean velocity of the coolant fluid due to larger exit area. The injected coolant stayed closer to the wall rather than getting lost by penetration into the main stream. They also concluded that it is not the mass velocity ratio but the momentum ratio or dynamic pressure ratio, which is the key parameter in determining the penetration of the jet for fluids of different density.

Gritsch et al., (2000) investigated three film cooling hole geometries including a cylindrical hole and two holes with a diffuser shaped exit portion in terms of local heat transfer coefficients as well as overall cooling performance. Tests were conducted for a coolant to main flow temperature ratio of 0.54 (density ratio 1.85) over a range of blowing ratios of M=0.25 - 1.75. Surface temperatures downstream of the injection location were measured by means of an infrared camera system and used as boundary conditions for a finite element analysis to determine the surface heat. The superposition method was applied to evaluate the overall film-cooling performance of the hole geometries investigated by combining heat transfer and adiabatic cooling effectiveness data. The results revealed that the holes with expanded exits have much lower heat transfer coefficients at elevated blowing ratios than that of a cylindrical hole. Combining the effects of reduced heat transfer coefficients and increased film cooling

effectiveness, holes with expanded exits provide significantly improved film cooling performance at elevated blowing ratios as compared to a cylindrical hole.

Investigations of the influence of compound angle injection on film cooling effectiveness were carried out in detail by Nasir et.al.,(2001) Tests were conducted in a low speed wind tunnel using a flat surface through a single row of discrete holes angled 55° along the stream wise and 0° and 60° in the lateral directions. Heat transfer coefficient and film effectiveness at blowing ratios of 0.5, 1.0 and 1.5 with a coolant-to-mainstream density ratio of 1.0 were presented. They used a transient liquid crystal technique to measure both the local heat transfer coefficient and the film effectiveness. It was found that the film effectiveness is significantly higher in the case of compound angle holes than that of simple angle injection geometry.

Folayan and Whitelaw, (1974) compared the measured and predicted values of adiabatic wall effectiveness for multi-slot film cooling and found them to be in close agreement of each other. The study concluded that the multi-slot film cooling is more effective than a single-slot cooling.

Narayan et al. ,(1986) carried out an experimental study of liquid film cooling with tangential injection of 2-D liquid film along a surface of a square duct with co-flowing hot combustion gases. They also carried out a simple heat transfer analysis to predict the liquid film cooled length. The study brought out the influence of free-stream temperature, velocity and coolant mass flow rate on film cooled length. The results showed that the wall temperature increases gradually up to a point and, thereafter, there is a sharp increase indicating the vanishing of liquid film. They also found that the film cooled length increases with an increase in coolant injection rate and decreases with an increase in free stream velocity and hot gas temperature. They found a good agreement with the predicted and measured film cooled lengths.

Kinney et al. ,(1952) investigated the effectiveness of liquid cooling films on the inner surfaces of tubes containing flowing hot air. Their experiments were carried out on 2" and 4" diameter straight metal tubes with air flows at temperature from 588 K to 1367 K and diameter Reynolds numbers varying from 2.2×10^5 to 14×10^5. They used water as the film coolant. Flow visualization of the experiments was done over a transparent tube with the help of a stroboscopic light. Their results indicated that the best possible way of cooling a given surface area, with as little coolant flow as possible,

is to introduce the coolant at several axial positions instead of a single position. They also concluded that the liquid film cooled length decreases with an increase in mass velocity.

Yu et al. (2004) have investigated the potential benefits of swirling the liquid film to reduce entrainment and to provide manageable wall thermal environments at a lower performance penalty. A critical review of published analyses of liquid film cooling for rocket engine combustors and a survey of experimental studies of the same were also performed by them. A comparison between different models was performed and the heat transfer coefficient was initially high and then decreased due to the growth of the vapor layer. An order of magnitude analysis was done on a swirling liquid film. Wall shear stress, centrifugal force, surface tension and liquid inertia were found to be the major forces. Swirling the liquid film may provide more efficient cooling by reducing entrainment and extending the liquid and vapor cooled regions of the chamber.

Brown and Saluja (1979) presented measurements of film cooling effectiveness for coolant injection through a single hole and rows of holes with pitch to diameter ratios of 8.0, 5.33 and 2.67 with an injection angle of 30° to the free stream flow direction. They found that the influence of injecting a small fraction of the coolant through narrow slits located three diameters downstream from the row of holes is found to be significant, in the case of a row of holes with a pitch to diameter ratio of 5.33. They also measured the effects of free stream turbulence and velocity gradient and found that an increase in free stream turbulence reduces film cooling effectiveness. It is also observed that from the various effectiveness measurements, the optimum blowing rate for all values of pitch-to-diameter (p/D) ratio is about 0.5.

Yuen and Martinez-Botas (2005) studied experimentally the film cooling effectiveness on rows of cylindrical holes with stream wise angles of 30°, 60° and 90°, in a flat plate test facility with a zero pressure gradient. This investigation commenced with a single row of holes with two pitch-to-diameter ratios (p/D), 3 and 6. The effects of introducing inline and staggered rows for each stream wise angle and pitch-to-diameter ratio was also analyzed. The row spacing in the inline and staggered rows is 12.5 diameters in the stream wise direction. The short but engine representative hole length (L/D = 4) is constant for all geometries. The blowing ratio ranges from 0.33 to 2, and the free stream Reynolds number based on the free stream velocity and hole diameter

(Re_D) was 8563. Both local values and laterally averaged ones are presented, the latter refers to the averaged value across the central hole. The results are compared with the experimental results obtained by other researchers, the effects of the additional inline and staggered rows, and of the variations in injection angle, pitch-to-diameter ratio are described. The maximum effectiveness was achieved with a blowing ratio of 0.5 approximately at x/D equal to, or smaller than 5.2 for one row of 30° holes with pitch-to-diameter ratios of 3 and 6. The blowing ratio at which the maximum effectiveness occurred increased with stream wise distance, since stronger jets travelled farther downstream. This finding reinforces the need to specify the axial location when comparing the blowing ratio at which the maximum effectiveness occurred. The maximum effectiveness with one row of 60° holes occurred with blowing ratios of less than 0.5 at x/D equal to, or smaller than 5.2 with pitch-to-diameter ratios of 3 and 6. The row of 90° holes gave lower values than the 30° and 60° holes due to greater vertical momentum and penetration. It is worth noting that the steeper the hole, the lower the blowing ratio at which the maximum effectiveness occurred in the near-hole region. The span wise uniformity and coverage in effectiveness were improved with the smaller pitch, particularly for the intermediate and far downstream regions. The effectiveness and coverage with two-inline rows were generally better than one row even for the same injected mass flow. The benefits of the inline rows were greatest with the 30° holes, and became most apparent with blowing ratios greater than unity.

In another paper Yuen and Martinez-Botas (2005) presented their experimental results on the same test facility and the same operating conditions and blowing ratios. They used the liquid crystal thermography and the steady state heat transfer method as the measurement technique. The results were presented in the form of h/h_o, which is the ratio of heat transfer coefficient with film cooling to that of without film cooling. The 30° holes gave the largest h/h_o values with a row of holes and p/D ratio of 6 for blowing ratio from 0.33 to 1.67 at all axial locations, followed by the 60° and 90° holes in descending order. The row of 90° holes with a p/D ratio of 3 gave larger h/h_o values than that of the 60° holes of the same pitch. This was probably caused by the greater shear due to the higher velocity gradient, which increased the heat transfer from the wall. Larger h/h_o means here a large heat transfer from the main stream to the turbine blades. The effectiveness and coverage with the two in-line rows were observed to be generally

better than one row even for the same injected mass flow. The combined performance of effectiveness and heat transfer coefficient suggests that the two in-line rows are likely to be advantageous in the film cooling, (of turbine blades) with good coverage for unit mass flow of cooling air and lower thermal stresses because of the smaller heat load. The staggered rows improved the span wise uniformity in effectiveness, but the h/h_o values were larger than those with the in-line rows of the same pitch for all blowing rows with the 30° holes.

A numerical study to investigate the liquid film cooling in a rocket combustion chamber was performed by Zhang et al. (2006). Mass, momentum and heat transfer characteristics through the interface were considered in detail, and by solving the respective governing equations for the liquid film and the gas stream coupled through the interfacial matching conditions, they concluded that the heat transfer at the gas-liquid interface in a rocket combustion chamber with insulated wall is mainly dominated by convection of the free stream and transport of latent heat associated with the evaporation of the liquid film. When the wall is cooled by an external coolant, however, the sensible heat transfer becomes significant, and accordingly the convective transfer increases and latent heat flux decreases, leading to the elongation of the liquid film length. The interfacial temperature increases quickly in the entrance region and soon reaches the saturated temperature of the liquid film. The wall temperature is very low in the liquid film cooling region and increases sharply just beyond the point of the dry-out. The liquid film length decreases with the increase of the gas stream Reynolds number with an invariable coolant mass flux. The liquid film length increases with the increase of the external cooling intensity but decreases with increasing the coolant inlet temperature.

Nasir et.al. (2003) investigated the effect of discrete data (or triangular) shaped tabs with different orientations on the film cooling performance from a row of cylindrical holes. Three tab orientations were investigated. Measurements were carried out in a low-speed wind tunnel using the transcend liquid crystal technique. The main stream velocity and free - stream turbulence intensity in the low – speed wind tunnel are 9 m/s and 7 % respectively and the mainstream Reynolds number based on the hole diameter is around 7100. Three blowing ratios of 0.56, 1.13 and 1.7 are tested. The tabs oriented downwards provide the highest effectiveness at a blowing ratio of 0.56 while the tabs

oriented horizontally provides highest film effectiveness at blowing ratios of 1.13 and 1.7.

The film cooling performance is evaluated by Ahn et al. (2003) for film hole configuration with opposite orientation angles; and the effects of blowing ratios on boundary layer temperature distributions are investigated. They observed that at a blowing ratio of 0.5, the injectant is centered near the surface regardless of the configuration to provide high adiabatic effectiveness level. At the higher blowing ratios of 1.0 and 2.0 the interaction between injectant from the upstream and downstream holes become important to film cooling effectiveness. The downwash flow at the hole exit makes the injectant well attached to the wall to yield the high film cooling effectiveness, whereas the upwash flow deteriorates it. For the film cooling with two rows of holes, the previous data usually showed that the lower blowing ratio such as M=0.5 provides the highest adiabatic film cooling effectiveness in the near-hole region, whereas the higher blowing ratio gives better protection in the further downstream region. However, the trend could be reversed depending mainly on hole arrangement and configuration such as the orientation angle. In this study, the highest film cooling effectiveness is obtained at the blowing ratio of 0.5 for staggered hole configuration throughout the measured surface.

Maiteh and Jubran (1999) investigated a combination of one row of simple angle holes and one row of compound angle holes on film cooling. They used an open suction-type wind tunnel with a cross sectional area of 30cm x 30cm and a length of 200 cm. Increasing the free stream turbulence intensity was found to reduce the film cooling effectiveness for compound angle holes or combination of simple and compound angle holes. They also deduced that the averaged film cooling effectiveness from an injection model of either two rows of compound angle holes or one row of compound angle holes and one simple angle holes row can be correlated by using a two-dimensional film cooling correlation provided that the momentum ratio I is incorporated in the correlation.

Lakehal et al. (1998) investigated the film cooling effectiveness of a flat plate using a row of laterally injected jets applying a Navier-Stokes equation solver, which employs a finite-volume method with a multi block technique. The paper compares measured and calculated temperature and velocity fields obtained with the standard k-ε and the k-ε based two layer turbulence model for various blowing rates. The resolution

of the viscosity-affected near-wall region with a one-equation turbulence model yielded a noticeable improvement in the prediction of film cooling effectiveness compared to results obtained with wall functions.

Burns and Stollery (1969) studied the influence of foreign gas injection and slot geometry on film cooling effectiveness. They conducted experiments using two-dimensional plate geometry in a low-speed wind tunnel. They concluded that the increasing the velocity ratio of coolant to mainstream produces higher effectiveness though improvements in effectiveness are small for pure Arcton – 12 as coolant. For helium injection, the effectiveness continues to improve with increasing velocity ratio. The influence of mainstream boundary layer thickness on effectiveness is, in general, small. However, it can become important, if the density ratio of coolant to mainstream is low, presumably since the momentum deficit in the boundary layer of the same order of magnitude as the momentum of injectant. Thickening the slot lip would decrease the film cooling effectiveness. This effect is particularly serious for low values of density ratios of coolant to mainstream. For a given mass flow of injectant, the lightest gas results in higher effectiveness.

A careful study of the literature review reveals that the use of compound angle in a cylindrical chamber as in the case of the combustion chamber of a liquid propellant rocket has not been evaluated thoroughly for its effects on film cooling effectiveness, film cooled length and its uniformity. The present work addresses the role of the injection of coolant into a cylindrical chamber for various configurations of injection angles.

Chapter 3

THRUST CHAMBER HEATING MECHANISM

Higher temperature is essential in a thrust chamber to achieve higher specific impulse and therefore it has to be managed by suitable hardware design. As discussed, the thrust chamber wall needs to be protected within safe limits by providing appropriate cooling heat transfer techniques. The heat loads from convection and radiation from the hot gases to the chamber walls has to be dissipated out to maintain a tolerable temperature within the hardware.

3.1 Heat transfer from the hot gases to the walls

The significant part of the heat transferred from the hot combustion gases to the chamber walls is by convection. The amount of heat transferred by conduction is small and that transferred by radiation is usually less than 25%, of the total [Sutton, 1963]. As the wall temperature determines the yield strength of the material and the thermal stresses induced, the chamber walls have to be kept at a temperature such that the wall material strength is adequate to prevent failure. Material failure is usually caused either by increased wall temperature on the gas side so as to weaken, melt, or damage the wall material or by the increased wall temperature on the liquid coolant side so was to vaporize the liquid next to the wall. The consequent failure is caused because of the sharp temperature rise in the wall caused by non-availability or storage of the coolant. The design of such regenerative coolant passage therefore has to be within the nucleate boiling regime to avoid burn through.

Once the wall material of an operating rocket engine begins to fail, final burn-through and engine destruction are extremely rapid (Fig. 3.1). Even a small pinhole in the chamber wall will almost immediately (within a second) open into a large hole since the hot chamber gases (2,500 to 3,600 K) will oxidize or melt the adjacent metal, which is then blown away exposing new metal to the hot gases.

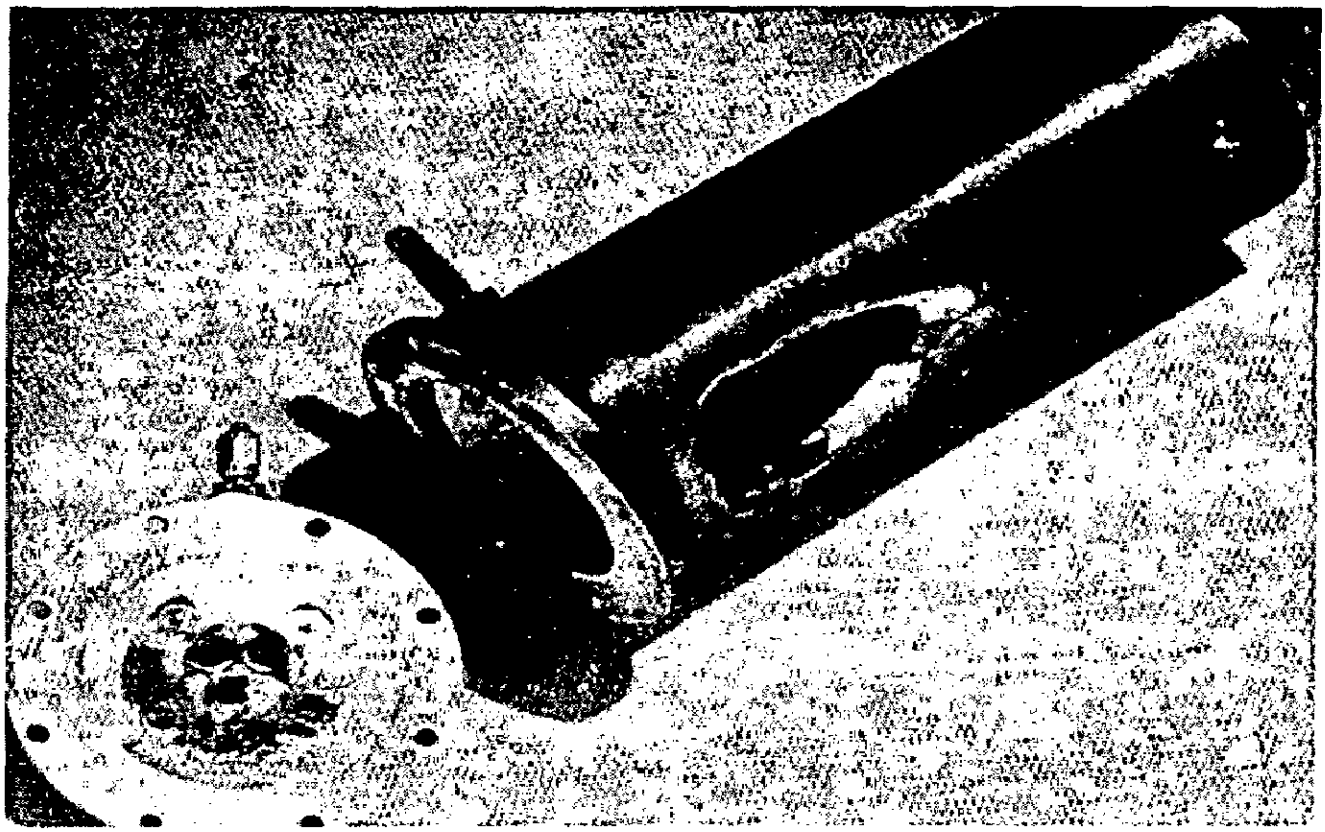

Fig. 3.1 Eroded test chamber and the injector(Sutton, 1963)

The heat transfer process is very important in every single system such as combustion chamber, nozzle, liquid propellant gas generator, injector, and feed lines. In cooled combustion devices the heat transfer usually reaches a thermal equilibrium condition. In an uncooled unit the operating time is usually short and the heat transfer is in transient state.

3.2 Thrust chamber cooling techniques

The heat created during combustion in a rocket engine is contained within the exhaust gases. Most of this heat is expelled along with the gas that contains it, however, heat is transferred to the thrust chamber walls in quantities sufficient to require attention.

Thrust chamber designs are generally categorized or identified by the hot gas wall cooling method or by the configuration of the coolant passages, where the coolant

pressure inside the regenerative coolant passage may be as high as 500 atmosphere. The high combustion temperature (2,500 to 3,600 K) and the high heat transfer rates (up to 160 MW/m^2) encountered in a combustion chamber present a formidable challenge to the designer. To meet this challenge, several chamber cooling techniques have been utilized successfully. Selection of the optimum cooling method for a thrust chamber depends on many considerations, such as type of propellant, chamber pressure, available coolant pressure, combustion chamber configuration, and combustion chamber material.

Regenerative cooling is the most widely used method of cooling a thrust chamber and is accomplished by flowing high-velocity coolant over the back side of the chamber hot gas wall to convectively cool the hot gas liner. The coolant with the heat input from cooling the liner is then discharged into the injector and utilized as a propellant (Fig. 3.2). Such systems are successfully utilized in cryogenic, semi-cryogenic and earth storable rocket propulsion systems.

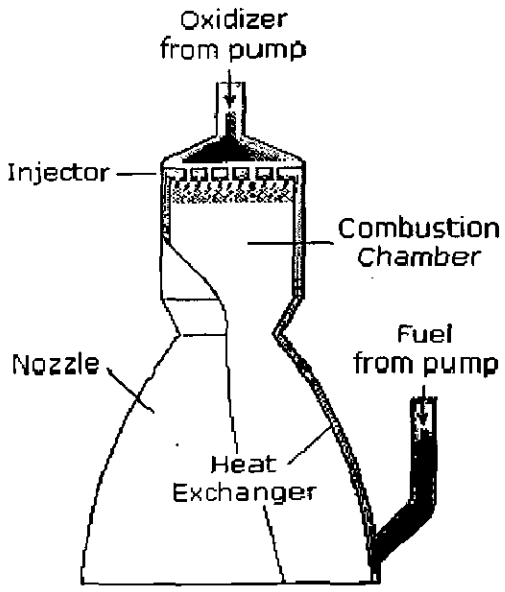

Fig. 3.2 Regenerative cooling. (http://www.braeunig.us/space/propuls.htm)

In addition to the regeneratively cooled designs mentioned above, other thrust chamber designs have been employed for rocket engines using dump cooling, film cooling, transpiration cooling, ablative liners and radiation cooling. Although regeneratively

cooled combustion chambers have proven to be the best approach for cooling large liquid rocket engines, other methods of cooling have also been successfully used for cooling thrust chamber assemblies. Same of the examples are detailed below.

Dump cooling, is similar to regenerative cooling because the coolant flows through small passages over the back side of the thrust chamber wall. The difference, however, is that after cooling the thrust chamber, the coolant is discharged overboard through openings at the aft end of the divergent nozzle. This method has limited application because of the performance loss resulting from dumping the coolant overboard. However, small amount of dump cooling is provided in many smaller thrusters.

*With **ablative cooling**, combustion gas-side wall material is sacrificed by melting, vaporization, charring and chemical changes to dissipate heat (Fig. 3.3). As a result, relatively cool gases flow over the wall surface, thus lowering the boundary-layer temperature and assisting the cooling process. Such systems are generally employed in earth storable rocket systems.*

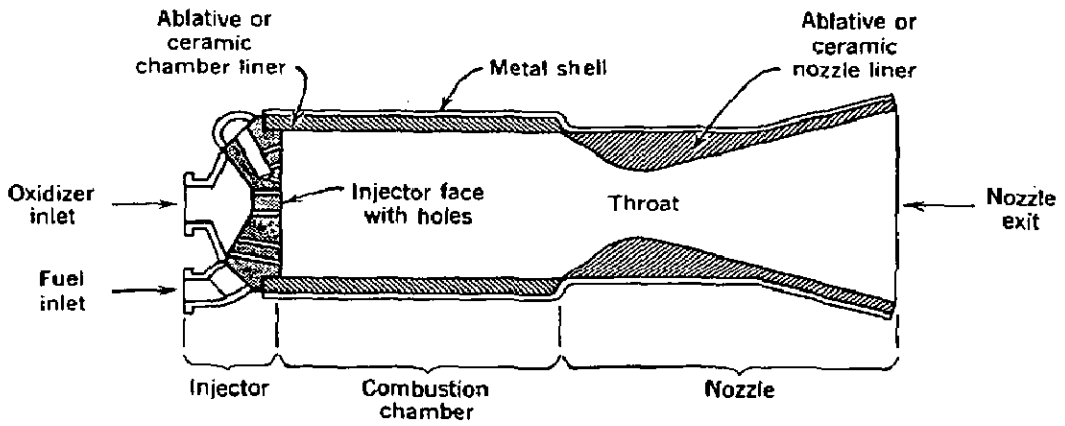

Fig. 3.3 Uncooled liquid propellant thrust chamber with ceramic liners

(Sutton, 1963)

Film cooling provides protection from excessive heat by introducing a thin film of coolant or propellant through orifices around the injector periphery or through manifolded orifices in the chamber wall near the injector or chamber throat region

(Fig. 3.4). This method is typically used in high heat flux regions and in combination with regenerative cooling and is the most popular among all chamber cooling techniques.

Transpiration cooling provides coolant (either gaseous or liquid propellant) through a porous chamber wall at a rate sufficient to maintain the chamber hot gas wall to the desired temperature. The technique is really a special case of film cooling and is also called as sweat cooling.

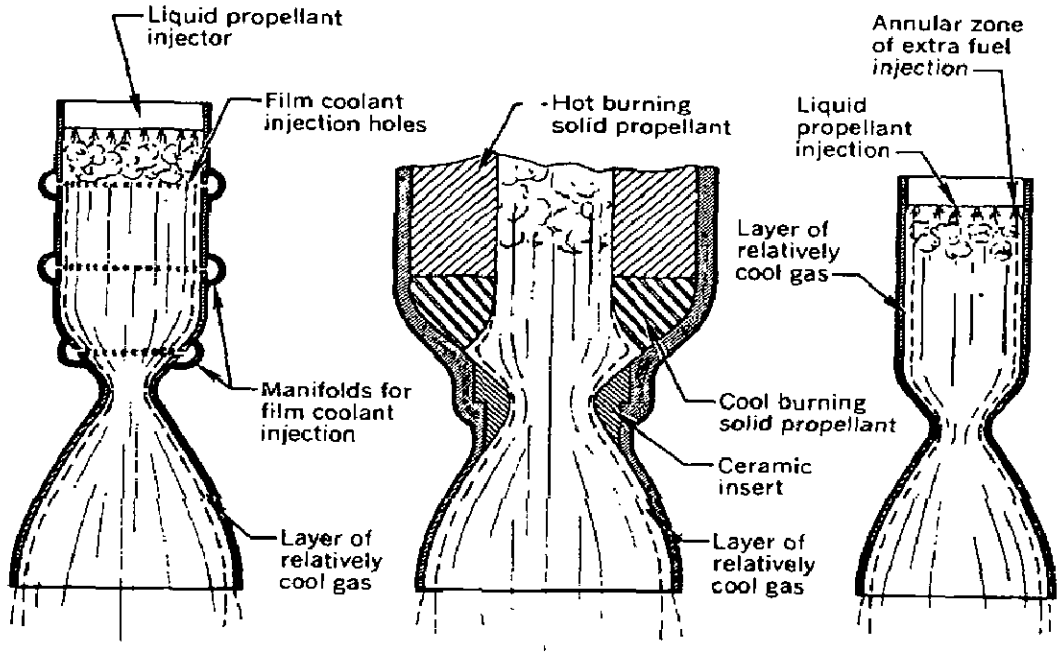

Fig. 3.4 Three ways of cooling the combustion chamber
(Sutton, 1963)

With **radiation cooling**, heat is radiated from the outer surface of the combustion chamber or nozzle extension wall. Radiation cooling is typically used for small thrust chambers with a high-temperature wall material (refractory) and in low-heat flux regions, such as a nozzle extension.

3.3 Rocket thrust chamber heat transfer

Heat is transferred to all parts exposed to hot gases, such as injector faces, nozzles and chamber walls. The heat transfer rate varies within the rocket and is usually highest at, and immediately upstream of, the nozzle throat, with local wall temperatures having the highest values in the region as shown in Fig. 3.5.

The amount of heat transferred by conduction from the chamber gas to the walls in a rocket thrust chamber is negligible. By far the largest part of the heat is transferred by means of convection. A part of the transferred heat is attributed to radiation.

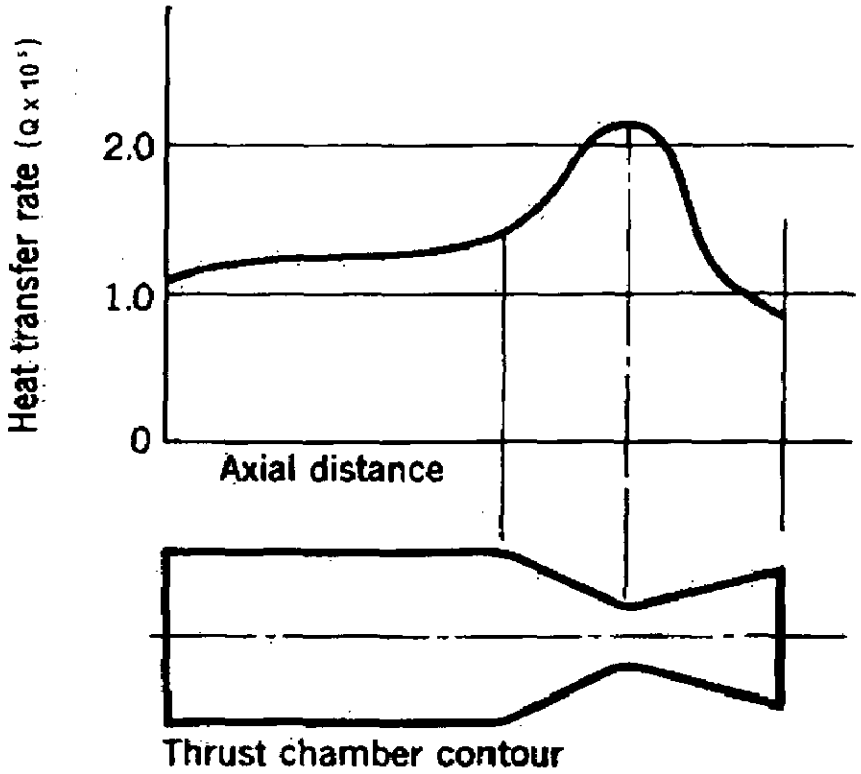

Fig. 3.5 Heat transfer rate distribution along thrust chamber wall

(Sutton, 1963)

3.4 General steady-state heat-transfer relations.

For heat-transfer conduction the general relation applies:

$$Q/A = -k(dT/dL) = -k\,\Delta T/L \qquad (3.1)$$

The negative sign indicates that temperature decreases as thickness increases.

The convective heat transfer through the chamber wall of a rocket chamber can be treated as a series type, steady-state heat-transfer problem with a large temperature gradient across the gaseous film on the inside of the chamber wall, a temperature drop across the wall, and, in cases of cooled chambers, a third temperature across the film of the moving cooling fluid. It is shown schematically in Fig. 3.6.

The general steady-state heat-transfer equations can be expressed as :

$$Q/A = h(T_g - T_l) \tag{3.2}$$

$$= \frac{(T_g - T_l)}{(1/h_g + t_w/k + 1/h_l)} \tag{3.3}$$

$$= h_g (T_g - T_{wg}) \tag{3.4}$$

$$= (k/t_w).(T_{wg} - T_l) \tag{3.5}$$

$$= h_f (T_{wl} - T_l) \tag{3.6}$$

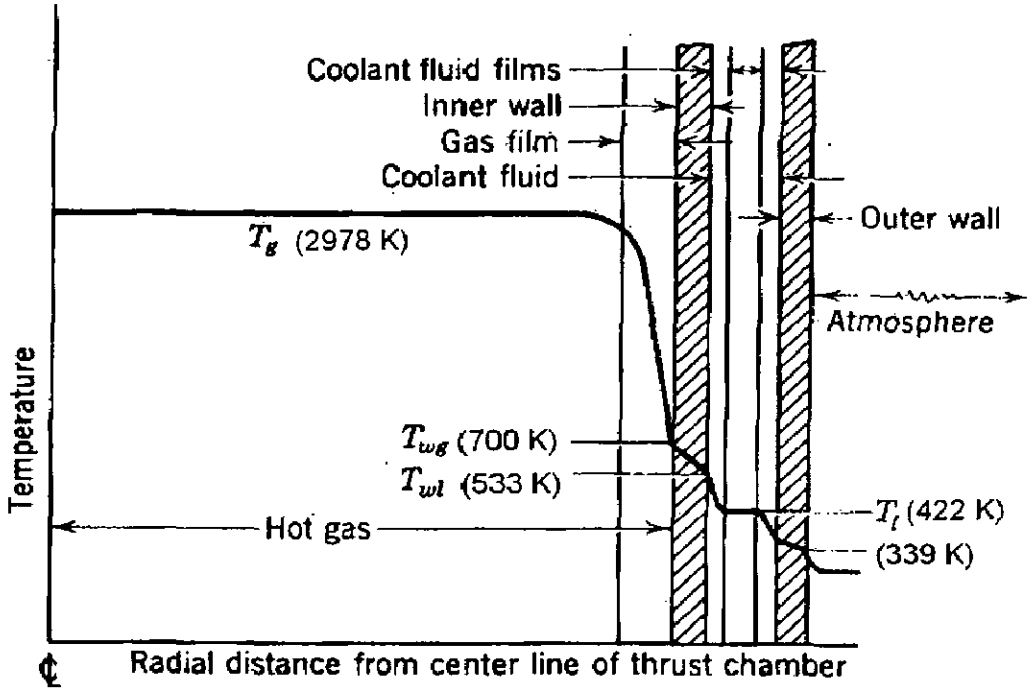

Fig. 3.6 Temperature gradients in rocket thrust chamber
(Values are typical) (Sutton, 1963)

The important quantities for controlling the heat transfer across a rocket chamber wall are fluid film boundaries established by the combustion products on one side of the wall and the coolant flow on the other. The gas film coefficient largely determines the numerical value of the heat transfer rate, and the liquid film largely determines the value of the wall temperatures.

3.5 Film cooling effectiveness (η)

In most film cooling applications the heat transfer from the hot gas to the surface to be protected is not zero. For a given main stream and allowable wall heat transfer the requirement may be to predict the secondary flow needed to maintain the surface temperature below some critical value.

The heat flux with film cooling would be,

$$Q/A = h\Delta T = h(T_w - T_{aw}) \tag{3.8}$$

The adiabatic wall temperature is not only a function of the geometry and the primary and secondary flow fields but also the temperatures of the two gas streams. To eliminate this temperature dependence a dimensionless adiabatic wall temperature, η, *called the film cooling effectiveness is used. For low speed, constant property flow, the* film cooling effectiveness is given by,

$$\eta = \frac{T_{aw} - T_\infty}{T_c - T_\infty}, \tag{3.9}$$

In general, $T_{aw} < T_\infty$ and $T_c < T_\infty$ in a film cooling application. The film cooling effectiveness usually varies from unity at the point of injection (where $T_{aw} = T_c$) to zero far down-stream where because of diffusion of the secondary flow, the adiabatic wall temperature approaches the free stream temperature (Goldstein).

3.6 Blowing ratio (M)

Blowing ratio refers to the ratio of mass fluxes (density x velocity) of the coolant to the hot gas fluid (main stream) and is given by

$$M = \frac{(\rho V)_c}{(\rho V)_\infty} \tag{4.0}$$

A low value of blowing ratio may result in inadequate cooling and a high value leads to an excessive loss in output power (as more working fluid is tapped out from the compressor). Hence optimization of the blowing ratio is essential for improving the efficiency of film cooling.

Chapter 4

EXPERIMENTAL SET UP AND MEASUREMENT PLAN

The experiments were carried out with hot air as the main-stream gas. Nitrogen gas is used as the coolant. The set-up comprises a hot gas generating unit, a feed back system, flow conditioner, a test section made of copper, an expander and an exhaust system. A schematic diagram of the experimental set-up is given in Fig. 4.1. The subsystems of the test rig are detailed below. The fabrication drawings of each component are given in Fig. 4 1A to 4.1I.

4.1 Flow system

The flow system shown in Fig. 4.2 was considered same for all experiments. It consisted of essentially three parts, viz. (i) a hot air source with a temperature range of 300 to 800 K, (ii) a test section and (iii) an exhaust system.

The air source consisted of a 10 kW blower which supplies air at a maximum pressure of 1.077 bar at a flow rate of 0.13 m^3/s. The atmospheric air from the blower is passed through an electric heater of 100 kW, which heats up the air to a free-stream temperature that can be set from 300 to 800 K. The temperature of the hot gas is controlled using a feedback loop with a temperature controller. It keeps the temperature constant at a particular value by switching on and off the various heater sections with the help of relay system. The maximum flow Reynolds number that can be obtained is of the order of $6x10^4$.

The flow conditioner consists of a flow straightener (Fig. 4.3) made of stainless steel of 1500 mm long. The hot air from the flow conditioner enters the test section chamber through a calming section. The flow duct made of stainless steel is circular in cross section with an inside diameter of 100 mm up to the coolant injector and the diameter has been changed accordingly to accommodate the coolant injection manifold with the test section.

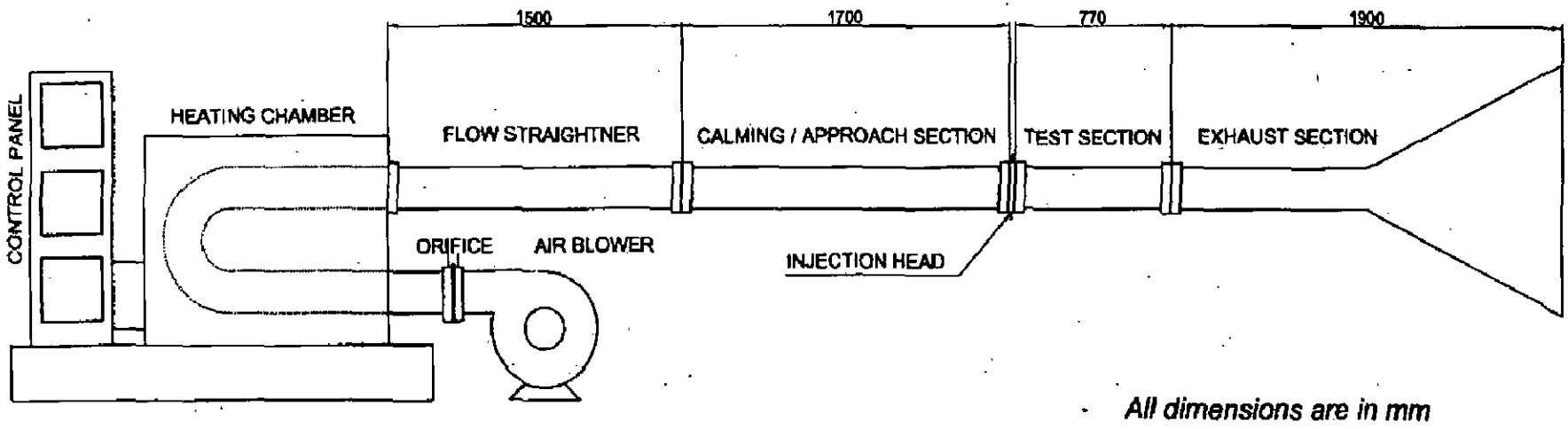

Fig. 4.1 Schematic of experimental set-up

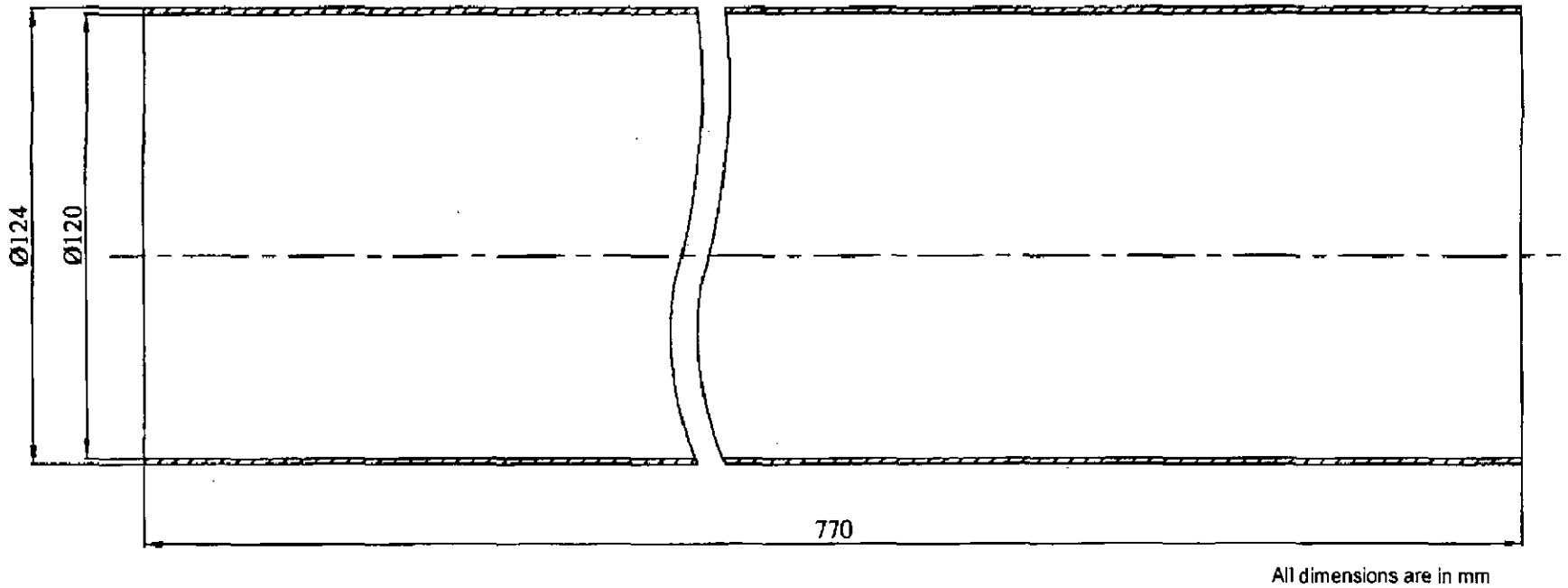

Fig. 4.1A Test section-Copper

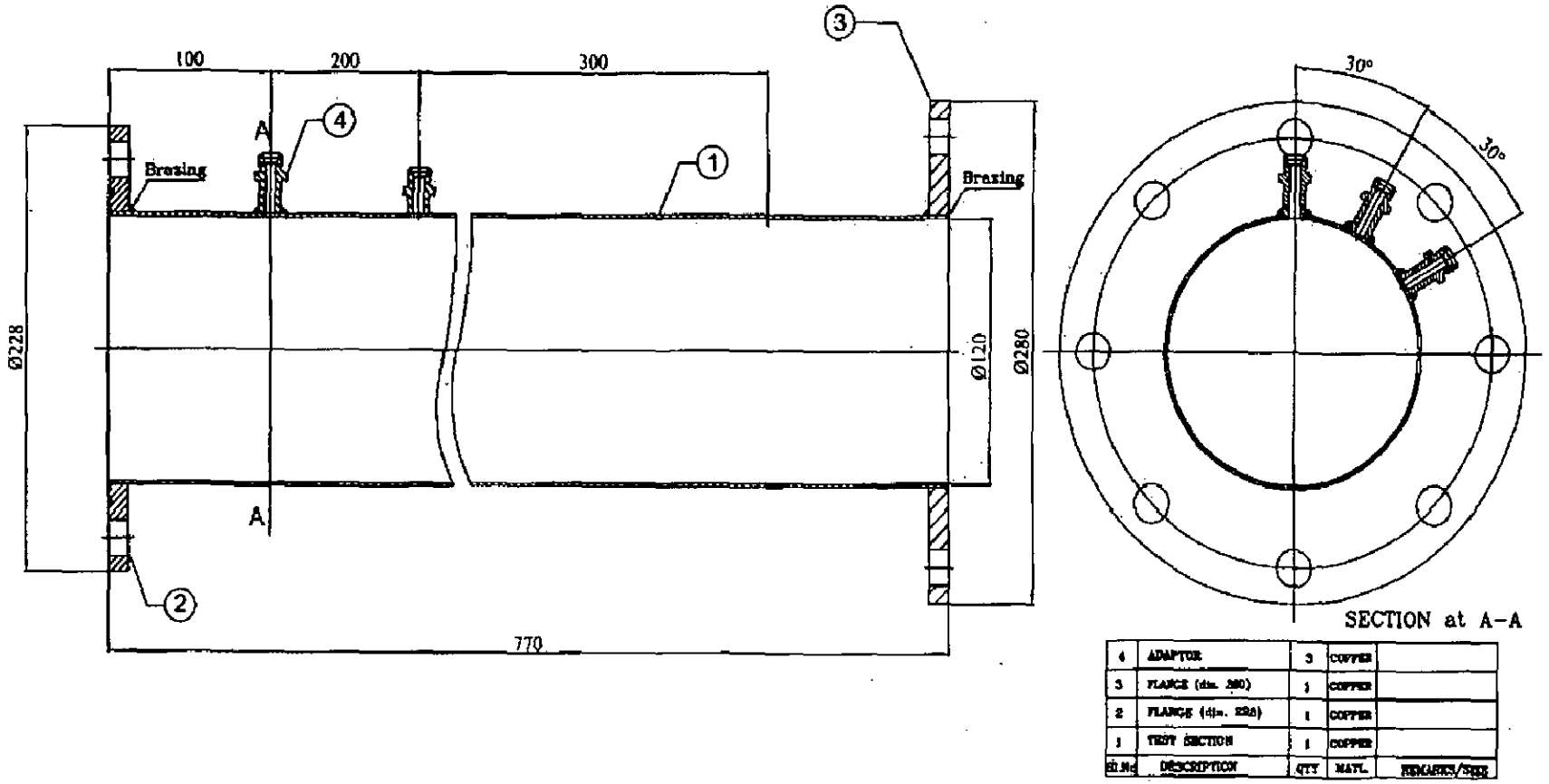

4	ADAPTOR	3	COPPER	
3	FLANGE (dia. 280)	1	COPPER	
2	FLANGE (dia. 228)	1	COPPER	
1	TEST SECTION	1	COPPER	
Sl.No	DESCRIPTION	QTY	MATL	REMARKS/SIZE

All dimensions are in mm

Fig. 4.1B Test section assembly

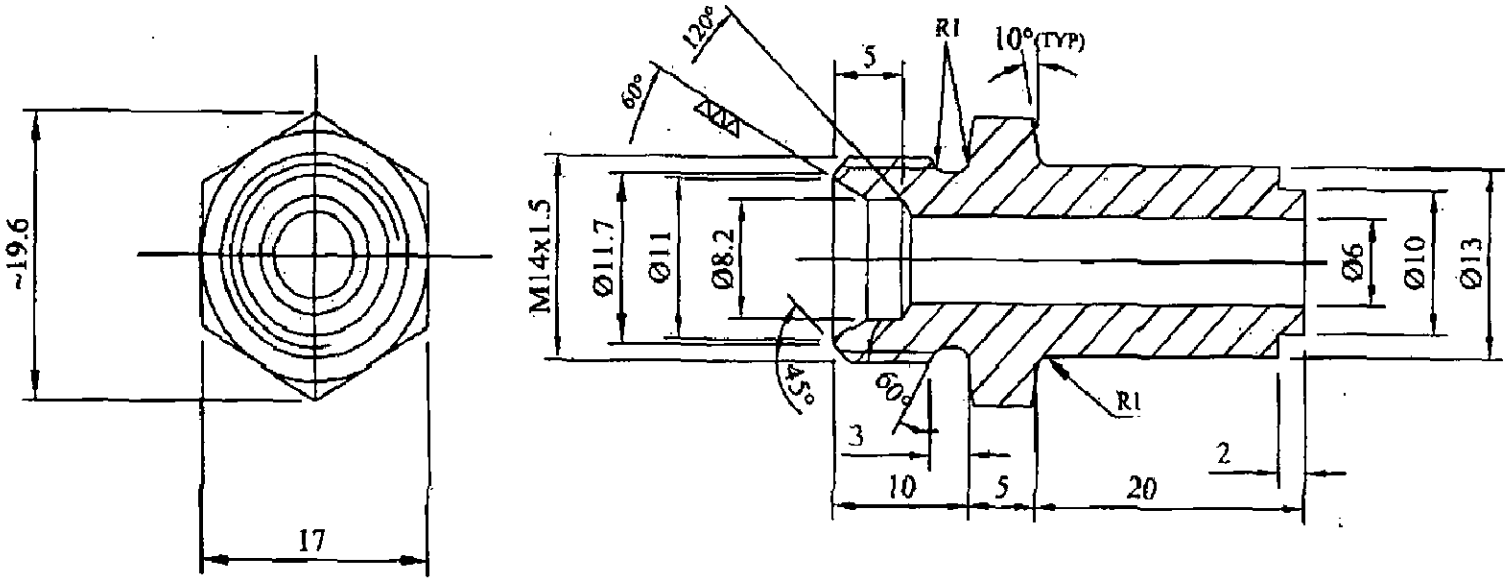

All dimensions are in mm

Fig. 4.1C Pressure adaptor of test section

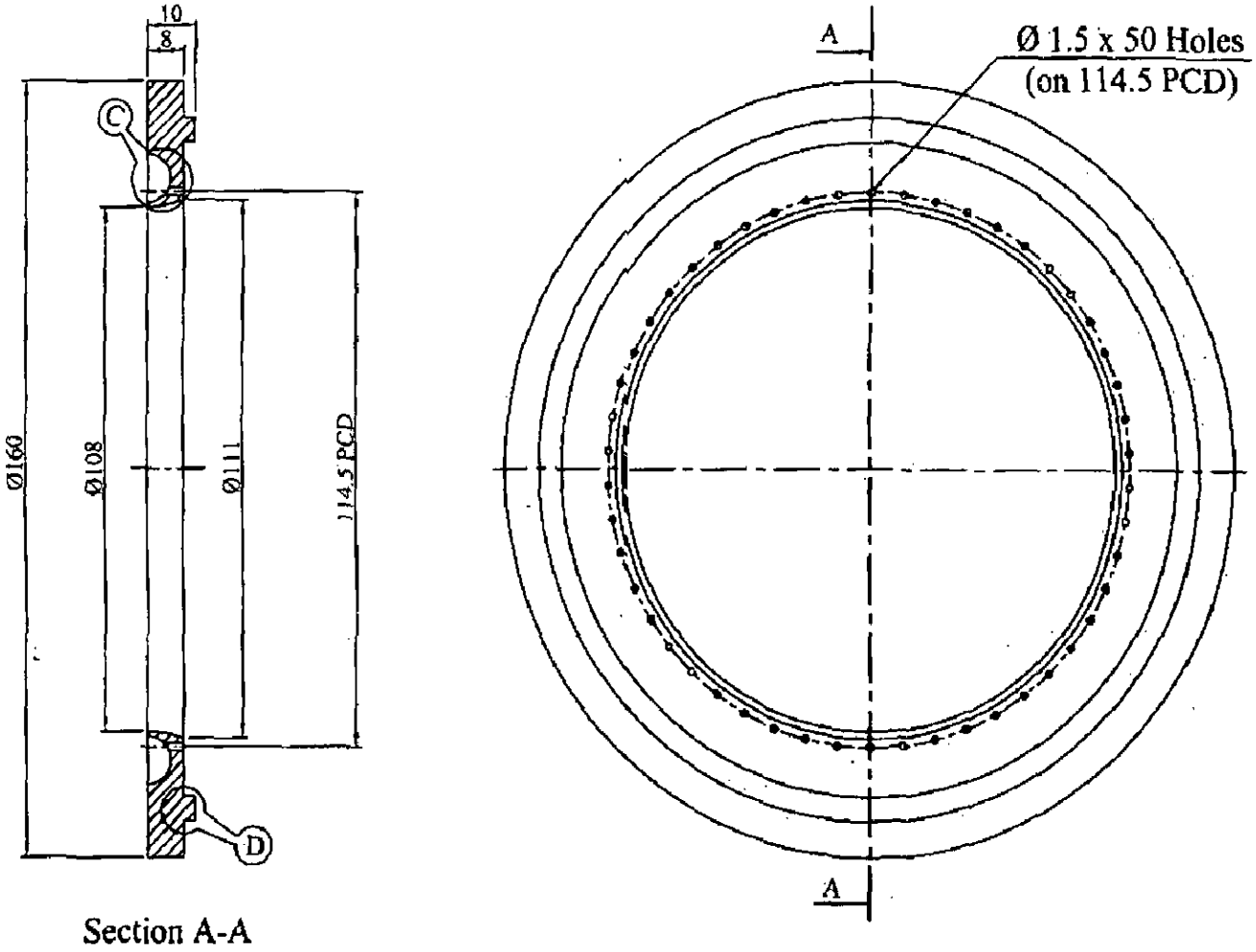

All dimensions are in mm

Fig. 4.1D Injector-straight orifice

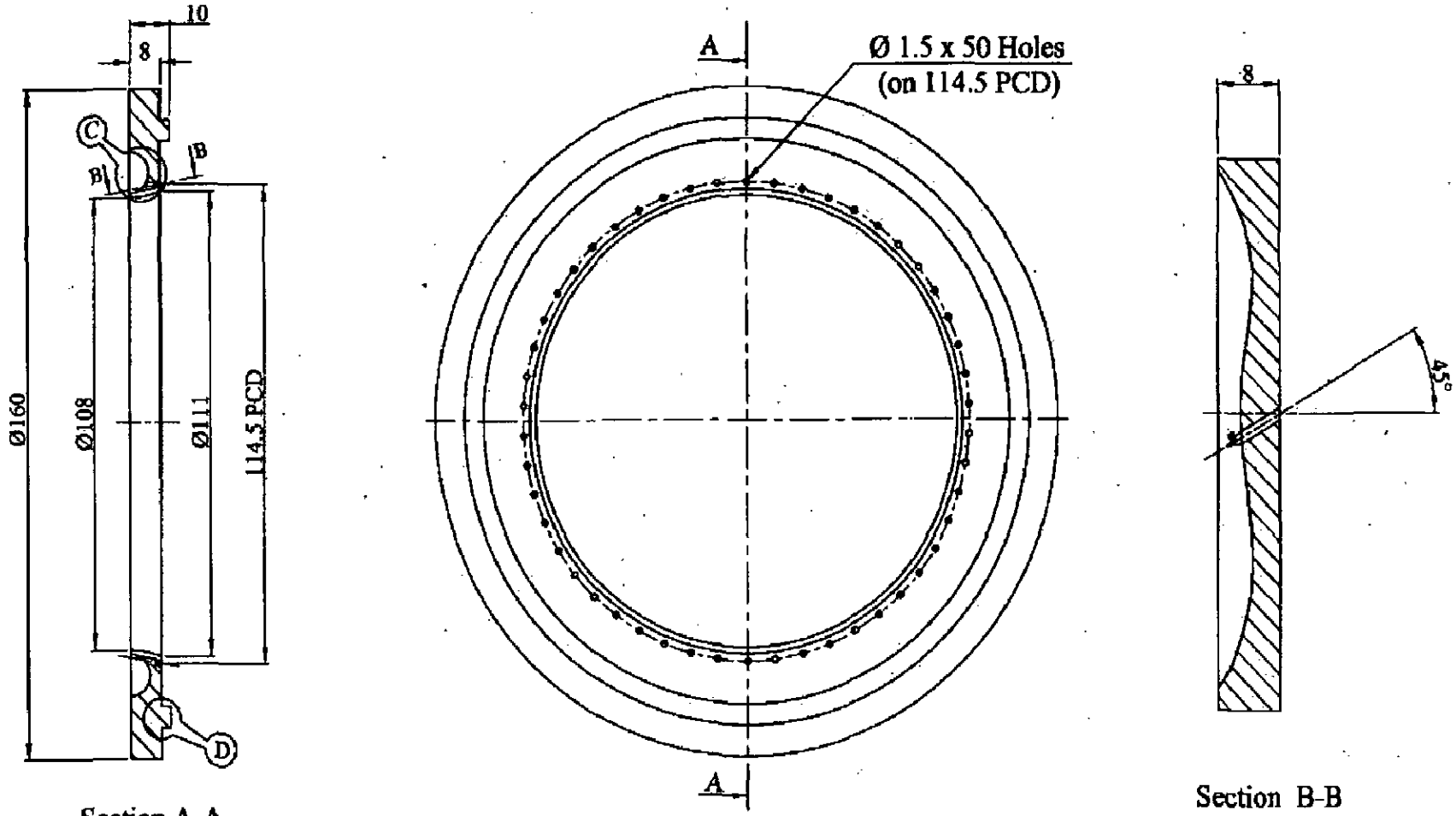

All dimensions are in mm

Fig. 4.1E Injector-Part I of 45° – 10°

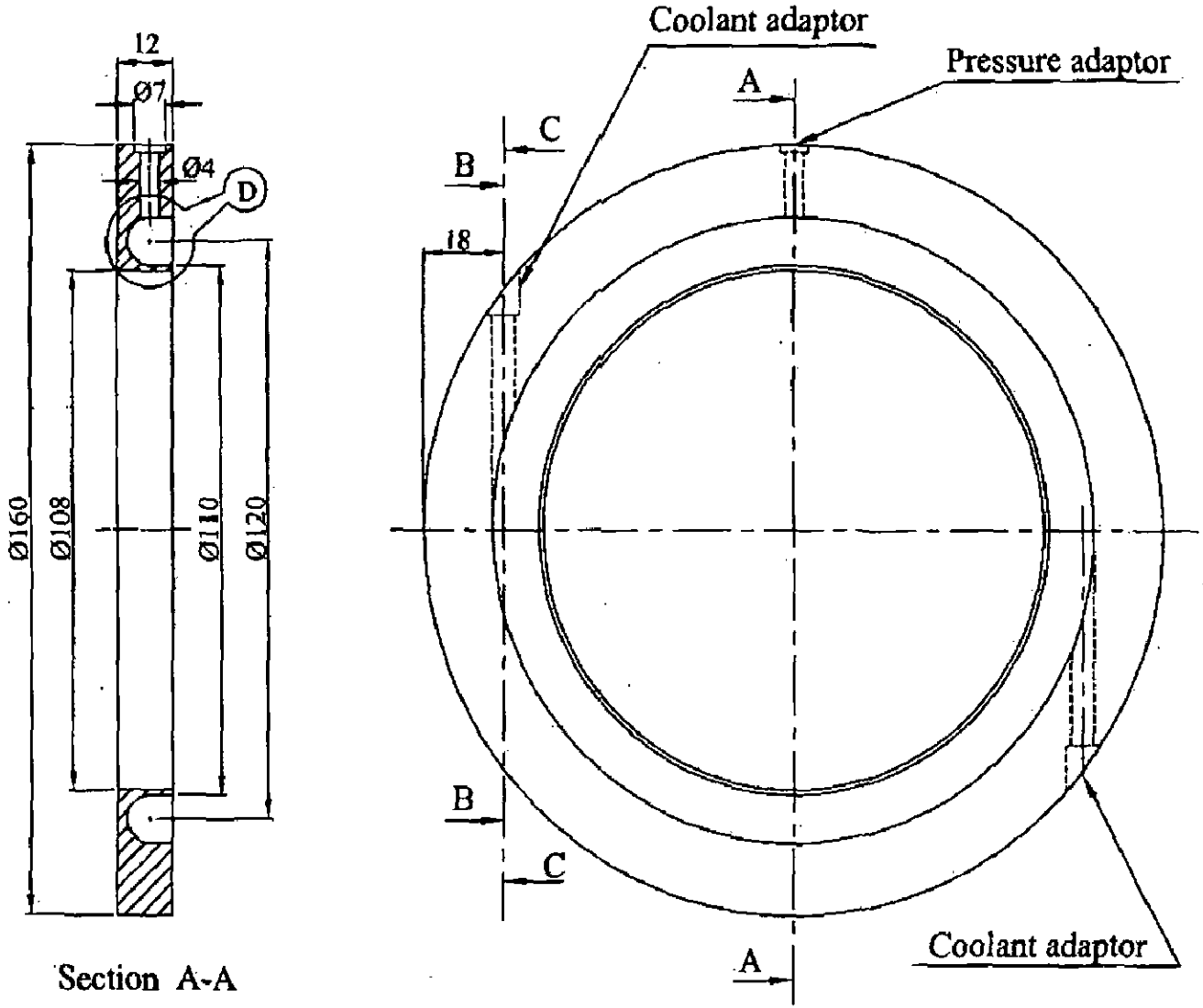

All dimensions are in mm

Fig. 4.1F Injector-Part II (Typical)

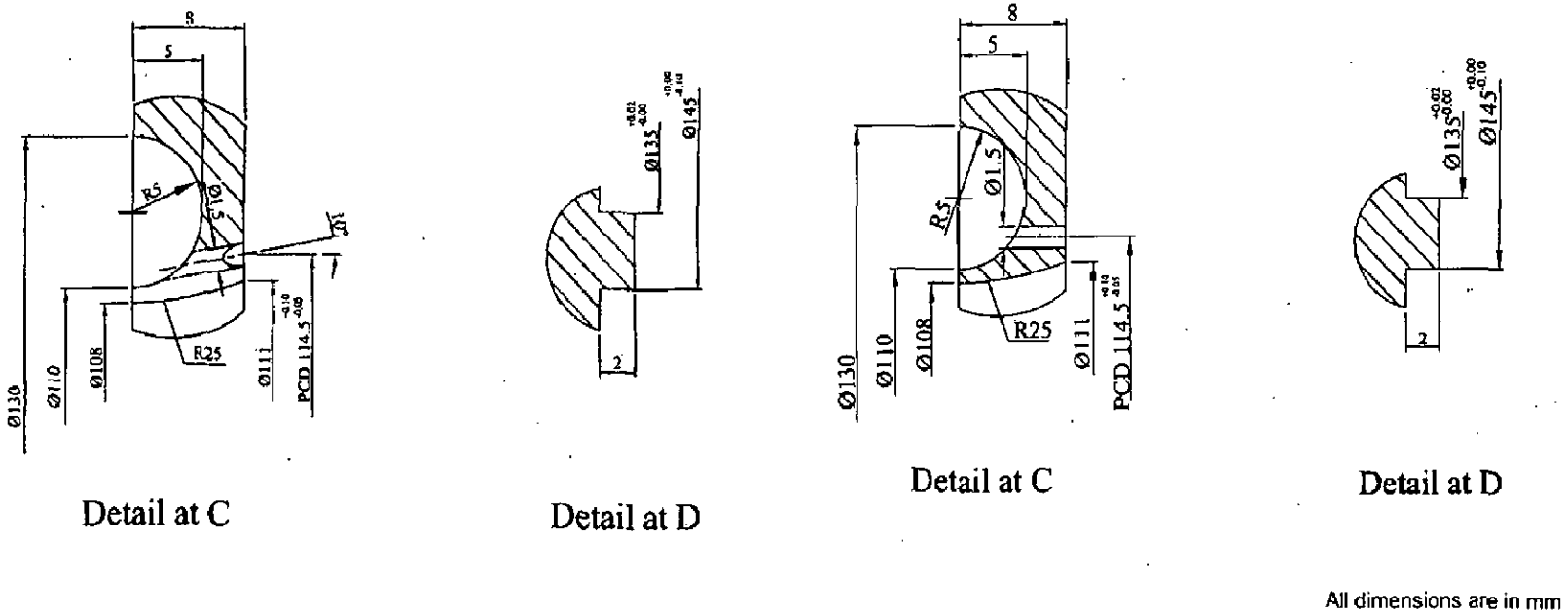

Fig. 4.1 G Details of Injector Orifices

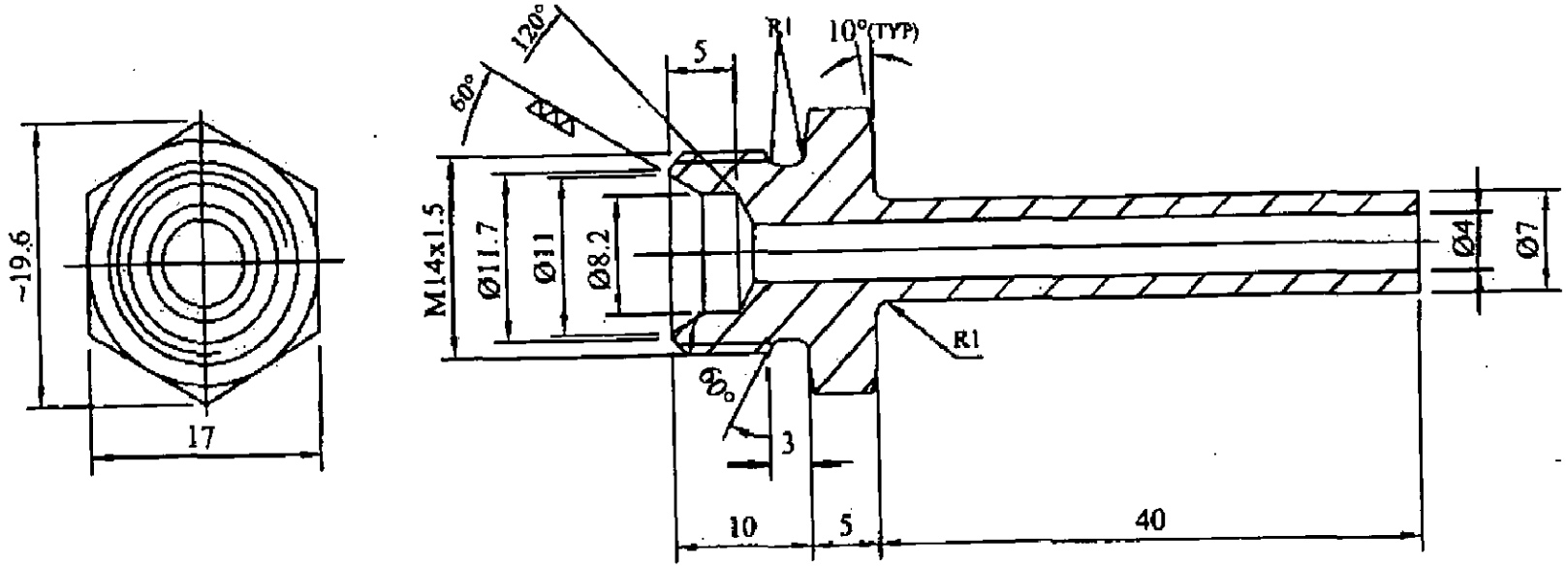

All dimensions are in mm

Fig. 4.1H Pressure adaptor of injector

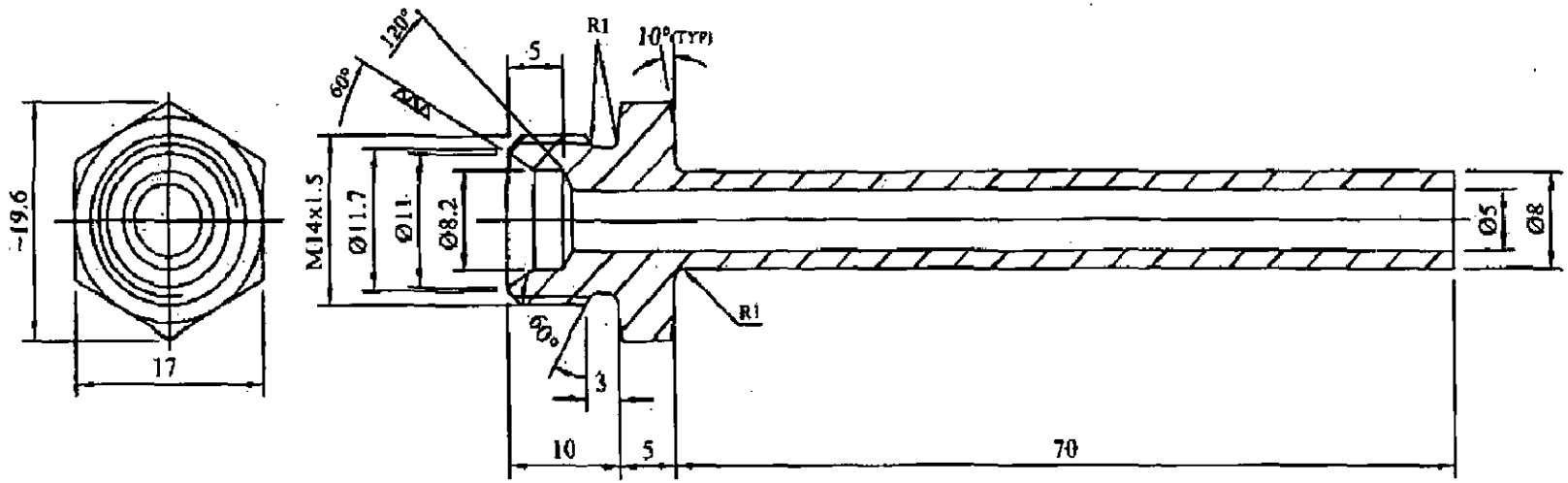

All dimensions are in mm

Fig. 4.1I Coolant adaptor of injector (2 no.)

4.6 Test matrix

Operating parameters considered for the experiments are given in the test matrices. Tables 4.1 listed the parameters used for the straight injection orifice configuration. The compound angle injection orifice configuration of 30°-10° is given in table 4.2 and table 4.3 details the parameters used for the compound angle injection orifice configuration of 45°-10°.

4.7 Test procedure

A few numbers of trial runs are done to identify the extent to which the furnace has to be heated to ensure a specific initial air temperature. Initially the temperature of the furnace is brought up to the desired temperature with the help of the control system attached with the heater in steps of 50 K from the room temperature. The control system keeps the temperature constant at the set value.

Once the furnace temperature for the desired value of gas temperature has stabilized, the blower is switched on and the ambient air allows entering the furnace and thereby the air gets heated. Simultaneously the nitrogen gas as the coolant is also allowed to pass through the coolant injector. When the flow and temperature conditions stabilized, as indicated by the constant readings in the monitoring temperature indicators, the main-stream hot gas and test section surface wall temperatures will be recorded for a particular mass flow rate of the coolant and main-stream. The digital manometer and rotameter readings were also may noted. The experiments were repeated for all the test section configurations for different blowing ratios.

4.8 Uncertainty in measurements

The major uncertainties in measurements are caused due to the inaccuracies in temperature and pressure measurements. Though the thermocouples are calibrated within $\pm$ 2 K accuracy, due to repeated thermal cycling, the temperature measurements are known within $\pm$ 2 K and the lowest temperature difference measured that is used for computing film cooling effectiveness is 30 K for nitrogen gas, this would formulate to an uncertainty of 6.6 %. The pressure uncertainty would account to less than 2 %. The combined uncertainty for the estimation of film cooling effectiveness with respect to blowing ratio would therefore be $(0.02^2 + 0.066^2)^{0.5} \approx 6.9\%$.

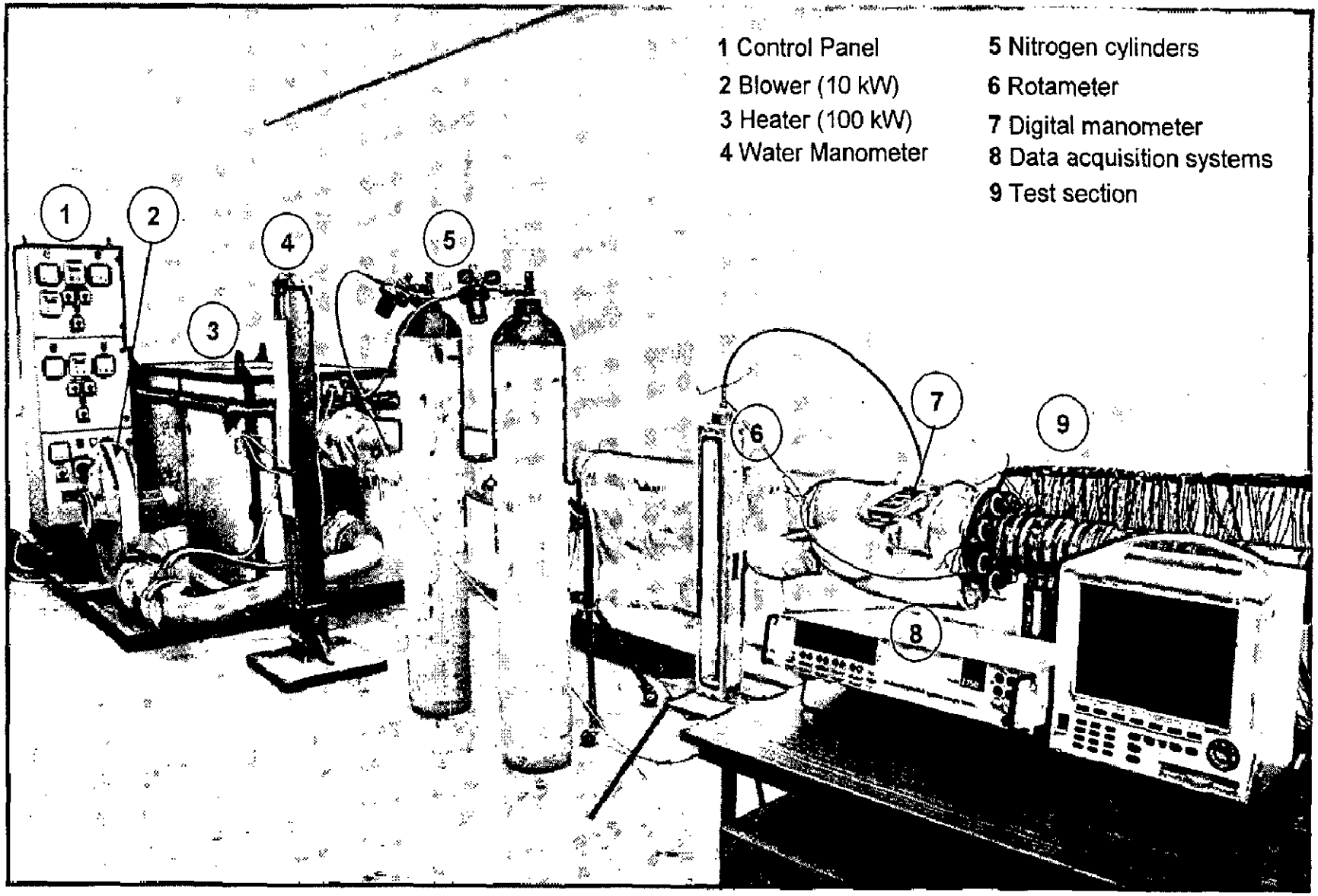

Fig.4.2 Photographic view of experimental set up

4.2 Coolant injection system

The coolant injection system consisted of nitrogen supply cylinder with pressure regulators, rotameter to measure the flow rate of coolant and coolant injector with an in-built coolant reservoir. Nitrogen gas is used as the coolant for all the cooling experiments. Nitrogen gas exits through the regulator at pressures of 1.4 to 2.3 bar. A rotameter, capable of measuring nitrogen gas flow up to 12 Nm^3/hr is used to measure the coolant flow rate. The injector is made of two parts, for easy fabrication and welded together. It consisted of an elliptical grove as a reservoir and orifices of 50 holes of 1.5 mm diameter were drilled, as in Fig. 4.4, from the reservoir groove with straight and compound angles of 30°-10° and 45°-10° to inject the coolant. Two adaptors were provided diametrically and tangentially opposite to supply the coolant to have a uniform flow and an even distribution throughout the injector orifices. The three different configurations of the injector orifices fabricated are shown in Fig. 4.5.

4.3 Test section chamber

The test section is a 120 mm inside diameter, 2 mm wall thick and 770 mm long rolled copper tube, which is instrumented with T-type thermocouples to measure the surface temperature as well as the free stream hot air temperature. Thermocouples are fitted circumferentially on the surface of the test section with an equal interval of 30 mm. along the length of the test section up to the length of 480 mm. as shown in Fig. 4.6. Six such rows of thermocouples are fixed circumferentially in an equal angular displacement of 60 degrees on the test section. Each of these thermocouples are welded to the test section using a discharge type welding set and then fastened tight with a non-conducting flexible strip as can be seen from the figure. There are three pressure tappings provided spaced 100 mm, 200 mm and 300 mm respectively at an equal angular displacement of 30° each along the length of the test section. The inside surface of the chamber was machined after welding, and polished for reducing some surface roughness and waviness.

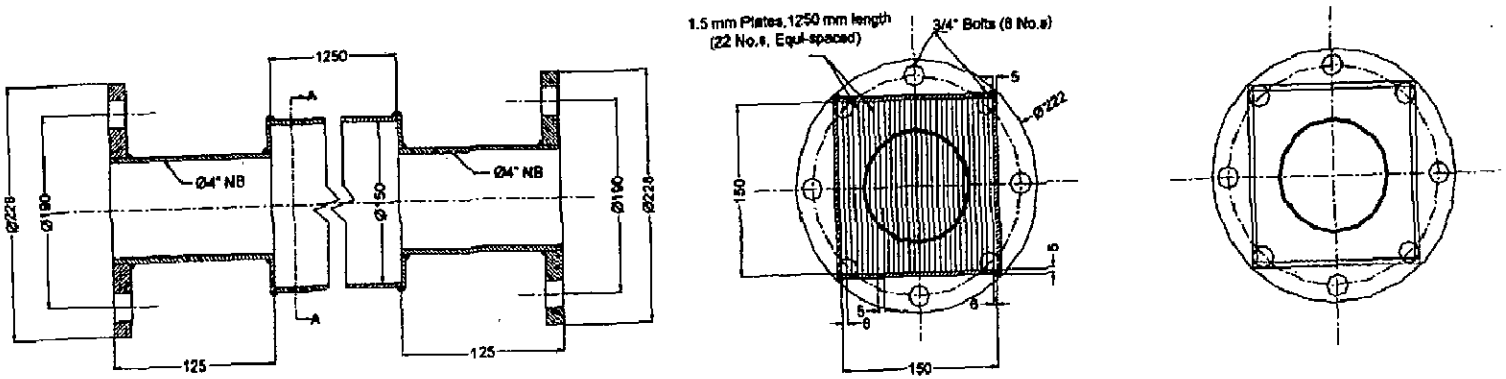

Flow Straightener

Section A-A

Chamber Wall Thickness:5mm

All Dimensions are in mm

Fig. 4.3 Flow straightener

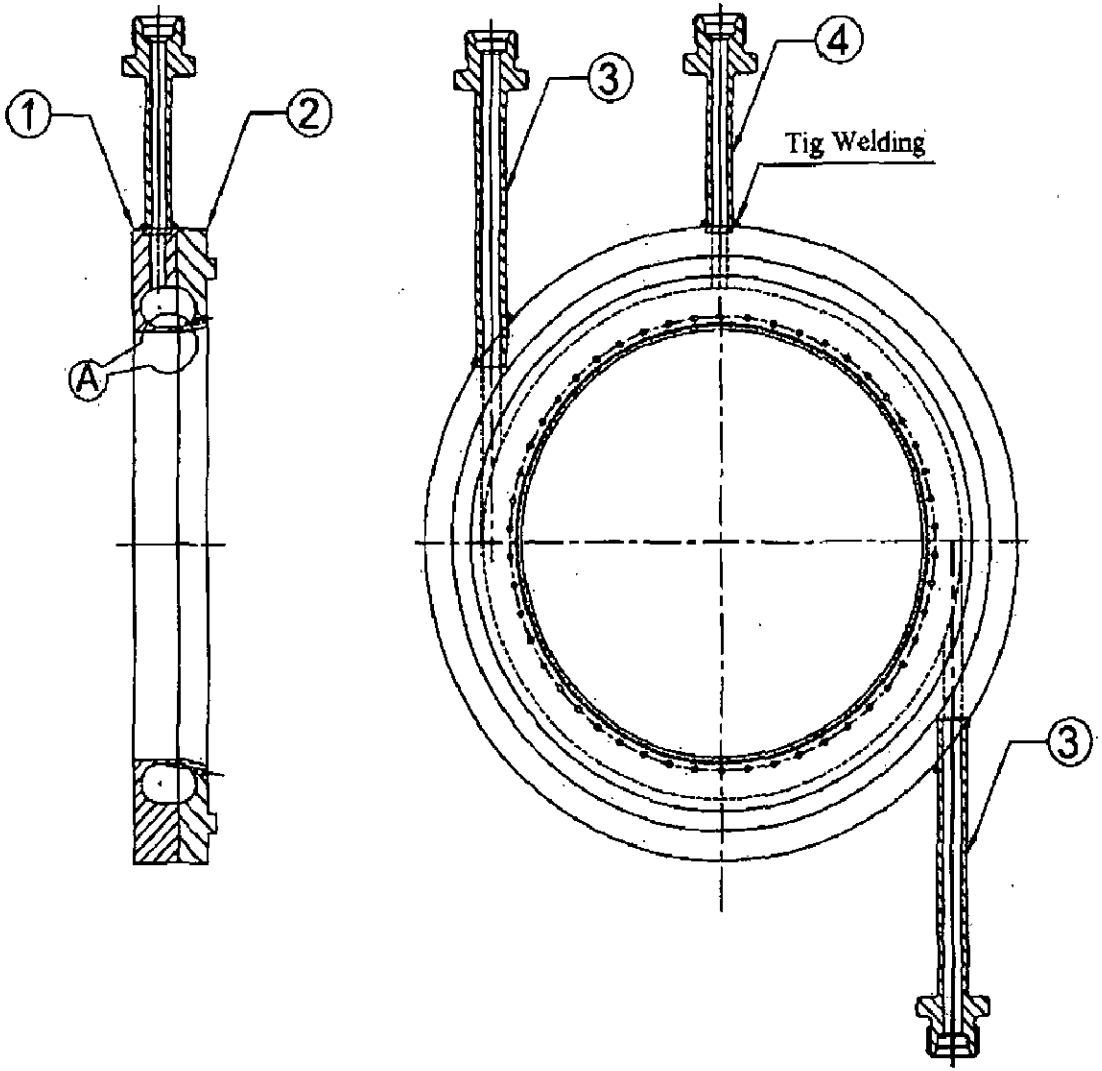

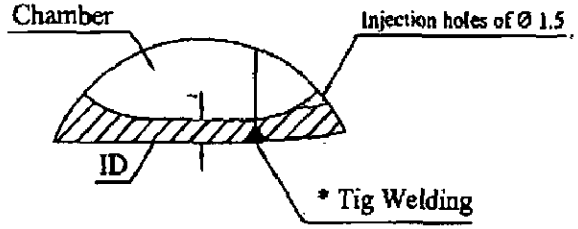

Detail at A

SL.No	DESCRIPTION	QTY	MATL.	REMARKS/SIZE
4	PRESSURE ADAPTOR	1	SS 304	
3	COOLANT ADAPTOR	2	SS 304	
2	INJECTOR PLATE (Part-2B)	1	SS 304	
1	INJECTOR PLATE (Part-1)	1	SS 304	

Fig. 4.4 Injection head assembly (Typical)

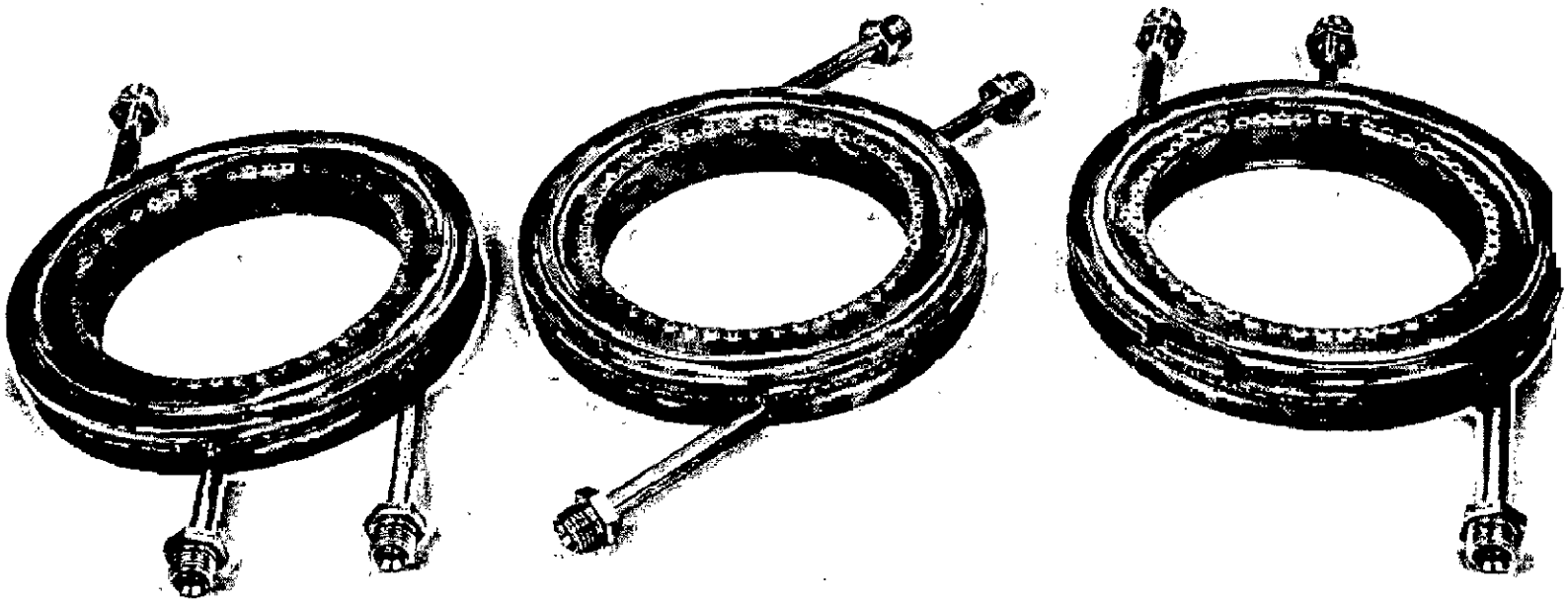

Straight orifices

Orifices with 30°-10°

Orifices with 45°-10°

Fig. 4.5 Photographic view of Injectors

4.4 Film coolant

Nitrogen gas at NTP is used as the coolant for all the experiments carried out. High pressure nitrogen cylinders were connected in parallel for long duration tests. The nitrogen flow is regulated using inline pressure regulator within the desired range.

4.5 Instrumentation

Flow rates of main-stream hot air and the coolant gas, temperature measurements of main-stream hot air, coolant, and the surface temperatures on the circumference of the test section are the primary measurements made throughout the experiments.

4.5.1 Flow rate

Hot air flow was measured for two main-stream flow rates by means of an orifice and a U-tube water manometer. The flow was controlled by adjusting the flow valve fixed on the pipeline from the blower to the heater. Coolant flows were measured by means of a rotameter, which is capable of measuring up to 12 Nm^3/hr.

4.5.2 Pressure

The static pressure of the main-stream hot air is measured during the experiments at 100 mm downstream with the use of U-tube water manometer. This measurement is used to determine the appropriate air densities and velocities at this position. A digital manometer is used to measure the pressure of coolant gas at the injector manifold.

4.5.3 Temperature

Temperatures of main-stream flow, the coolant and the surfaces of the test section are one of the primary measurements in the experiment. Apart from these, a measurement panel board arrangement with a temperature controller is attached with the heater system to measure the inside furnace temperature. This panel board will work as a feedback loop to vary the main-stream temperature. K-type sheathed thermocouples are used to measure the temperature inside the furnace, where nichrome heater coils are provided.

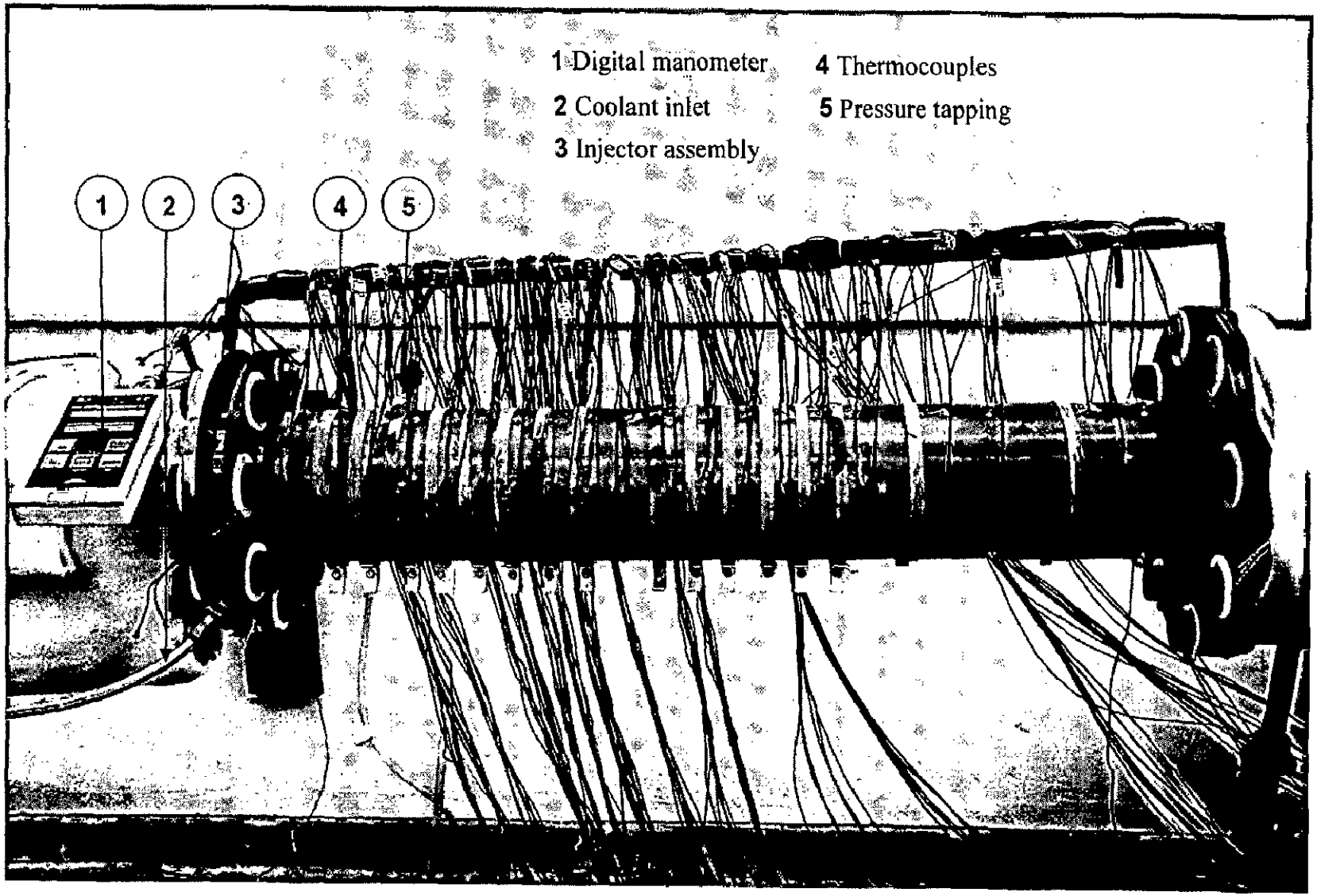

Fig. 4.6 Photographic view of injector and test section with thermocouples

The surface temperatures of the test section were measured by means of T-type thermocouples. The positions of the thermocouples on the test section are arranged in such a way that the temperature variation of wall is measured circumferentially and axially as shown in Fig. 4.6 and 4.7. A total of 96 thermocouples are located on the test section circumferentially and one thermocouple is inserted into the cylinder by ensuring it measures the inside main-stream hot air temperature at its centre.

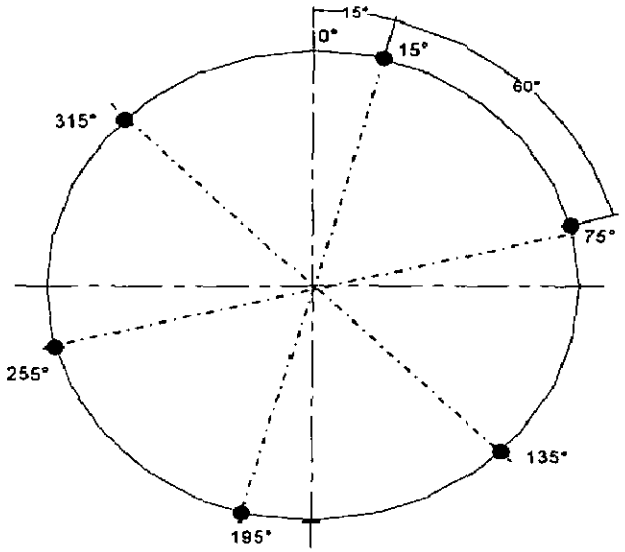

Fig. 4.7 Thermocouple positions on the test section

The thermocouples are fixed on the outer surface of the test section circumferentially and axially along the length till 480 mm at an equal interval of 30 mm in the horizontal direction. The T-type thermocouple is made with copper and constantan wires. The beads of all the T-type thermocouples are prepared with the help of a discharge type thermocouple welding unit. After making the beads they are calibrated using a microprocessor controlled dual temperature dry block calibrator with an operating range of 40 to 700° C. All the T-type thermocouples used to measure the surface temperature are welded on the test section and held firm with the help of non-conducting bands to ensure they are firmly fixed. The other ends of the thermocouples are fed into FLUKE digital multimeter (capable of measuring 20 channels), Yokogawa make mobile coder (for 30 channels) and Keithley multimeter model 2750 (capable of measuring 60 channels). The complete data acquisition system is shown in Fig. 4.8.

4.6 Test matrix

Operating parameters considered for the experiments are given in the test matrices. Tables 4.1 listed the parameters used for the straight injection orifice configuration. The compound angle injection orifice configuration of 30^{o}-10^{o} is given in table 4.2 and table 4.3 details the parameters used for the compound angle injection orifice configuration of 45^{o}-10^{o}.

4.7 Test procedure

A few numbers of trial runs are done to identify the extent to which the furnace has to be heated to ensure a specific initial air temperature. Initially the temperature of the furnace is brought up to the desired temperature with the help of the control system attached with the heater in steps of 50 K from the room temperature. The control system keeps the temperature constant at the set value.

Once the furnace temperature for the desired value of gas temperature has stabilized, the blower is switched on and the ambient air allows entering the furnace and thereby the air gets heated. Simultaneously the nitrogen gas as the coolant is also allowed to pass through the coolant injector. When the flow and temperature conditions stabilized, as indicated by the constant readings in the monitoring temperature indicators, the main-stream hot gas and test section surface wall temperatures will be recorded for a particular mass flow rate of the coolant and main-stream. The digital manometer and rotameter readings were also may noted. The experiments were repeated for all the test section configurations for different blowing ratios.

4.8 Uncertainty in measurements

The major uncertainties in measurements are caused due to the inaccuracies in temperature and pressure measurements. Though the thermocouples are calibrated within $\pm$ 2 K accuracy, due to repeated thermal cycling, the temperature measurements are known within $\pm$ 2 K and the lowest temperature difference measured that is used for computing film cooling effectiveness is 30 K for nitrogen gas, this would formulate to an uncertainty of 6.6 %. The pressure uncertainty would account to less than 2 %. The combined uncertainty for the estimation of film cooling effectiveness with respect to blowing ratio would therefore be $(0.02^2 + 0.066^2)^{0.5} = 6.9\%$.

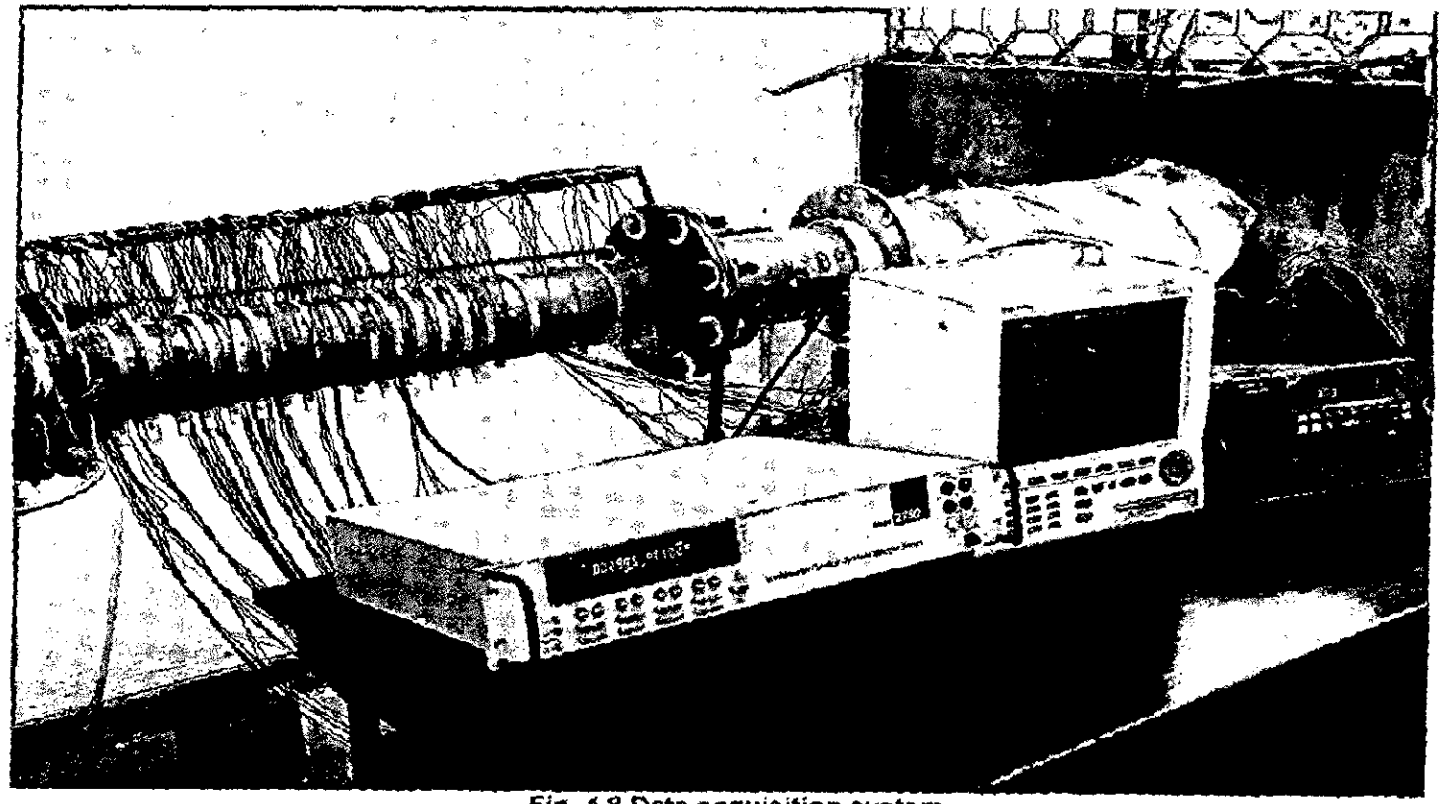

Fig. 4.8 Data acquisition system

Table 4.1 Matrix for straight injector orifice

Injector	Hot gas		Matrix No.	Coolant flow rate (N_2 gas) q_c (Nm^3/s)	Blowing Ratio (M)
	Temperature T_∞ (K)	Flow rate q_∞ (Nm^3/s)			
Straight ϕ1.5 x 50, 114.5 PCD	343 K	0.13	1	0.0028	2.4
			2	0.0021	1.8
		0.094	3	0.0028	3.4
			4	0.0021	2.5
	397 K	0.13	5	0.0028	2.8
			6	0.0021	2.1
		0.094	7	0.0028	3.9
			8	0.0021	2.9

Table 4.2 Matrix for compound angle injector orifice of 30°-10°

Injector	Hot gas		Matrix No.	Coolant flow rate (N_2 gas) q_c (Nm^3/s)	Blowing Ratio (M)
	Temperature T_∞ (K)	Flow rate q_∞ (Nm^3/s)			
Compound angle, 30^0-10^0, ϕ1.5 x 50 114.5 PCD	343 K	0.13	9	0.0028	2.4
			10	0.0021	1.8
		0.094	11	0.0028	3.4
			12	0.0021	2.5
	397 K	0.13	13	0.0028	2.8
			14	0.0021	2.1
		0.094	15	0.0028	3.9
			16	0.0021	2.9

Table 4.3 Matrix for compound angle injector orifice of 45°-10°

Injector	Hot gas		Matrix No.	Coolant flow rate (N_2 gas) q_c (Nm^3/s)	Blowing Ratio (M)
	Temperature T_∞ (K)	Flow rate q_∞ (Nm^3/s)			
Compound angle, 45^0-10^0, ϕ1.5 x 50 114.5 PCD	343 K	0.13	17	0.0028	2.4
			18	0.0021	1.8
		0.094	19	0.0028	3.4
			20	0.0021	2.5
	397 K	0.13	21	0.0028	2.8
			22	0.0021	2.1
		0.094	23	0.0028	3.9
			24	0.0021	2.9

Chapter 5

RESULTS AND DISCUSSIONS

As discussed earlier, three different coolant injection geometries were considered for the experiments, viz., one with a straight coolant injection and the other two with compound injection angles of 30^o and 45^o with an azimuth of 10^o. The experiments were conducted for main-stream hot gas entry temperatures of 343 and 397 K for each configuration of the coolant injection. Eight sets of blowing ratios were applied by varying the main-stream and coolant flow rates. Two flow rates of main-stream hot air, viz., 0.094 and 0.13 Nm^3/s and two flow rates of coolant, viz., 0.0021 and 0.0028 Nm^3/s were considered in this experimental investigation.

Initial experiments were conducted with hot air passing through the test section chamber to obtain the surface wall temperature of the test section in the absence of coolant gas for two different main-stream hot gas flow rates.

Prior to analyzing the data for film cooled length and effectiveness, an effort was made to determine the temperature uniformity around the test section without coolant. It is essential to identify the extent of film coolant wall adherence during film cooling experiments. Temperature uniformity for main stream hot air without coolant for two flow rates at a particular axial distance of 0.12 m and 0.06 m around 360° periphery of the test section is shown in Fig. 5.1. It shows a good agreement of within 1 K for hot air of 343 K at particular axial locations. For hot air of 397 K it is within 2 K and showed a higher non-uniformity as in Fig. 5.2.

The variations of temperature along the length of the test section with nitrogen gas coolant are presented in Fig. 5.3 to 5.10 for eight sets of blowing ratios for the three injector configurations. A comparison is made in all these figures with that of a case without the application of coolant. The temperature of the main stream hot air is almost constant over the test section length of 0.48 m. When film cooling is introduced, the wall temperature near to the coolant injection decreases as a film of coolant protects the wall from the hot air and the coolant mixes with main stream hot air in the downstream, thereby increasing the temperature on the surface of the test section.

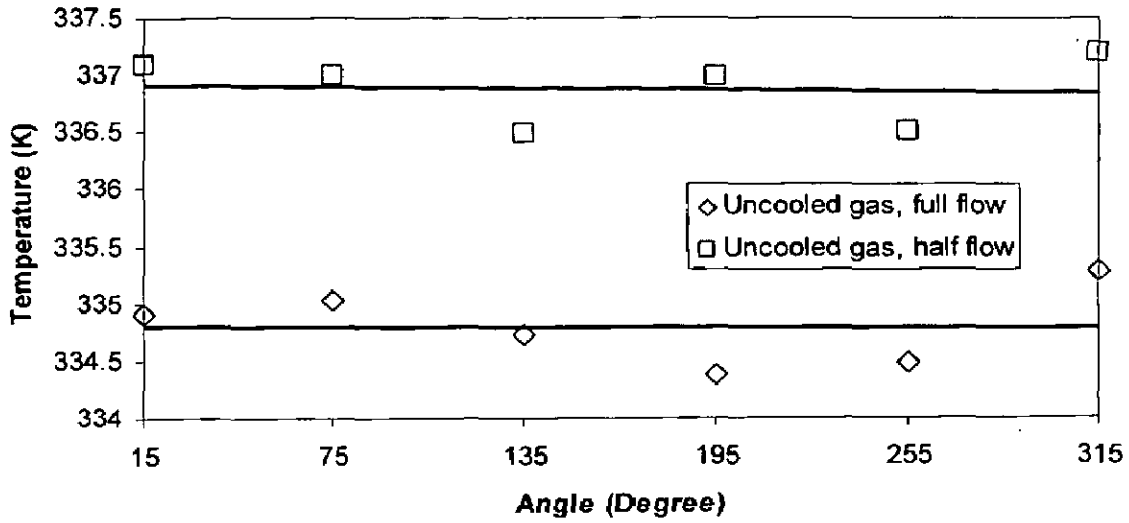

Fig. 5.1 Temperature distribution on the test section circumference (T_∞=343 K)

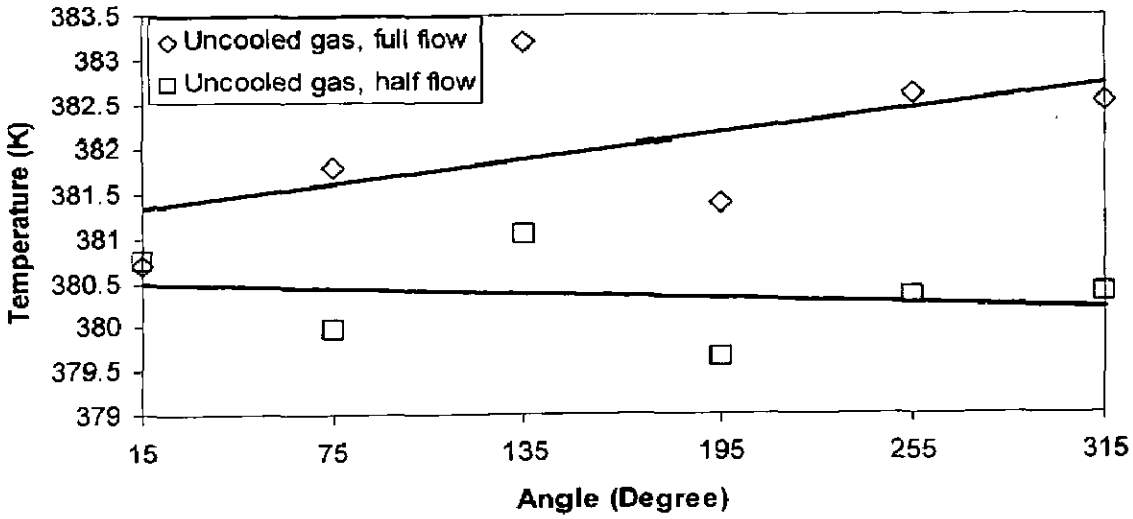

Fig. 5.2 Temperature distribution on the test section circumference (T_∞=397 K)

The temperature drop across all the sets of measurements made is higher as can be seen from Fig. 5.3 to 5.10 for the case of injector configuration of 30°-10° compared to the straight and 45°-10° configurations. It may however be noted that although these differences are not very significant they are not negligible. It is also important to note that in some cases the drop is significant as can be seen from Fig. 5.8, where a 30°-10° injector configuration brings about 5 K drop. These drop in

temperature are will be multiplied many fold while using a lower coolant injection temperature. The film cooled length is defined as the length of test section which is thermally influenced by film coolant. The extent of film cooled length for a range of operating parameters for the three coolant injection configuration is represented in Fig. 5.11 to 5.13. The changes in film cooled length with core gas temperature shows that the effective film cooled length to decrease with temperature of the core gas irrespective of the type of coolant injection configurations. This is to be anticipated as higher temperature leads stronger heat transfer across the film and the film itself gets heated up at an early phase reducing its effectiveness as a film. It may be noticed that small changes in blowing ratio (M) is caused by the core gas temperature due to the density of the coolant. The length of the film cooling influence is comparatively lesser for the compound angle injection configurations compared to that of straight. This attributed to the higher axial velocity component in the straight orifices and the film moves axially over a longer distance. Due to the significant angular component present in compound angle injector orifice, the film travels a lesser distance due to reduced effective angular momentum of the coolant jet. At high impingement angles, the film does not stick to the wall and may disintegrate leading to increased wall temperature shown in Fig. 5.3 to 5.10. The variation of film cooled length with blowing ratio is given in Fig. 5.14. The film cooled length is increasing with blowing ratio for both of the main stream temperatures. However, the film cooled length tends to reduces with higher mainstream temperature. Therefore the higher blowing ratio is good to increase the film cooled length.

The experiments were repeated for different blowing ratios and the results were summarized in a tabular form. The film cooled length is deduced from the Fig. 5.3 to 5.10 by which the points where the film temperature reaches the saturation and decomposition temperature. The film cooled length for the entire range of blowing ratios considered is presented in Table 5.1. Reducing the core gas flow increased the film-cooled length in all the three configurations. However, a considerable change in the temperature difference with respect to the different core gas flow rates was not noticed.

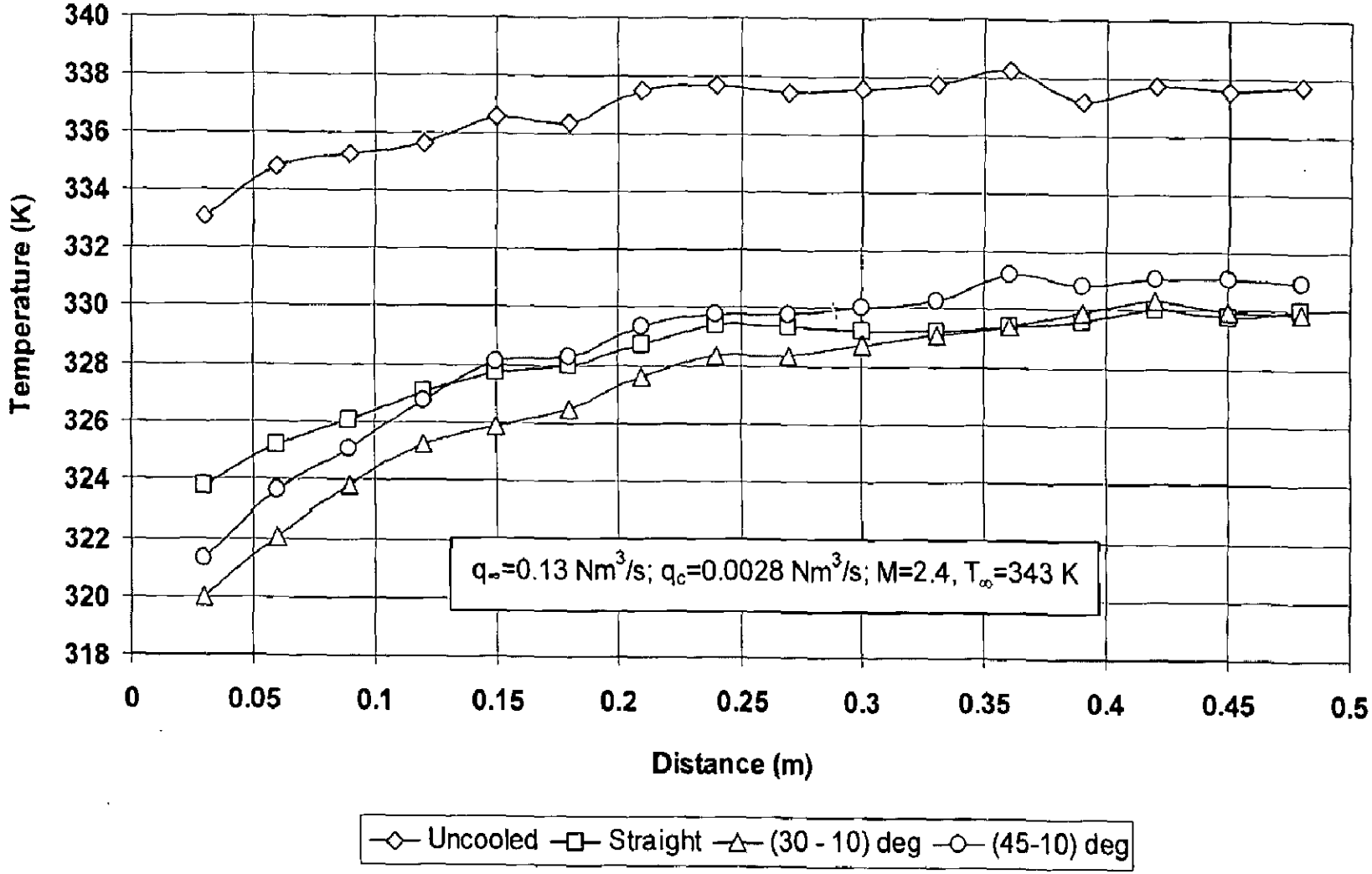

Fig. 5.3 Temperature profile for M = 2.4

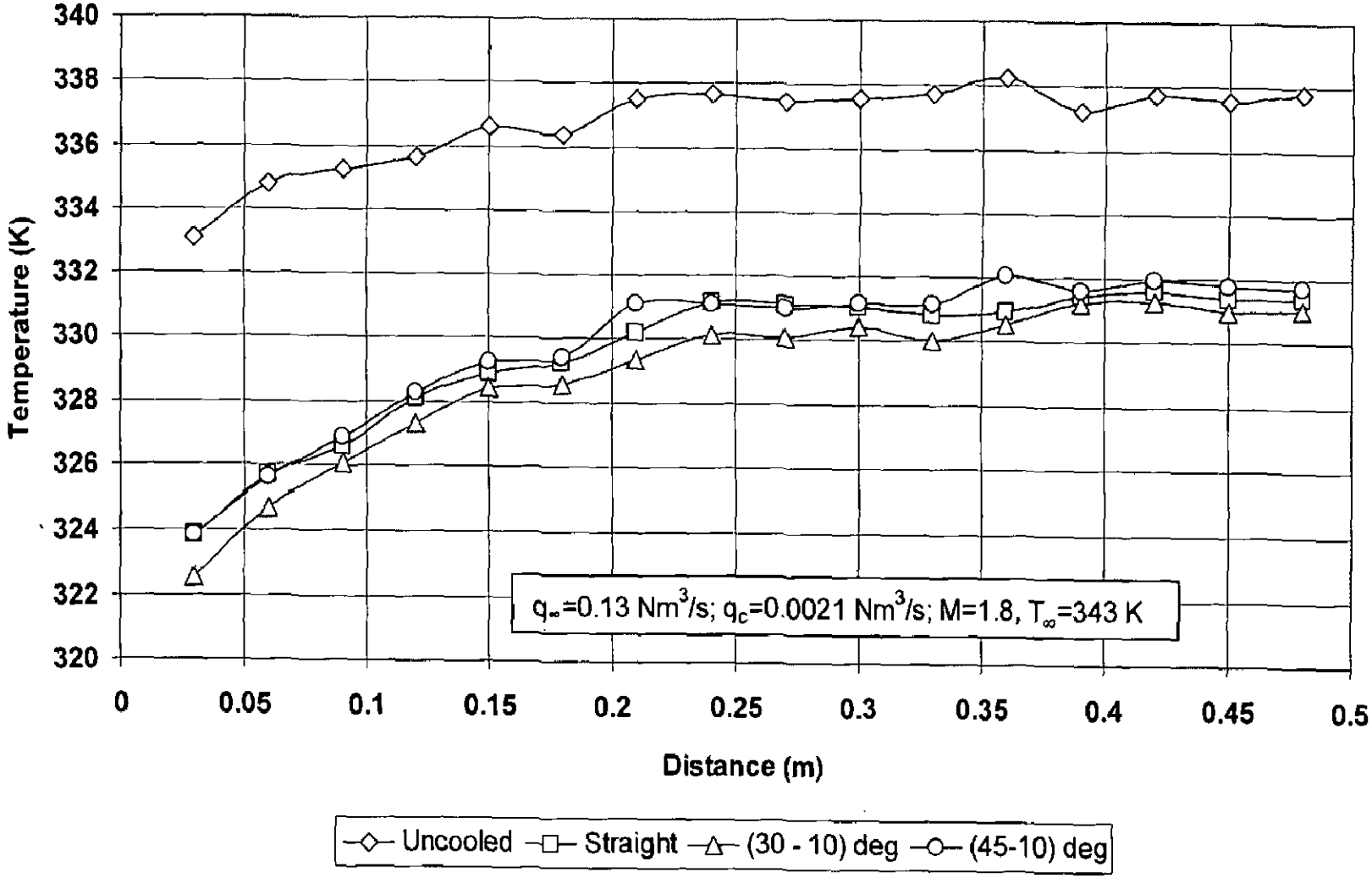

Fig. 5.4 Temperature profile for M = 1.8

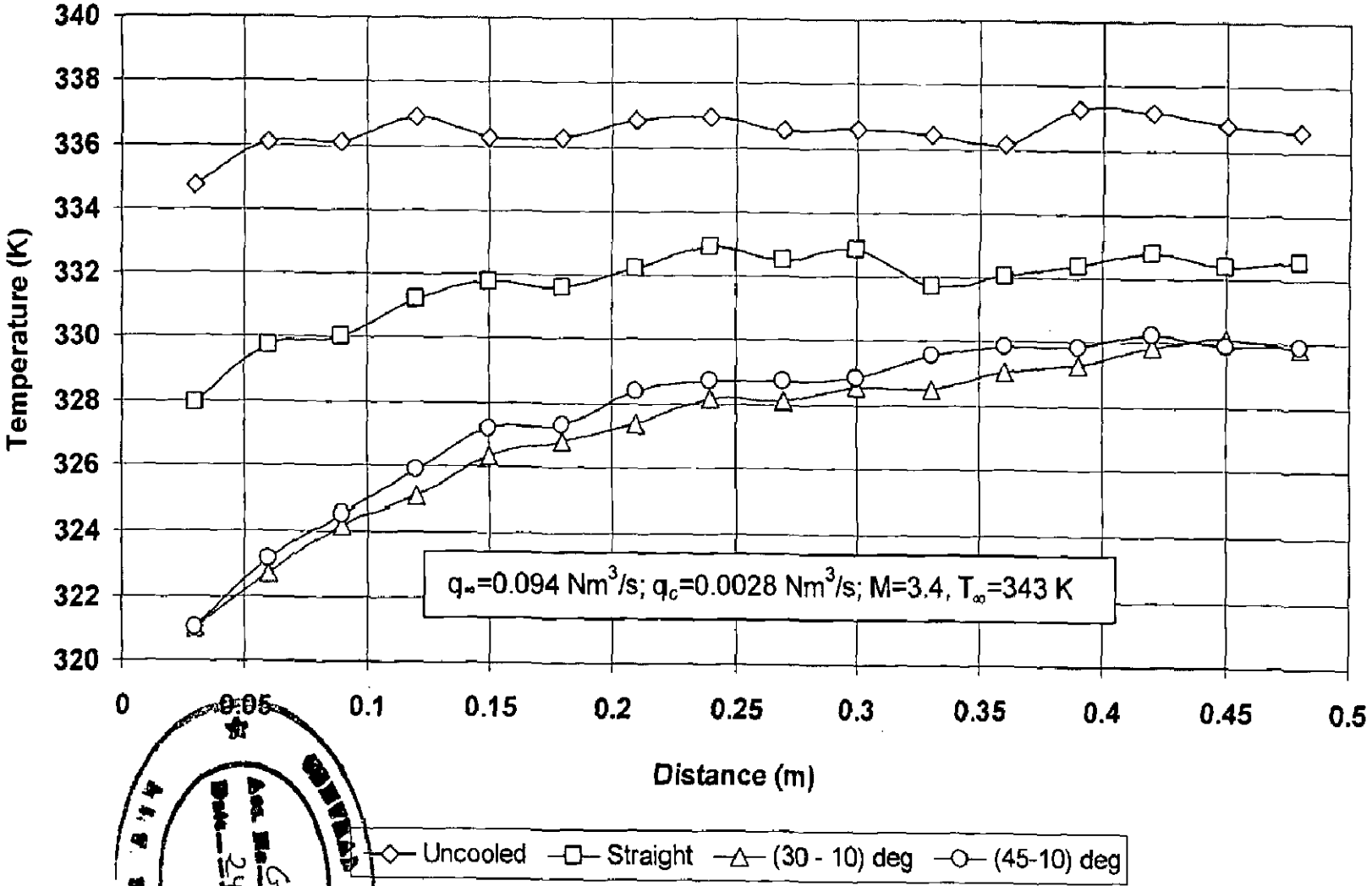

Fig. 5.5 Temperature profile for M = 3.4

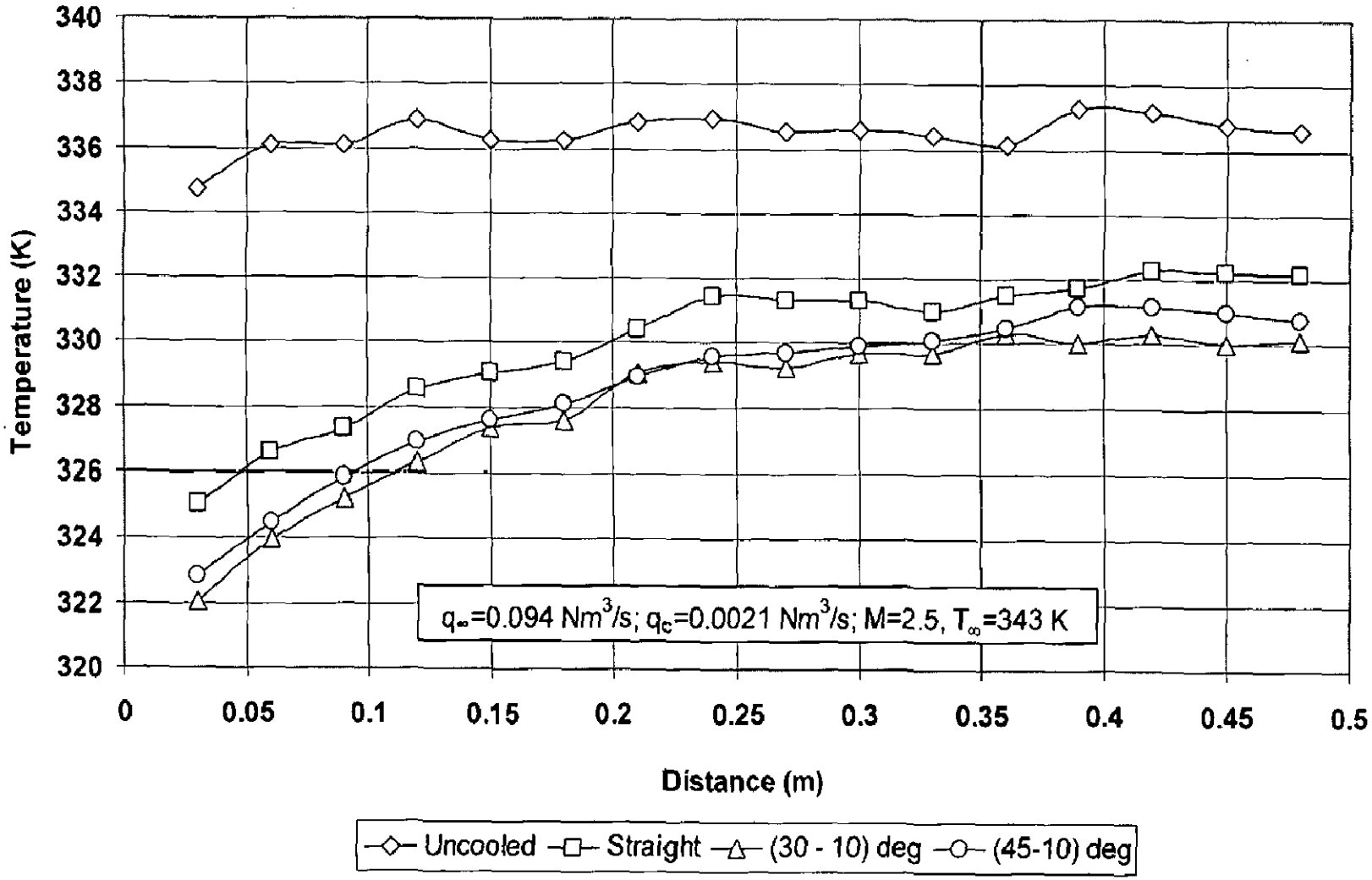

Fig. 5.6 Temperature profile for M = 2.5

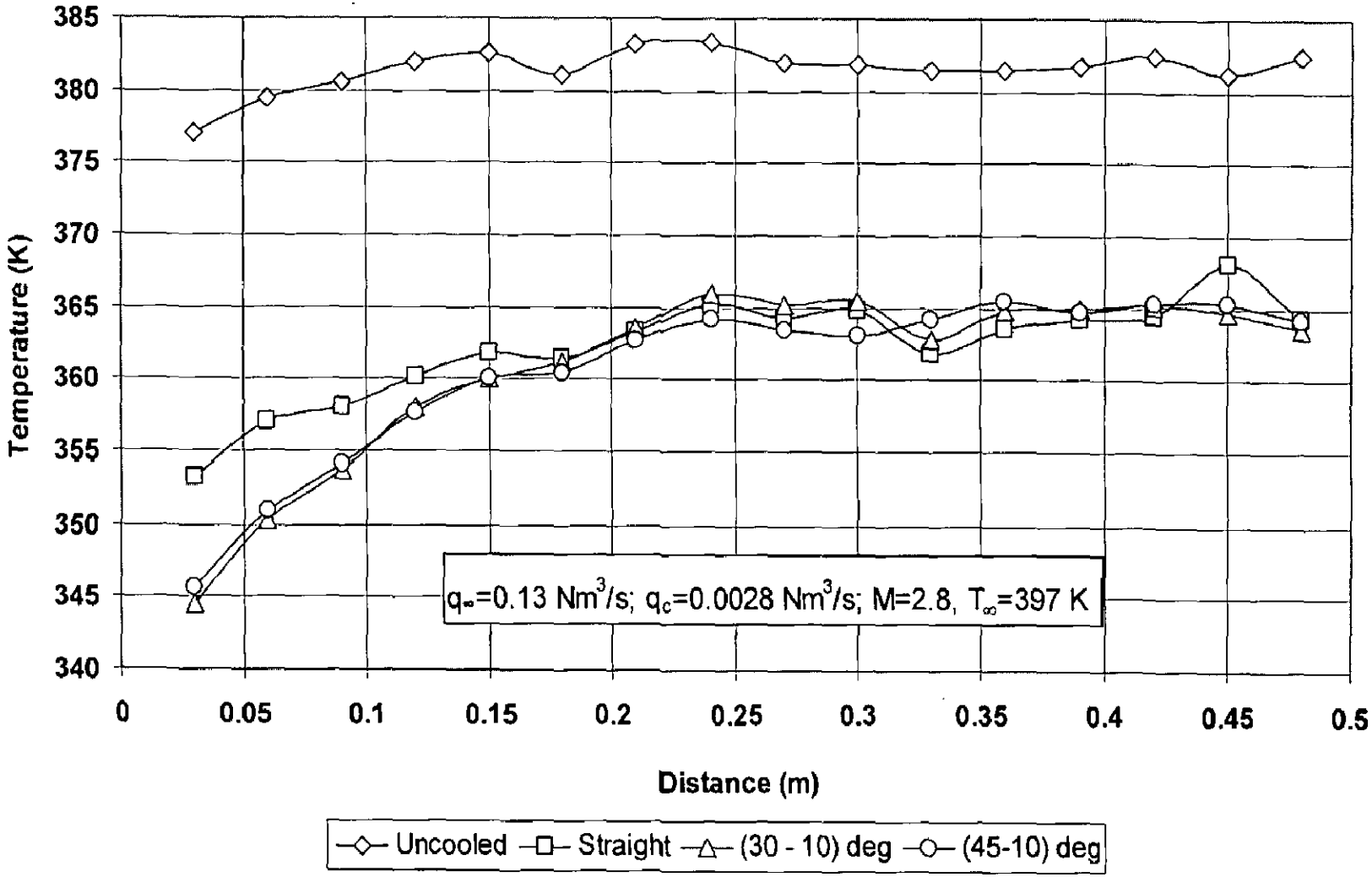

Fig. 5.7 Temperature profile for M = 2.8

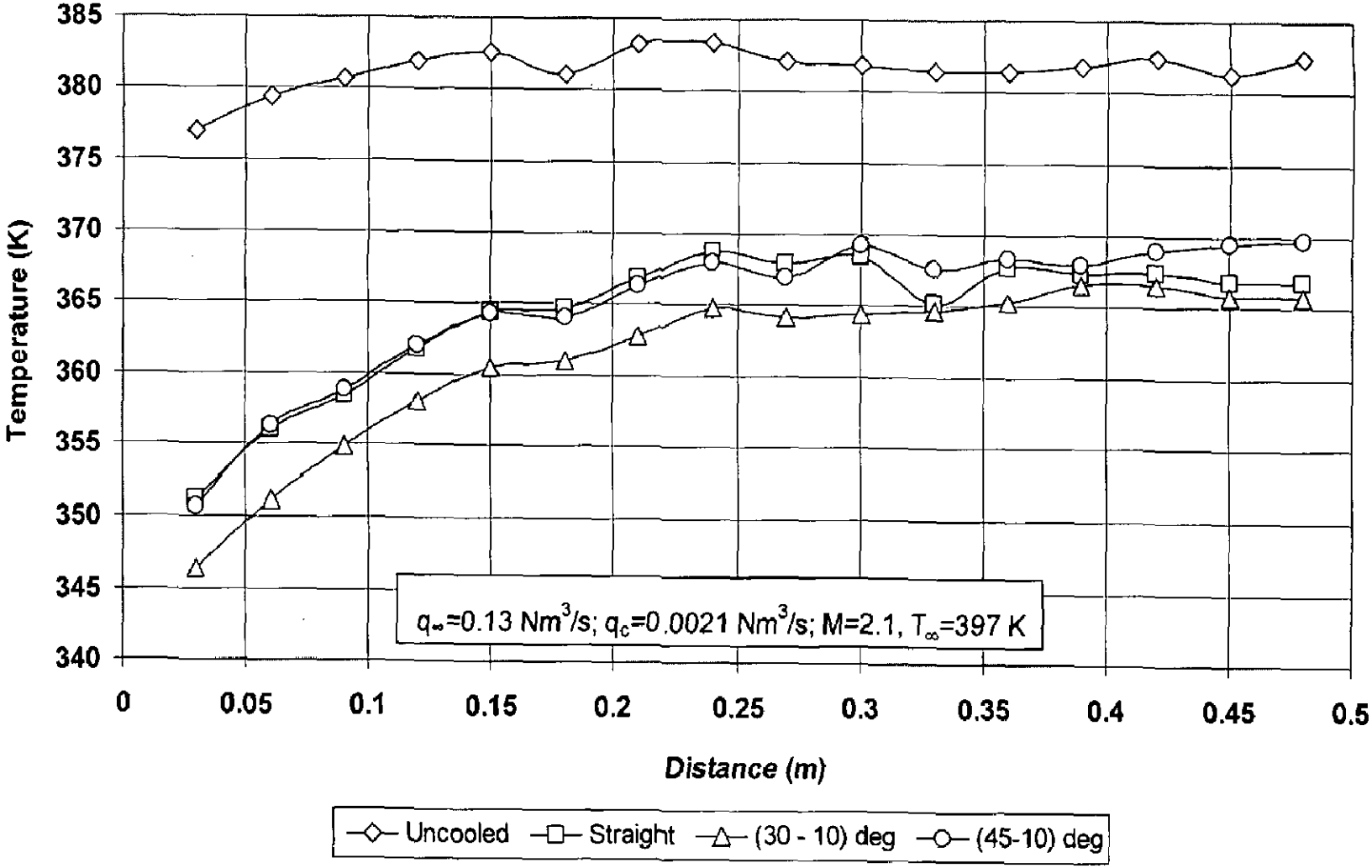

Fig. 5.8 Temperature profile for M = 2.1

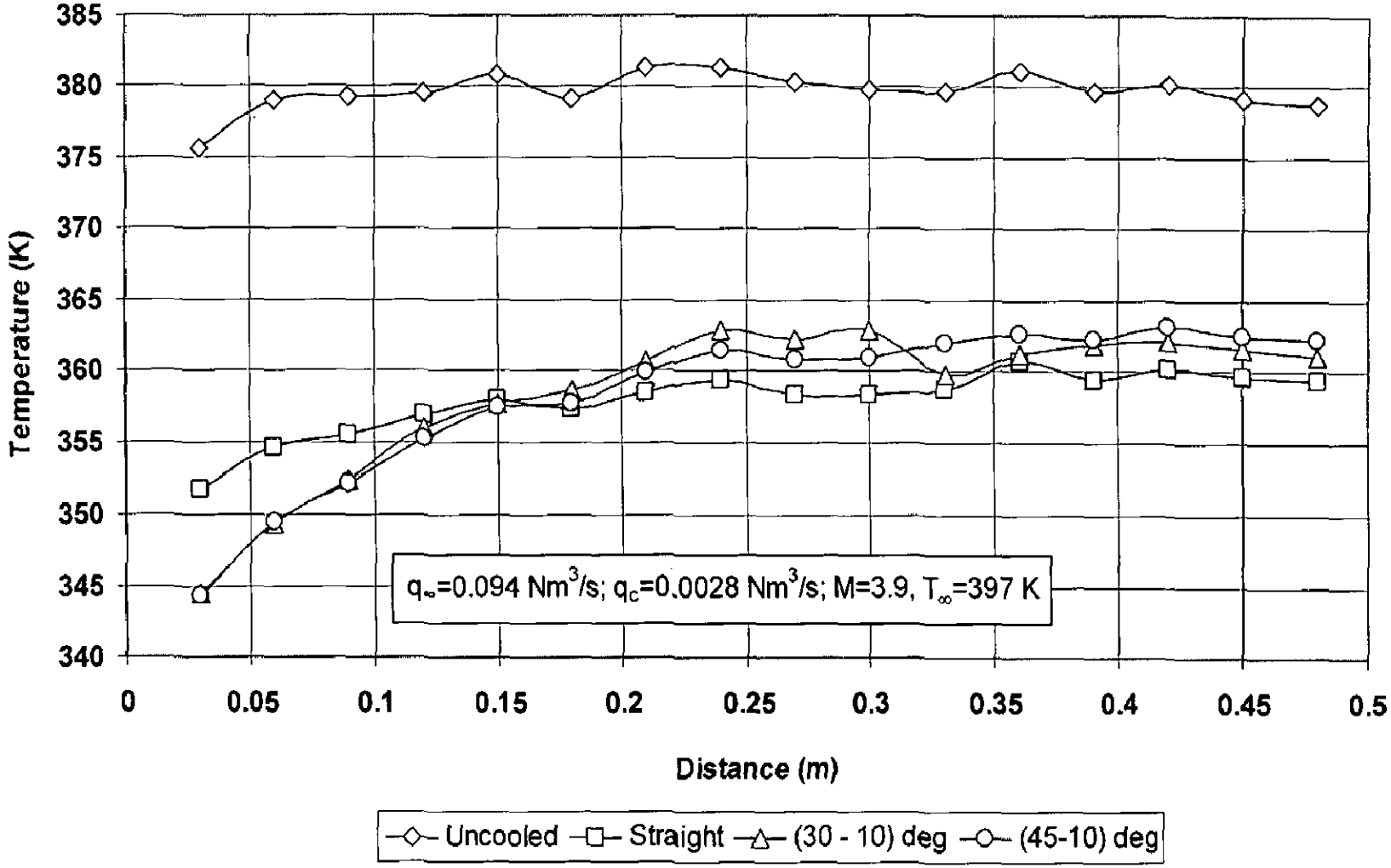

Fig. 5.9 Temperature profile for M = 3.9

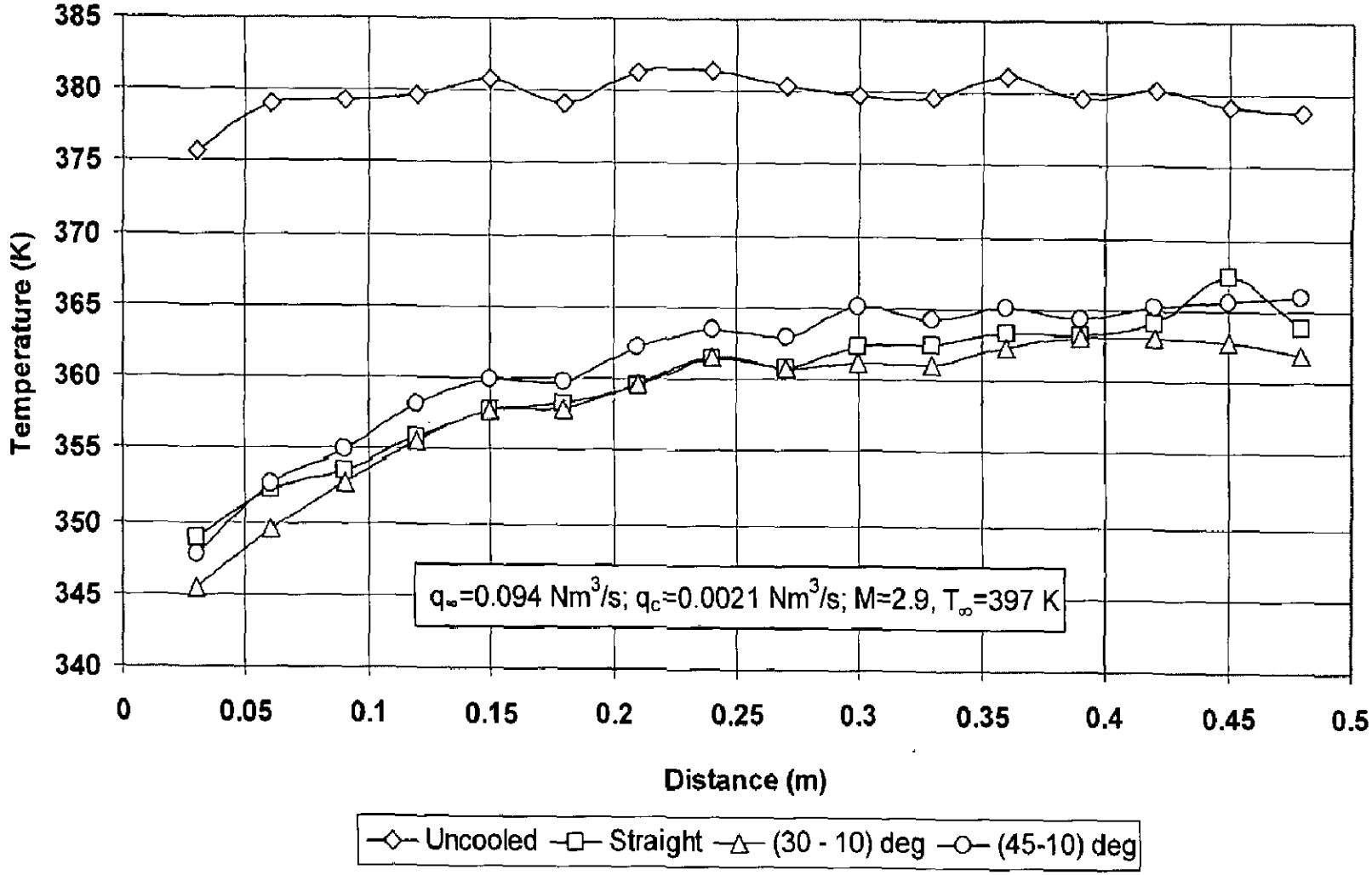

Fig. 5.10 Temperature profile for M = 2.9

Table 5.1 Comparison of film cooled length

Sl.No.	Main stream air temperature T_∞ (K)	Blowing ratio (M)	Main stream air flow rate q_∞ (Nm^3/s)	Coolant flow rate q_c (Nm^3/s)	Film Cooled Length (mm)		
					Straight	30° - 10°	45° - 10°
1	343	1.8	0.13	0.0021	260	250	240
2	343	2.4	0.13	0.0028	285	275	260
3	343	2.5	0.094	0.0021	290	275	260
4	343	3.4	0.094	0.0028	300	280	270
5	397	2.1	0.13	0.0021	235	230	220
6	397	2.8	0.13	0.0028	250	235	230
7	397	2.9	0.094	0.0021	250	240	230
8	397	3.9	0.094	0.0028	300	250	240

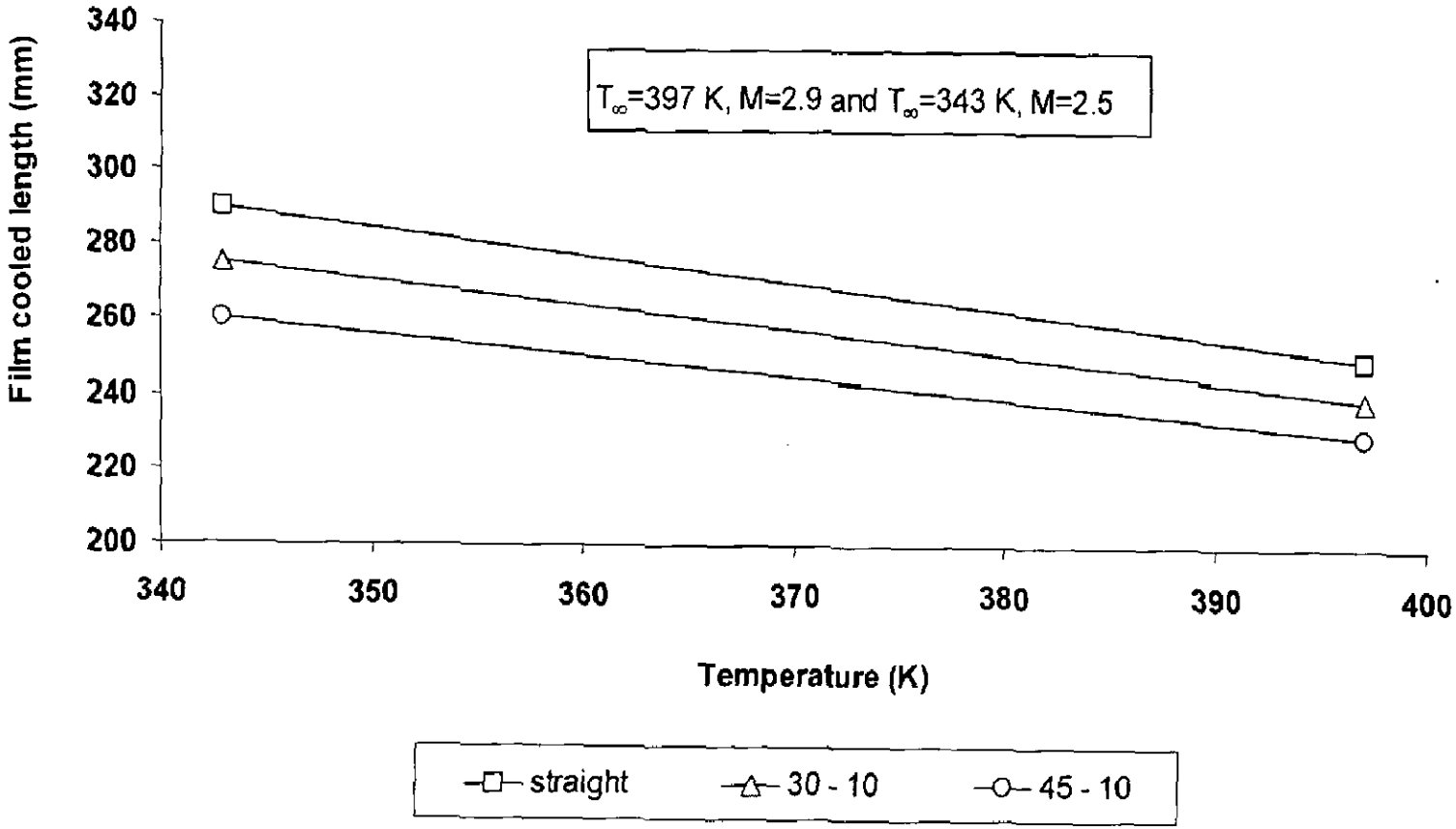

Fig. 5.11 Variation of film cooled length with temperature for M=2.5 and 2.9

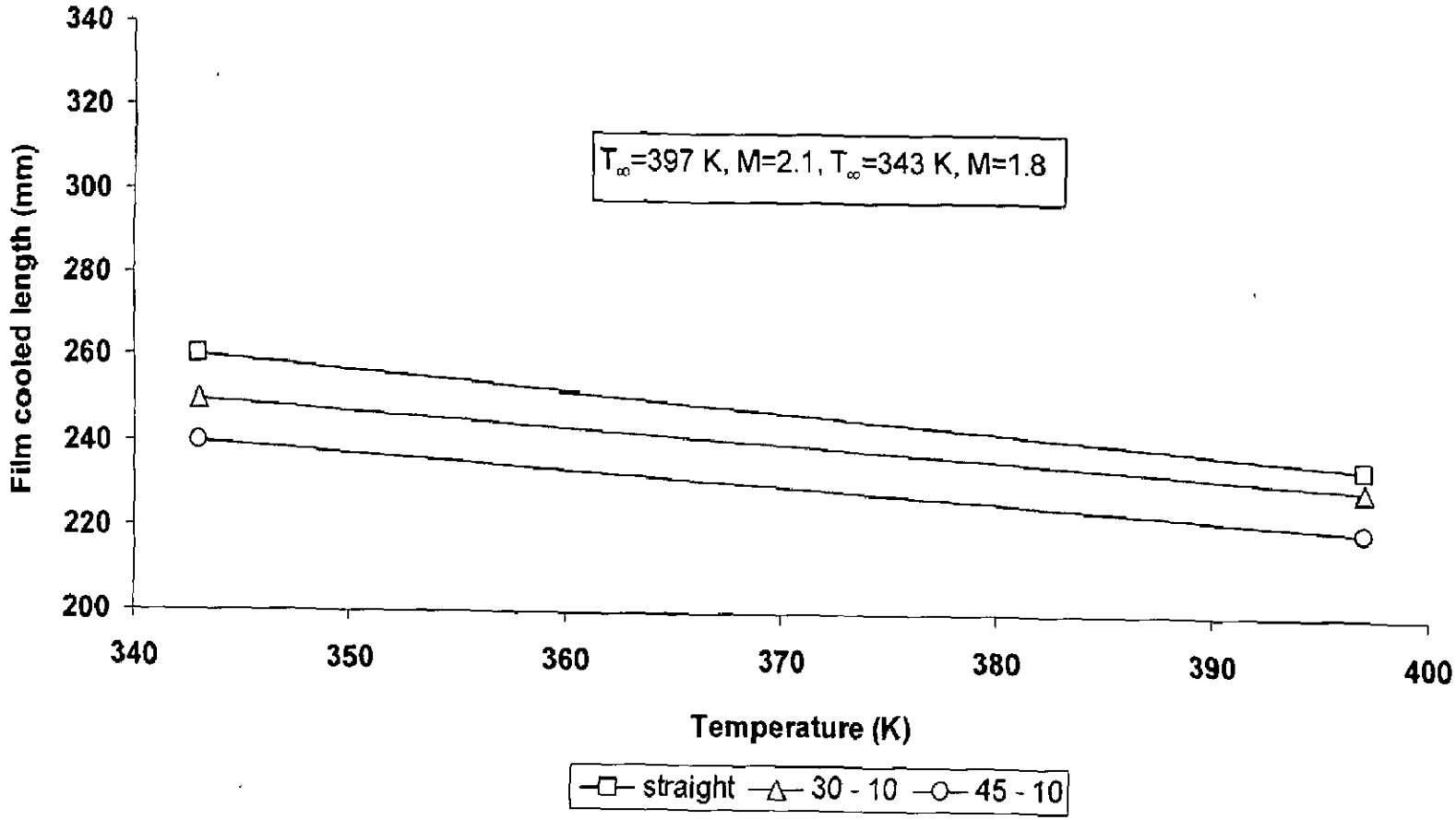

Fig. 5.12 Variation of film cooled length with temperature for M=1.8 and 2.1

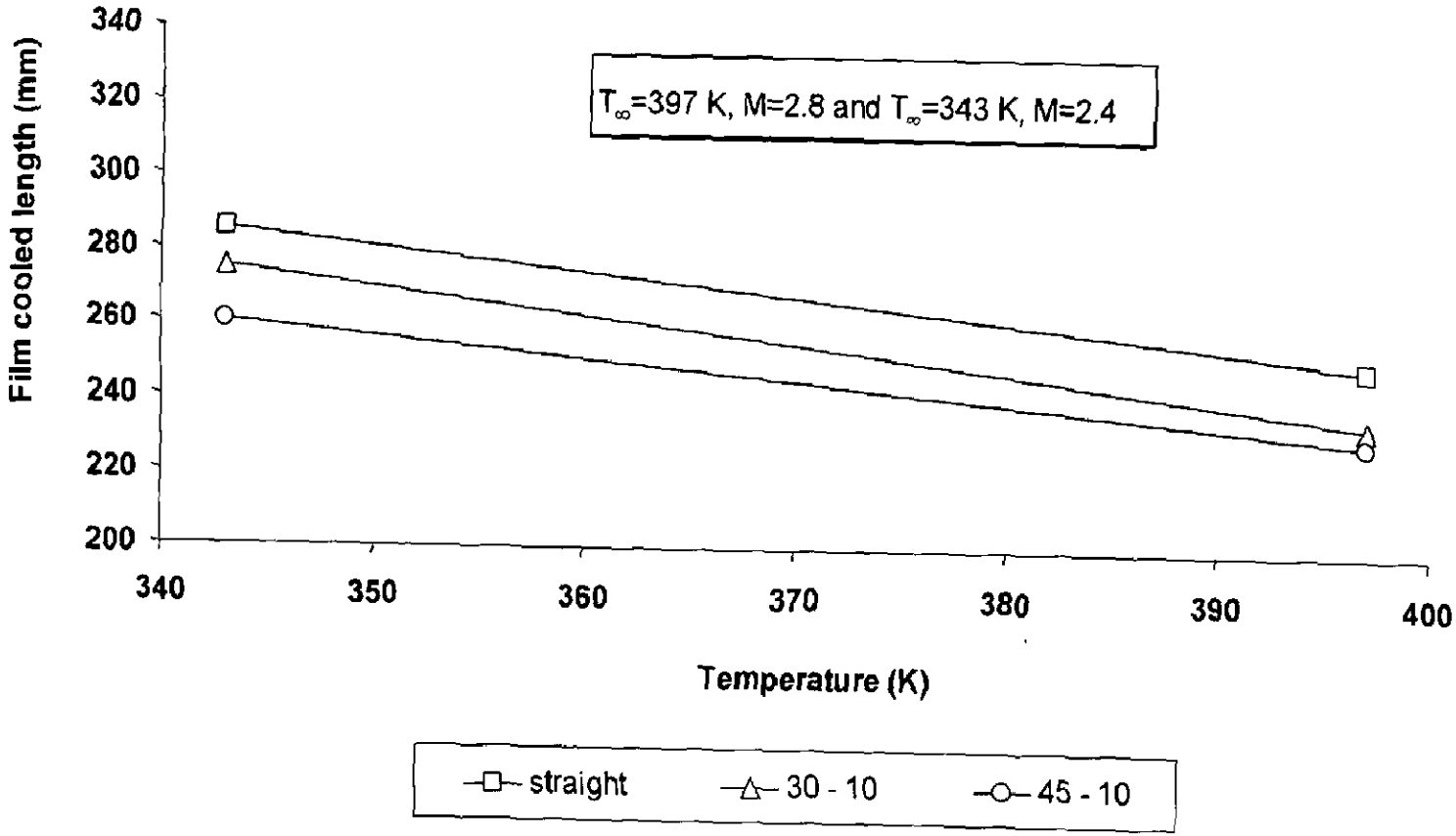

Fig. 5.13 Variation of film cooled length with temperature for M=2.4 and 2.8

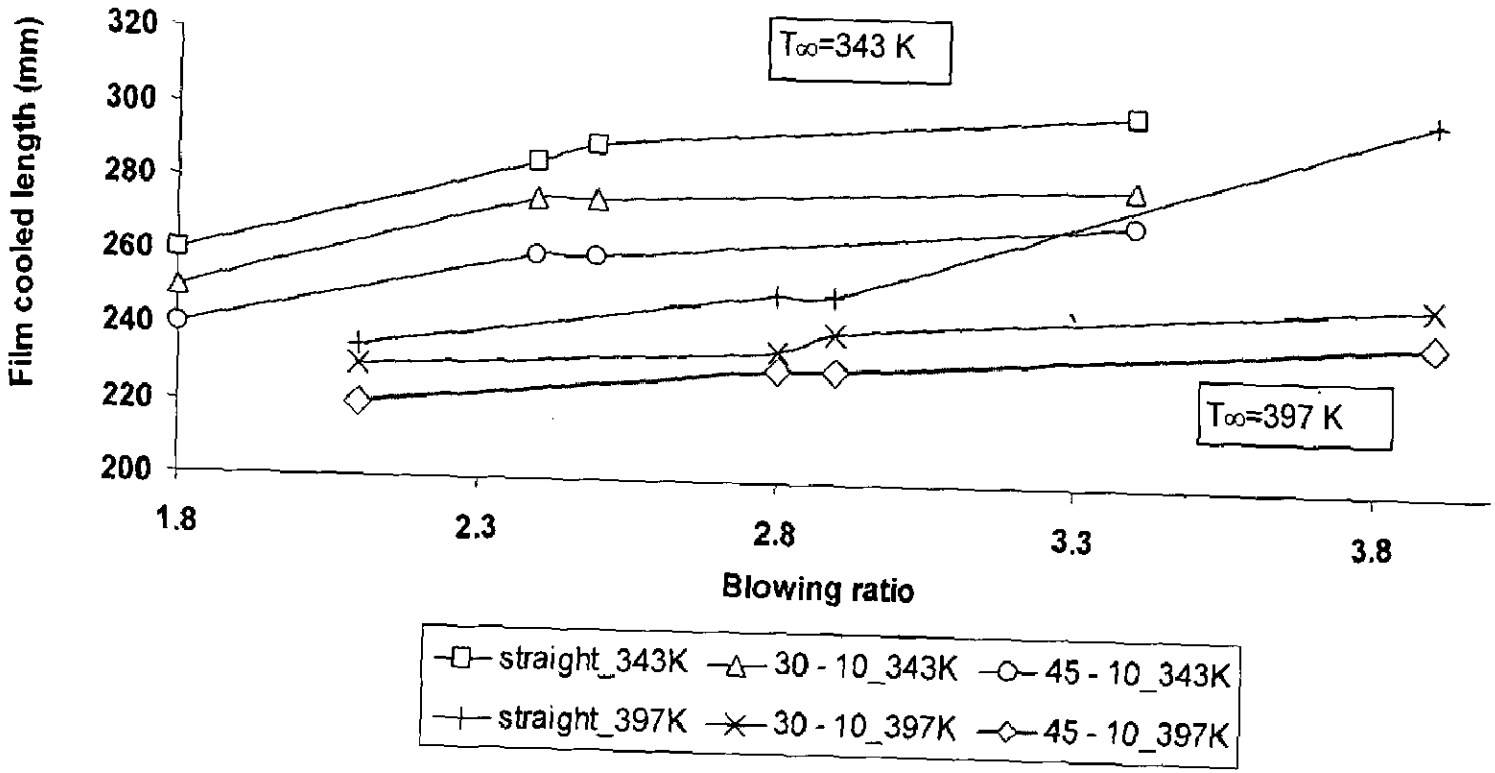

Fig. 5.14 Variation of film cooled length on blowing ratio

The film cooling effectiveness (η), the dimensionless wall temperature is computed from the ratio of the difference between the wall and main stream temperatures to that of the coolant and main stream temperatures. The variations of film cooling effectiveness for various blowing ratios on the non-dimensional length of the test section are shown in Fig. 5.15 to 5.22. Higher effectiveness for the orifice configuration of 30°-10° due to better cooling of the wall by the film adherence to the wall due to the higher angular momentum compared to the other two configurations. In the case of 45°-10° orifice configuration, the flow may not be adhered to the wall well due to direct impingement of the coolant on the wall and subsequent disintegration of the film.

The changes in effectiveness with the blowing ratios can be evaluated from the Fig. 5.17 and 5.18 for the main-stream temperature of 343 K, in which for M=2.5, the effectiveness is lower than that for M=3.4. Higher blowing ratio increases the angular momentum of the secondary fluid (coolant nitrogen) and hence the increase in the effectiveness. Similar effect can also be observed in Fig. 5.19 and 5.20 for the main-stream temperature of 397 K for M=2.1 and 2.8. This shows that the effectiveness is directly related to the blowing ratio.

The uniformity of coolant film around the test section for all the injector orifice configurations are shown in Fig. 5.23 and 5.24. Lower main stream temperature gives good coolant film uniformity at a distance of 0.06 m from the injection point as in Fig. 5.23 and a better uniformity attains from the orifice of 30°-10° as compared to the other two, which attributes to the good film smearing along the test section wall.

The standard deviation on temperature, σ measure the coolant film stability and is evaluated on the basis of a stable coolant film without breakage. Higher σ leads to higher fluctuations in the wall temperature indicating a non-uniform film or unstable film. Stability of the film is more with low main stream temperature as in Fig. 5.25. It can be seen from the Fig. 5.25 and 5.26 that for the same main stream temperature, higher blowing ratio tends to lower the film stability due to turbulence in the flow. High main stream temperature and high blowing ratio makes more fluctuation leading to an unstable coolant film as in Fig. 5.27.

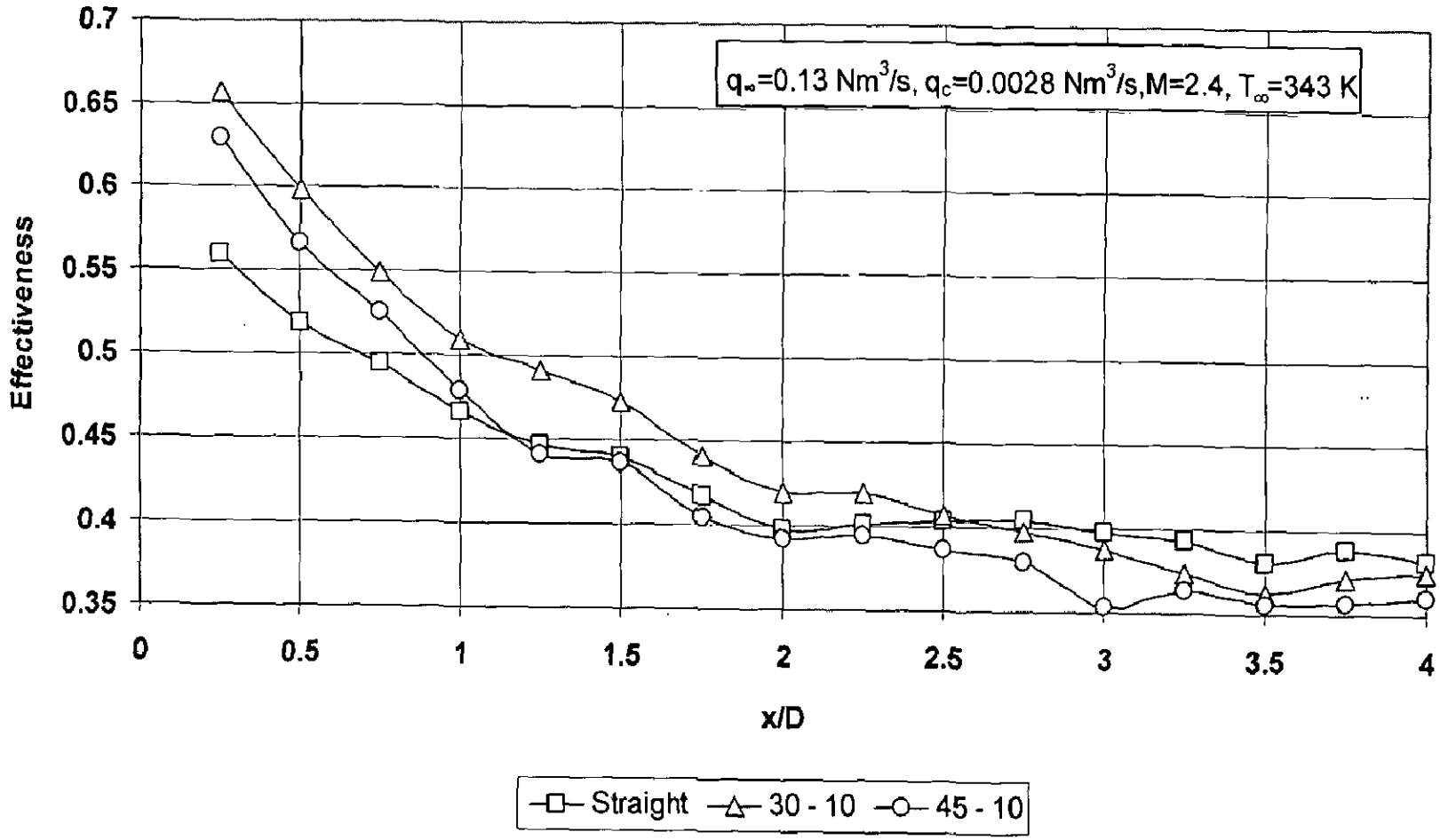

Fig. 5.15 Variation of Effectiveness for M=2.4

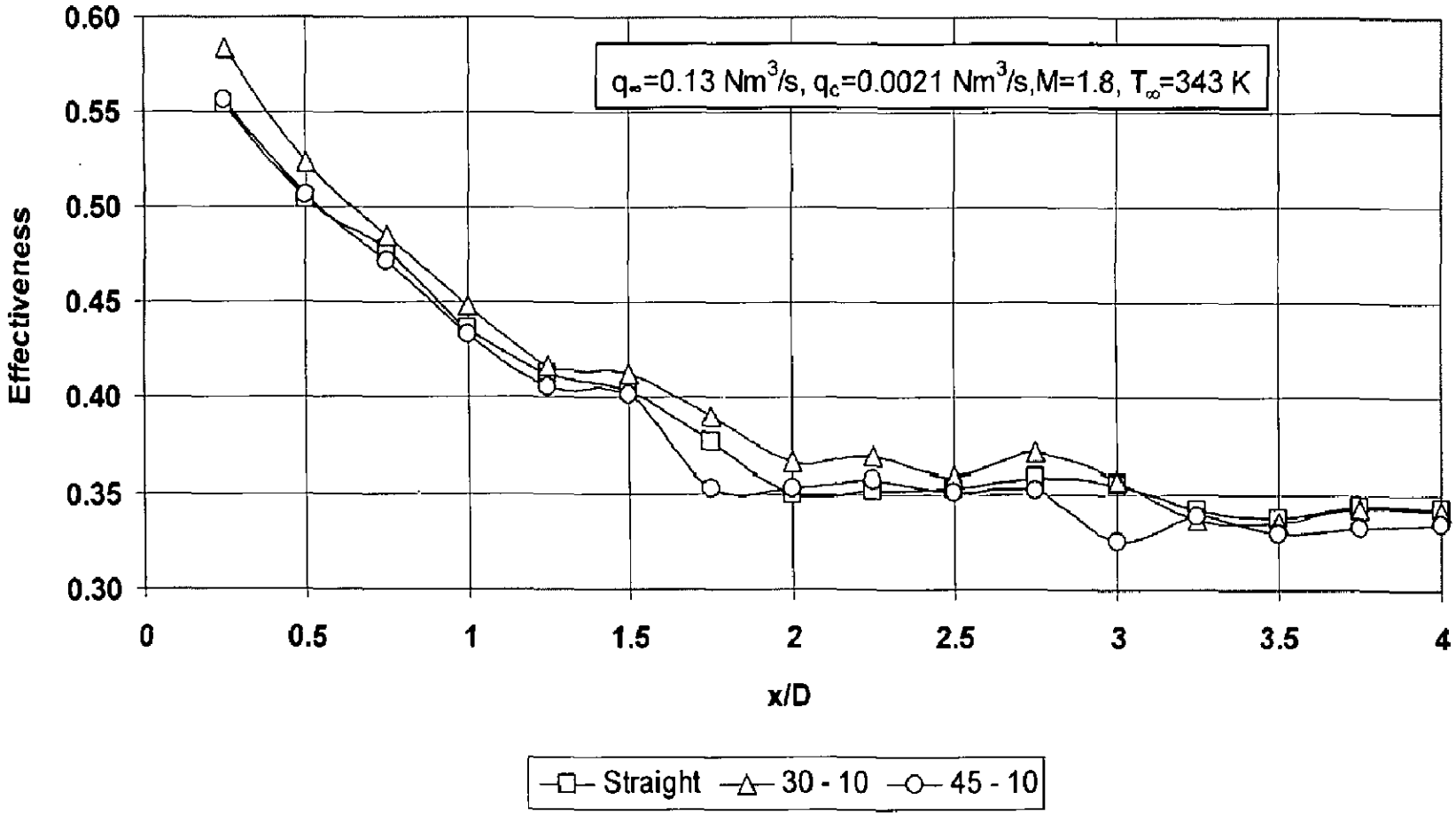

Fig. 5.16 Variation of Effectiveness for M=1.8

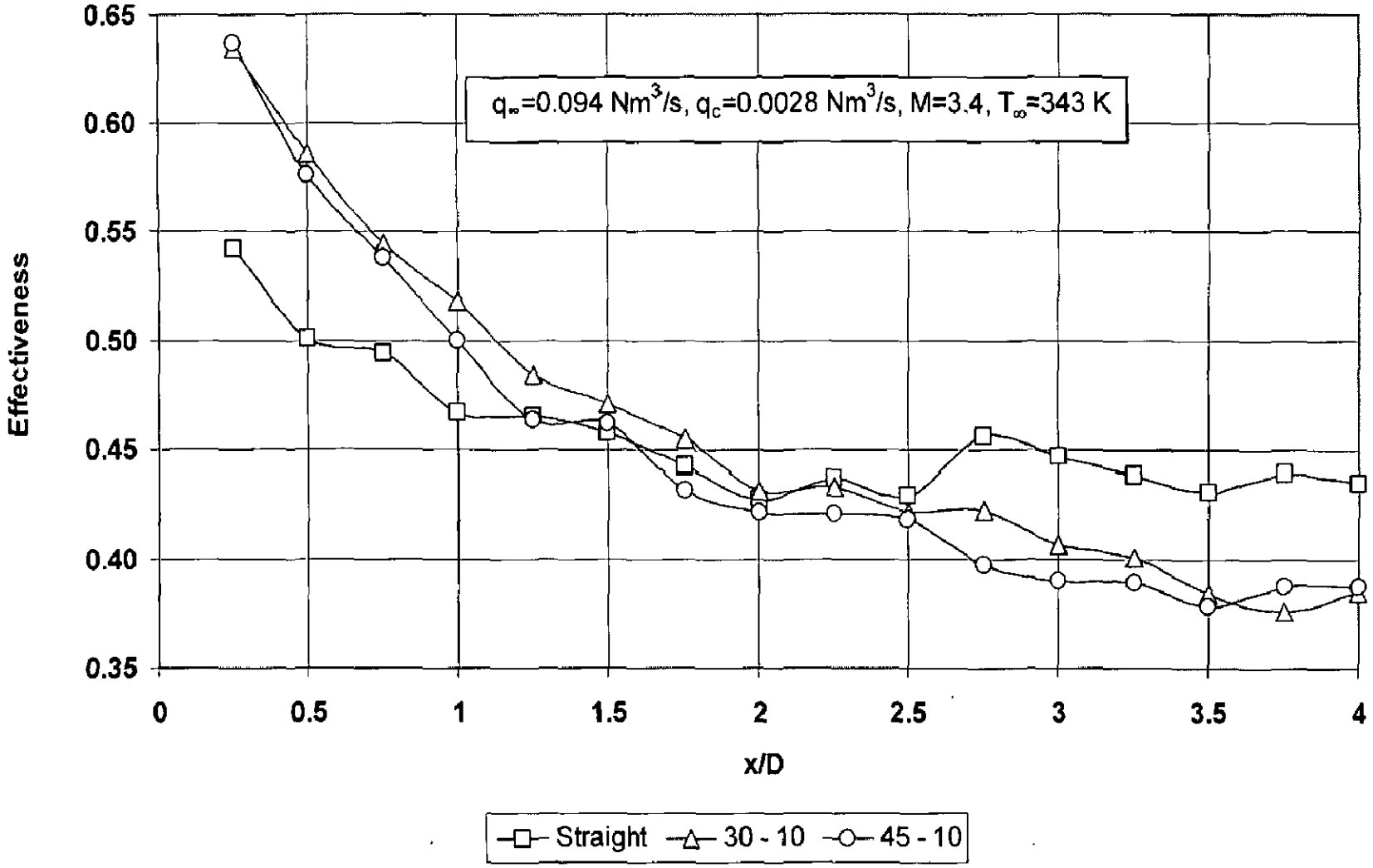

Fig. 5.17 Variation of Effectiveness for M=3.4

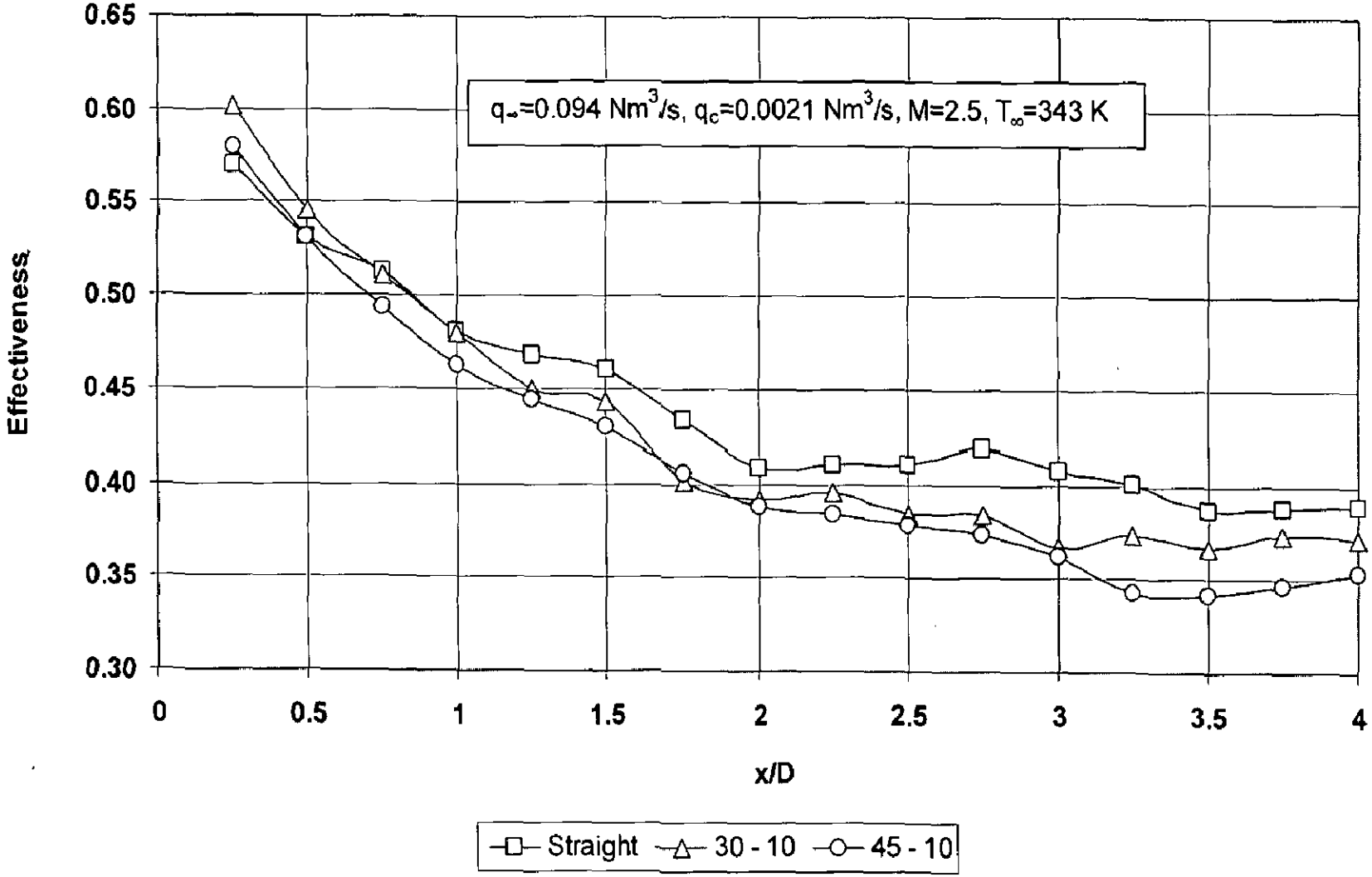

Fig. 5.18 Variation of Effectiveness for M=2.5

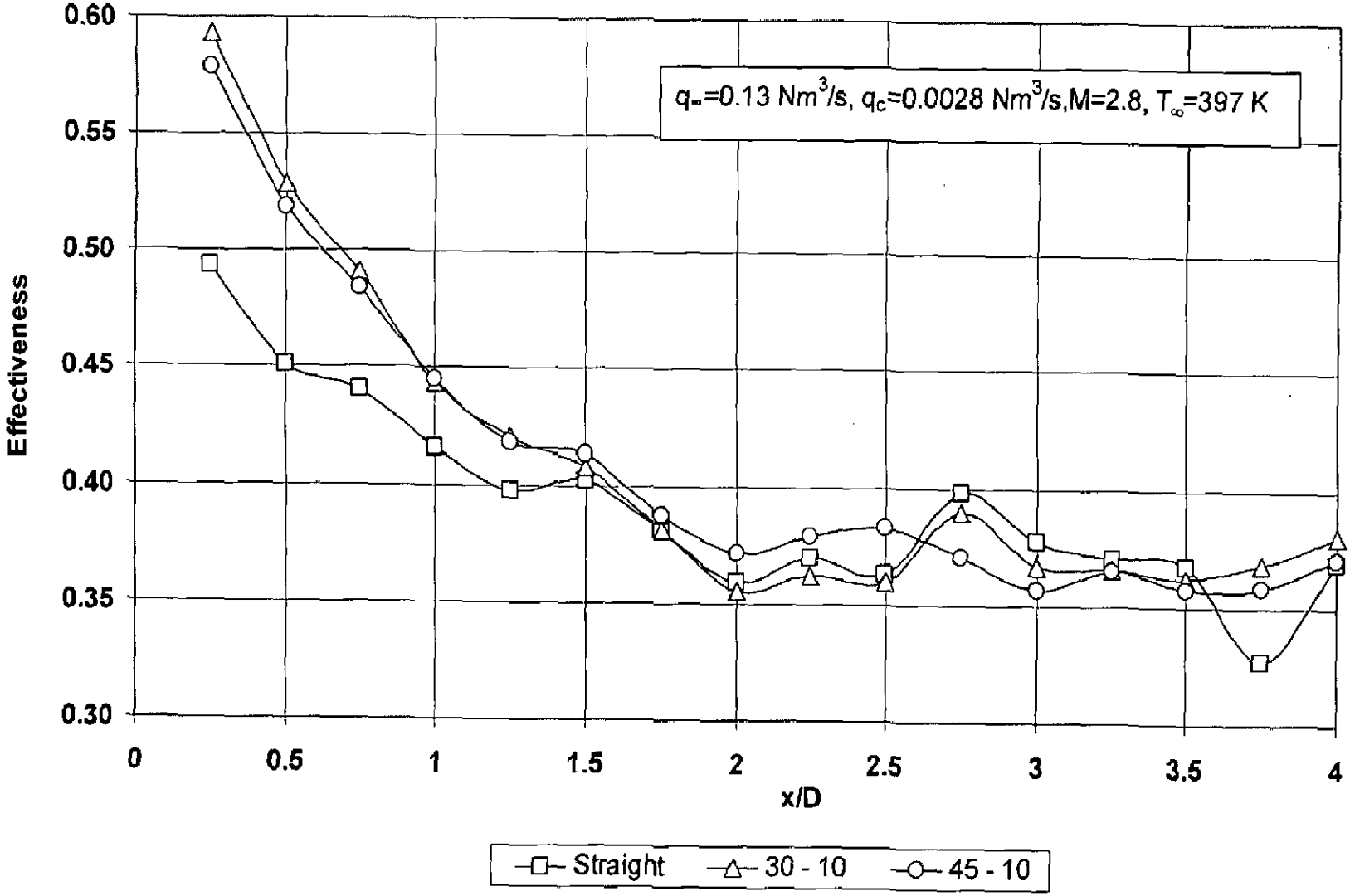

Fig. 5.19 Variation of Effectiveness for M=2.8

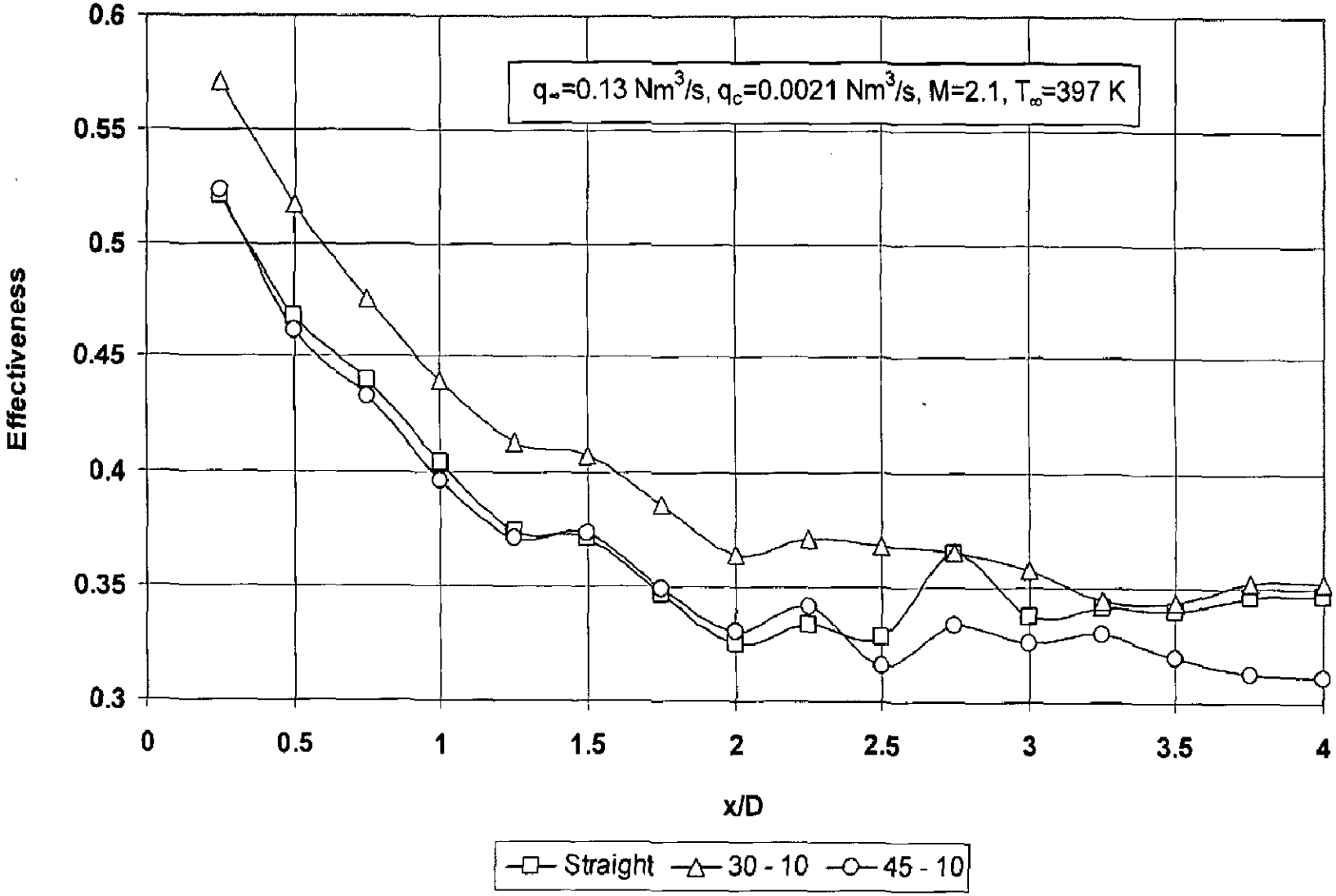

Fig. 5.20 Variation of Effectiveness for M=2.1

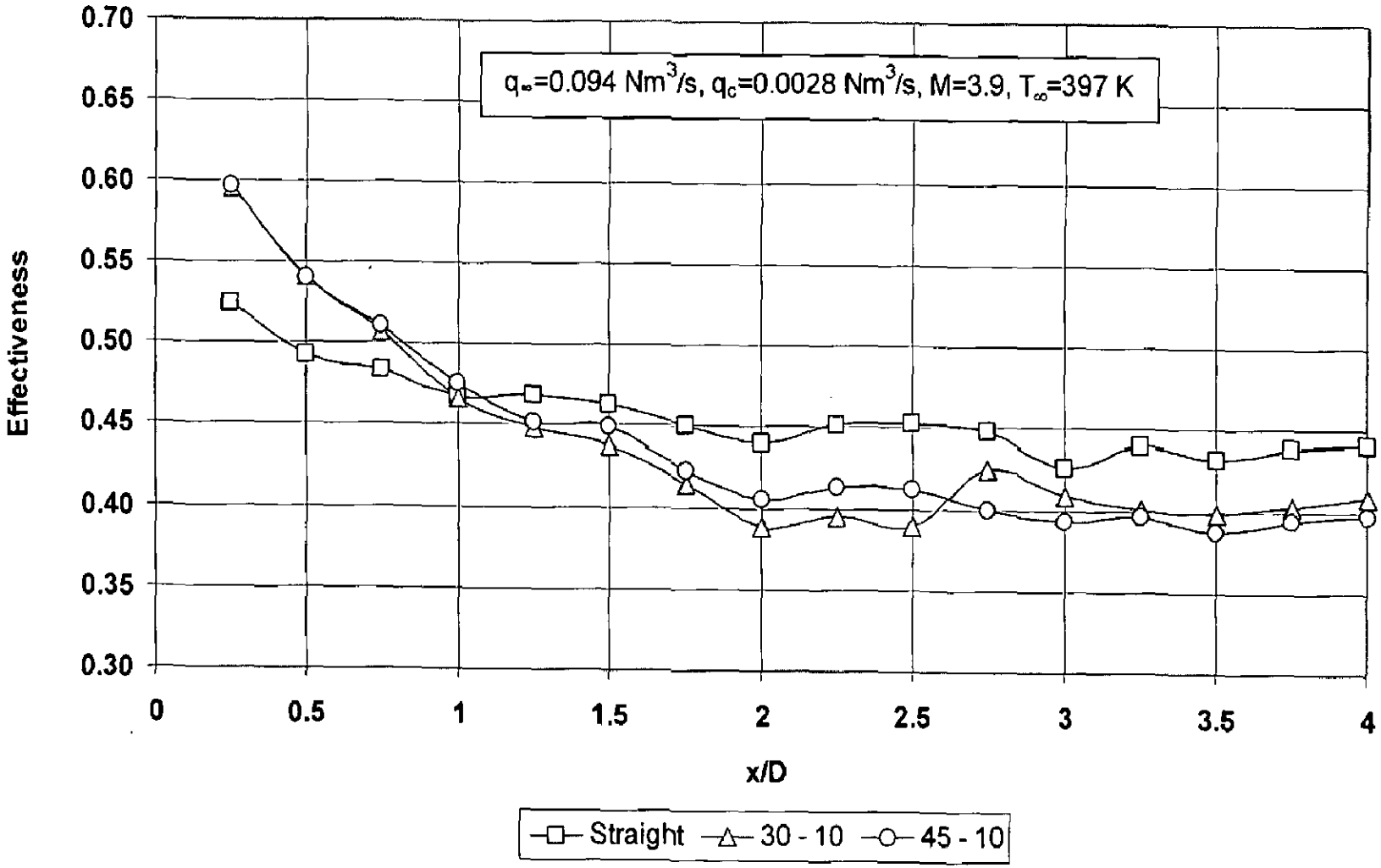

Fig. 5.21 Variation of Effectiveness for M=3.9

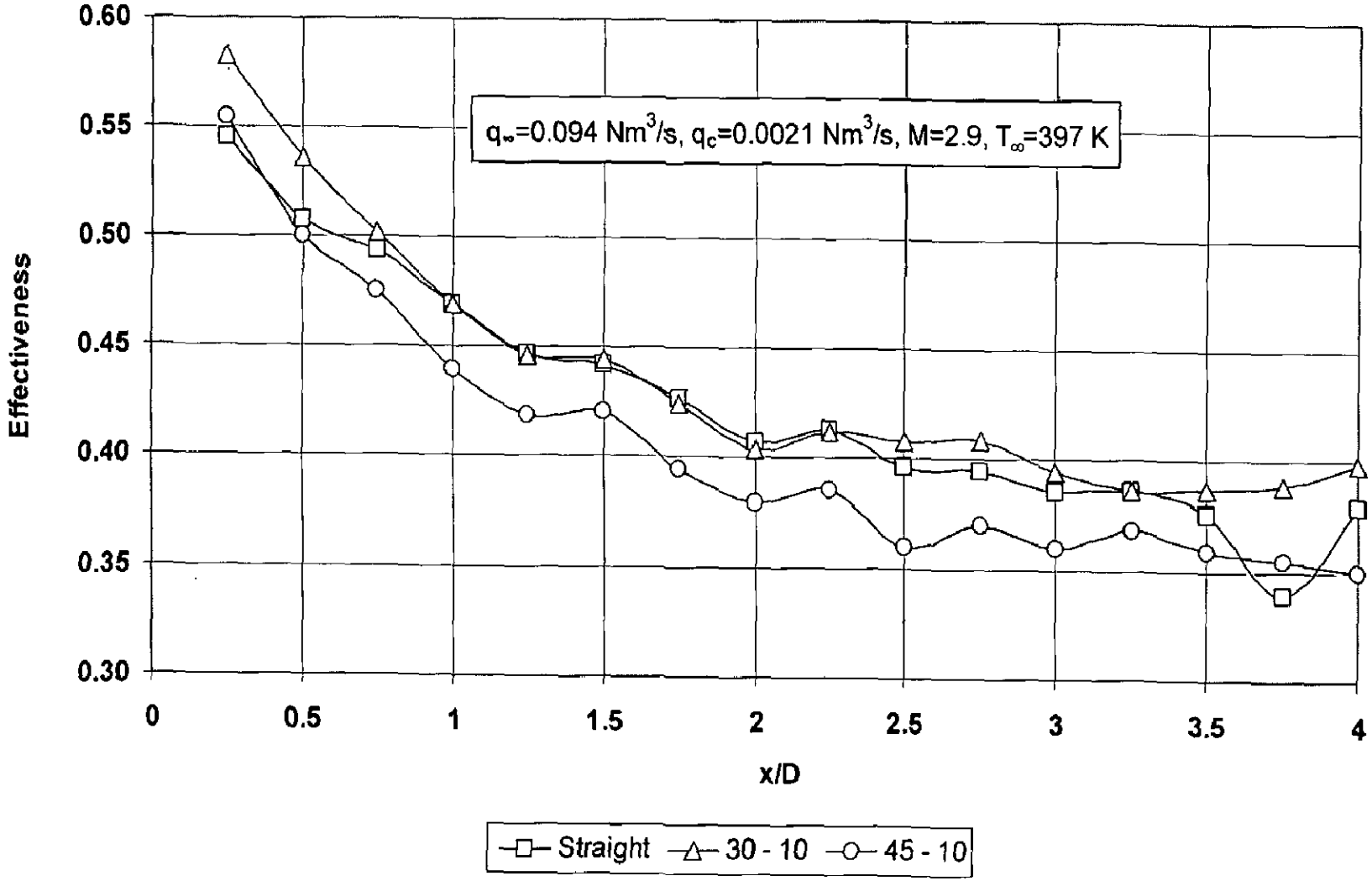

Fig. 5.22 Variation of Effectiveness for M=2.9

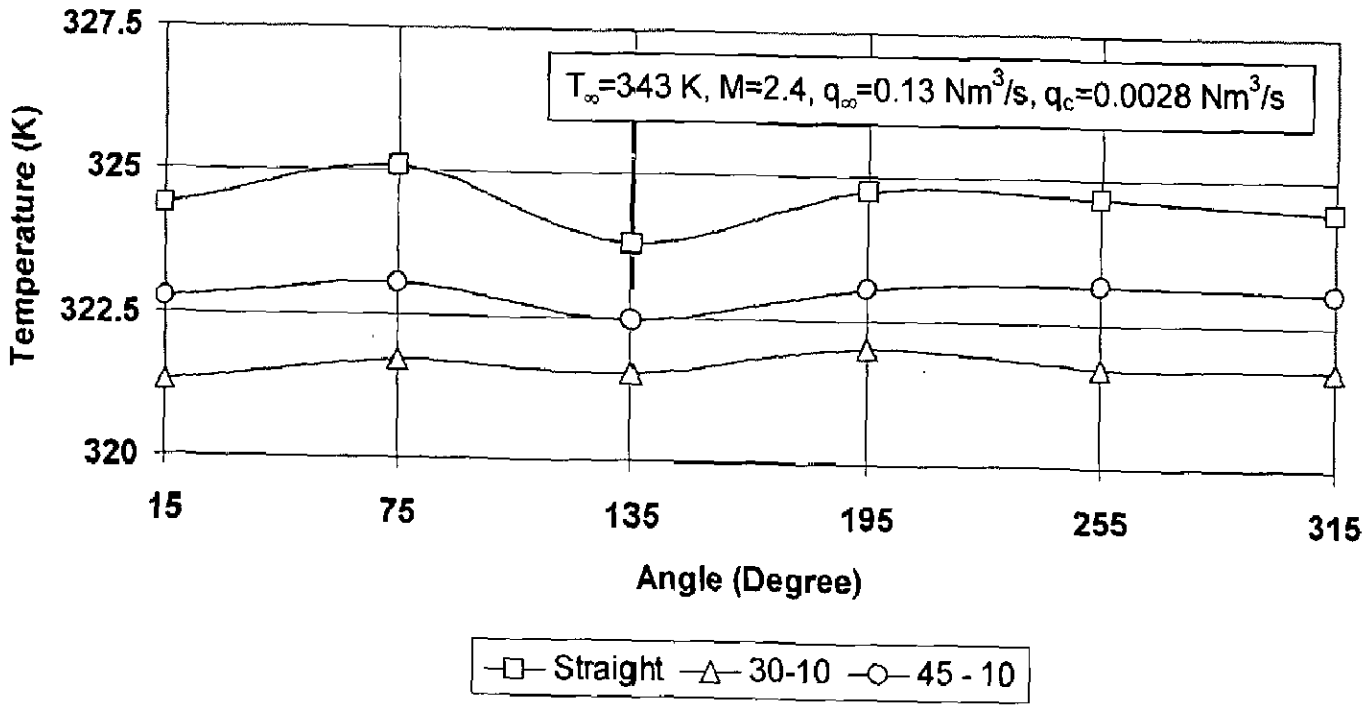

Fig. 5.23 Film uniformity along the circumference for M=2.4
(0.06 m from injection).

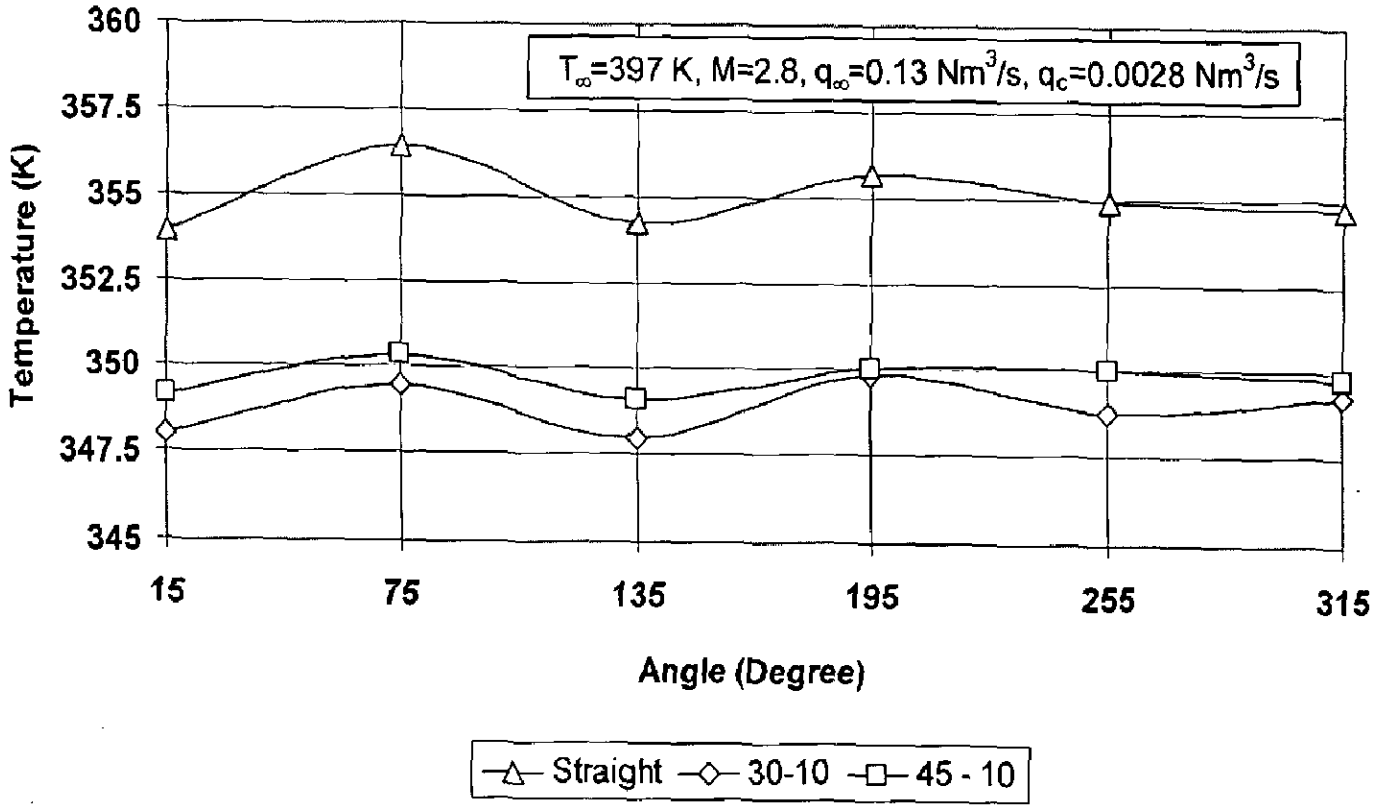

Fig. 5.24 Film uniformity along the circumference for M=2.8
(0.06 m from injection).

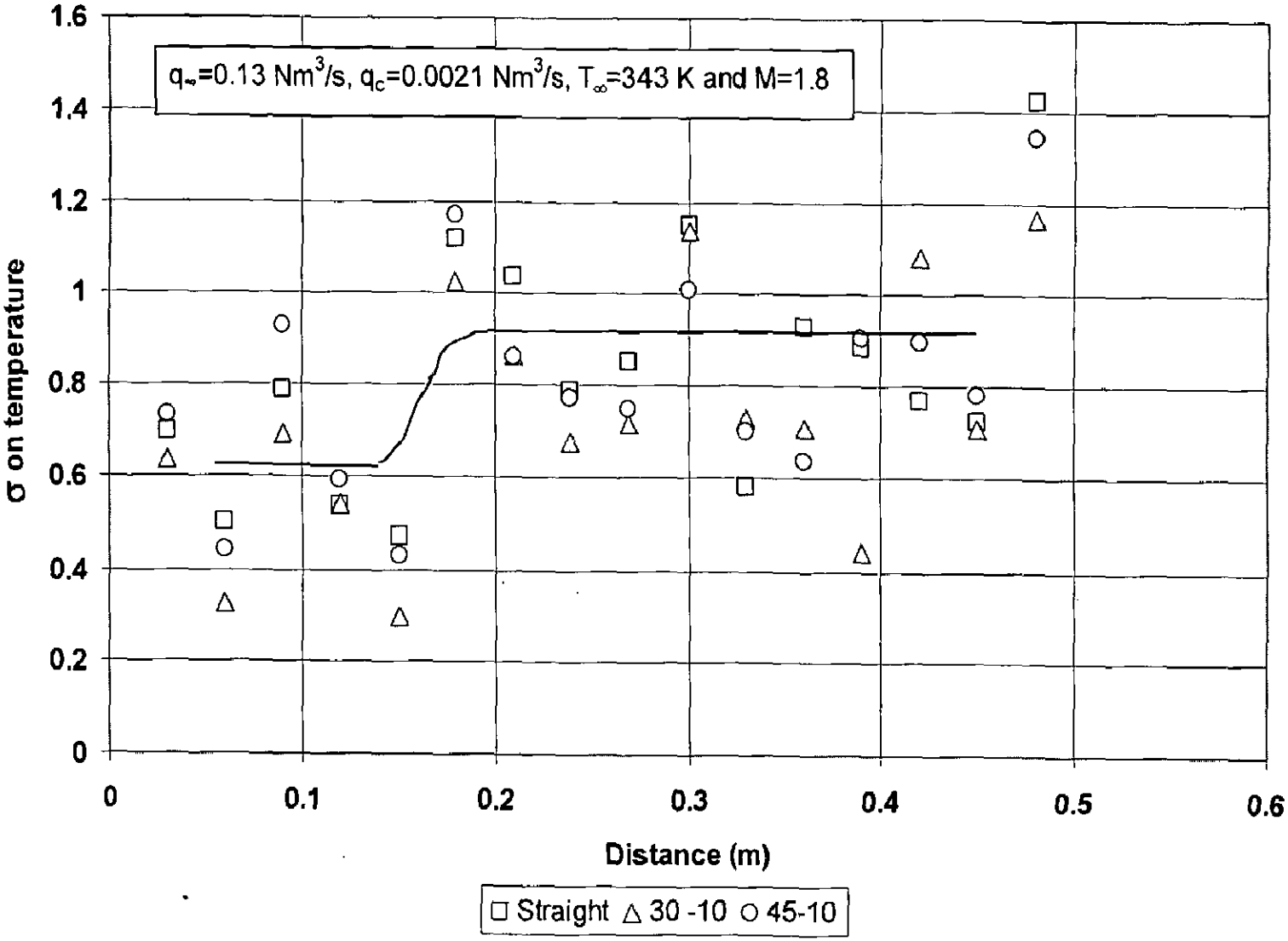

Fig. 5.25 Film stability for all injectors (M=1.8)

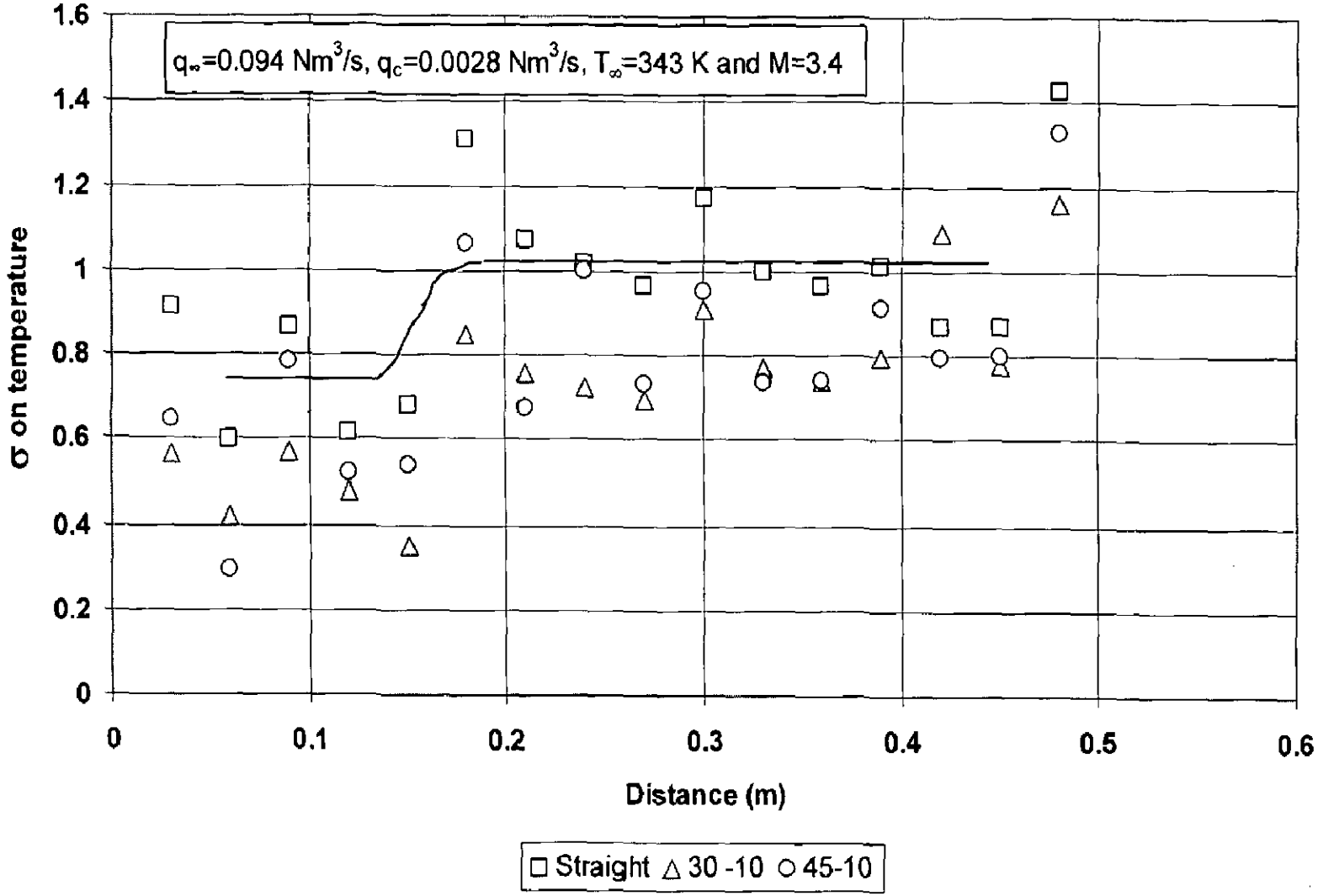

Fig. 5.26 Film stability for all injectors (M=3.4)

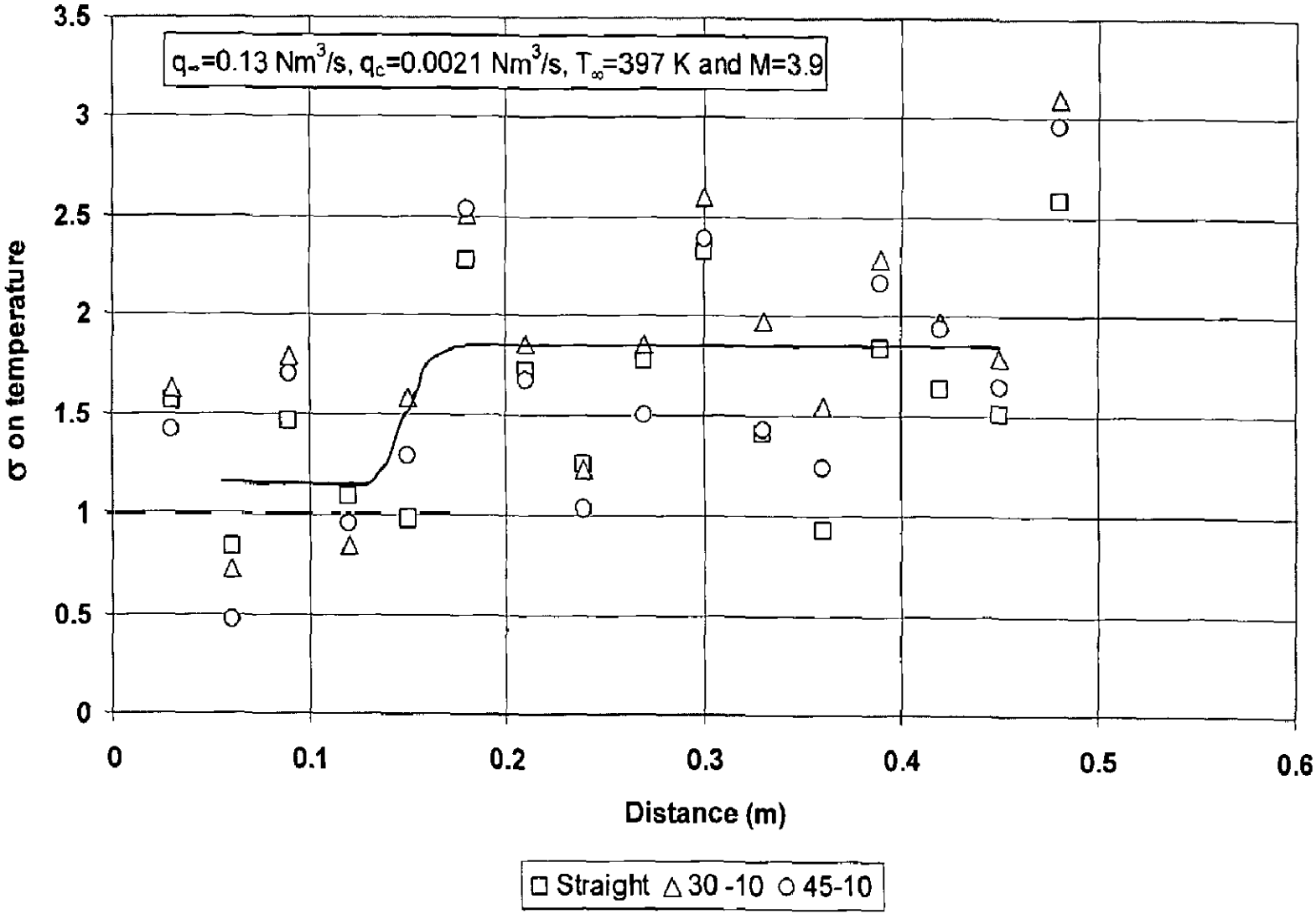

Fig. 5.27 Film stability for all injectors (M=3.9)

Chapter 6

CONCLUSIONS AND RECOMMENDATIONS

6.1 Conclusions

An experimental setup was made with a hot air source, flow straightner, insulated test section and an exhaust section to study the effect of different film coolant injection orifices on film cooling effectiveness, film cooled length and its stability. Detailed instrumentation for pressure, temperature and flow rates were made. Experiments were conducted for three different coolant injection configurations, viz., a straight injection orifice configuration and two compound angles injection configurations of 30°-10° and 45°-10°.

Measurements, which were carried out using nitrogen gas at NTP as coolant indicates the film cooling effectiveness as well as the film cooled length varies with blowing ratios and the injector configurations. It is also observed that better temperature uniformity is achieved on the test section in the case of compound angle injections compared to the straight injection. Higher film cooling effectiveness prevailed for the compound injection orifice of 30°-10° compared to straight and an angle of 45°-10° suggesting that an optimum compound injection angle do persists maximizing the film cooling effectiveness. On the other hand it was found that the extent of film cooled length is higher for straight injection orifice. The stability of the film was also found to be better for the compound angle of injection of 30°-10°. It was also noted that a relatively stable film prevails for low core gas temperature and higher blowing ratio tends to reduce the film stability. The film cooled length increases with higher blowing ratio but it reduces with higher core gas temperature. However higher blowing ratios are better at higher core gas temperature to achieve better film cooled length.

The choice of the angle of tangential and that of azimuth in the compound injection angle orifice configuration is found to be a significant factor in deciding the effectiveness of film cooling and the effective length of film cooling. There is high

potential for optimizing these angles to achieve maximum effectiveness and film cooled length, which is very essential for the part of view of engine operational safety.

6.2 Recommendations

On the basis of the present study, the following recommendations can be made for further studies.

1. It is understood from the study that there exist an optimum compound angle for the injection orifice that results in maximum film cooling effectiveness. Since it is extremely cumbersome to simulate all the possible combinations experimentally, it is suggested to carry out a 3-dimensional CFD modelling of the phenomena and validate it with few of the experiments. A subsequent parametric prediction study would yield an optimum configuration which then could be experimentally simulated using the setup.
2. Though gaseous film cooling is predominantly used in most of the cryogenic engines, earth storable and semi-cryogenic rocket engines use liquid propellant as the film coolant. Since the heat transfer process in gaseous film and a liquid film is entirely different and due to modeling difficulties of the processes in liquid film cooling, there exist an ambiguity over the film cooling effectiveness and length of film cooling. Further experiments in this direction will significantly improve the understanding of phenomenon and help the modelling activities. This could provide an opportunity to evaluate the heat transfer coefficients which are being used extensively in simulation models which is a major source of error.
3. The blowing ratio, M is one of the significant factor, which plays a direct role on the effectiveness, it is therefore it is essential that a parametric study is effected to optimize the same.

REFERENCES

1. Ahn. J., Jung. I. S. and Lee. J. S., Film cooling from two rows of holes with opposite orientation angles: injectant behaviour and adiabatic film cooling effectiveness, Int. J. Heat and Fluid Flow 24 (2003), 91–99.
2. Brown. A and Saluja C. L., Film cooling from a single hole and a low of holes of variable pitch to diameter ratio, Int. J. Heat and Mass Transfer, 22, (1979), 525 – 533.
3. Burns, W. K., and Stollery, J. L., The influence of foreign gas injection and slot geometry on film cooling effectiveness, Int. J. Heat and Mass Transfer, 12, (1969) 935 – 951.
4. Carl Stechman, R., Oberstone, J. L., and Howell, J. C., Design Criteria for Film Cooling for Small Liquid-Propellant Rocket Engines, AIAA 4th Propulsion joint Specialist conference., Cleveland, Ohio., 6 (2), (1969) 68 – 617.
5. Eriksen, V. L., Film cooling effectiveness and Heat transfer with injection through holes, NASA CR – 72991,(1971).
6. Folayan, C. O. and Whitelaw, J, H., Multi slot film cooling, Letters in Heat and Mass Transfer, 1, (1974), 31-36.
7. Georege P Sutton., Rocket Propulsion Elements.,3rd ed. John Wiley & Sons, Inc., New York and London (1963).
8. George. R. Kinney, Andrew. E. Abramson and John. L. Sloop, Internal liquid film cooling experiments with air stream temperatures to 2000°F in 2- and 4-inch diameter horizontal tubes, report 1087, Lewis Flight Propulsion Laboratory, National Advisory Committee for Aeronautics, Cleveland, Ohio., (1952).
9. Goldstein, R. J., Eckert, E. R. G., and Burggraf, F., Effects of hole geometry and density on three-dimensional film cooling, Int. J. Heat and Mass Transfer, 17, (1974), 595-607.
10. Goldstein, R. J., Rask, R. B., and Eckert, E. R. G., Film cooling with Helium injection into an incompressible air flow, Int. J. Heat and Mass Transfer, 9, (1966), 1341 – 1350.

11. Hasan Nasir, Srinath. V. Ekkad and Sumanta Acharya, Effect of compound angle injection on flat surface film cooling with large stream wise injection angle, J Experimental Thermal and Fluid Science, 25, (2001), 23-29.
12. Hassan Nasir, Sumanta Acharya and Srinath Ekkad, Improved film cooling from cylindrical angle holes with triangular tabs: effect of tab orientations, Int. J. Heat and Fluid flow, 24, (2003), 657–668.
13. Lakehal, D., Theodoridis, G. S., and Rodi. W., Computation of film cooling of a plat plate by lateral injection from a row of holes, Int. J. Heat and Fluid flow, 19, (1998) 418 – 430.
14. Lakshmi Narayanan, R., Pai, B. R., and Natarajan, R., Experimental study on liquid film cooling, Report, NAL Bangalore and IIT Madras, (1986).
15. Maiteh. B. Y. and Jubran. B. A., Influence of mainstream flow history on film cooling and heat transfer from two rows of simple and compound angle holes in combination, Int. J. Heat and Fluid flow, 20, (1999), 158–165.
16. Michael Gritisch, Achmed Schulz and Sigmar Wittig, Film cooling holes with expanded exits: near hole heat transfer coefficients, Int. J. Heat and Fluid Flow, 21, (2000), 146 – 155.
17. Richard J. Goldstein, "Film Cooling" – Literature.
18. Shyang-Lin Kuo, Neng-Li Zhang and Wen-Jei Yang., Role of Mainstream Flow Velocity in Film Cooling in a Duct, J.Thermophysics, 10 (2), (1996.)
19. Stephen Papell, S., Effect on gaseous film cooling of coolant injection through angled slots and normal holes, NASA Technical Note D – 299, (1960).
20. Yen Ching Yu, Reuben. Z. Schuff, William. E. Anderson, Liquid film cooling using Swirl in rocket combustors, 40th AIAA/ASME/SAE/ASEE Joint Propulsion Conference and exhibition, AIAA 2004-3360, (2004).
21. Yuen, C. H. N. and Martinez – Botas R F., Film cooling characteristics of rows of round holes at various streamwise angles in a cross flow: Part I. Effectiveness, Int. J. of Heat mass transfer 48, (2005), 4995–5016.
22. Yuen, C. H. N. and Martinez – Botas R F., Film cooling characteristics of rows of round holes at various streamwise angles in a cross flow: Part II, Heat transfer coefficients, Int. J. Heat mass transfer 48, (2005), 5017–5035.

23. Zhang. H. W., Tao. W. Q., He. Y. L. and Zhang. W., Numerical study of liquid film cooling in a rocket combustion chamber, Int. J. Heat and Mass Transfer 49, (2006), 349–358.